Photon – Photon Physics

From

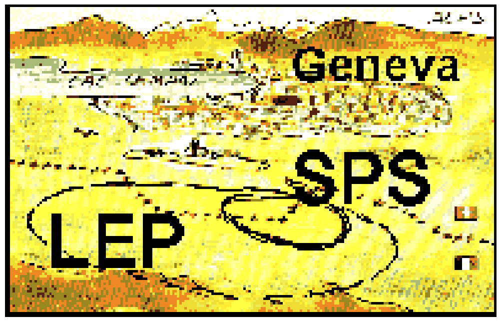

to

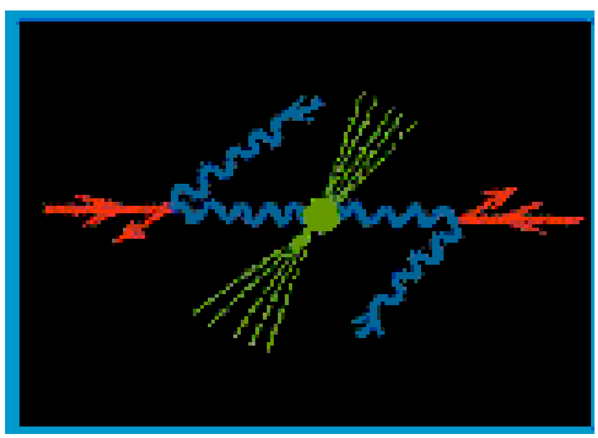

TESLA

Richard Nisius (CERN)
Holzhau, 2–7 October 1

The programme...

Introduction

1. The photon and photon structure
2. LEP and a LEP detector
3. The Linear Collider (LC)
4. Advantages of a Photon Collider (PC)
5. Compton backscattering and background

Photon–photon scattering

1. Total cross-section
2. Jet cross-sections
3. Heavy flavour production

Deep–inelastic electron–photon scattering

1. QED structure functions
2. The charm structure function $F_{2,c}^{\gamma}$
3. Bottom production
4. The hadronic structure function F_2^{γ}
5. Flavour decomposition of F_2^{γ}
6. Polarized structure functions
7. Hadronic structure function for virtual photons

...continued

Interactions of two virtual photons

1. QED signatures
2. BFKL signatures
   a) $\gamma^{\star}\gamma^{\star} \longrightarrow$ hadrons
   b) J/ψ production

New signatures

1. Higgs production
   a) $\gamma\gamma \longrightarrow h_0$
   b) MSSM Higgs
1. Production of W-pairs
2. Production of Z-pairs
3. Single top production

The 'history' of the photon

Date	Event
8.11.1895	Röntgen discovers the X-rays (first Nobel Prize for physics 1901).
1900	Planck interprets light as 'energy quanta' $E = h\,\nu$, with $h = 6.626 \cdot 10^{-34} Js$.
1905	Einstein explains the photoelectric effect by 'photons'.
1922	Discovery of Compton scattering $\mathrm{e}\gamma \rightarrow \mathrm{e}'\gamma'$.
1927	Heisenberg formulates the uncertainty principle e. g. $\Delta E \Delta t \geq \hbar$.
1930	Fist attempt to measure photon-photon scattering by Hughes et. al.
1936	First calculation of photon-photon scattering by Euler und Kockel.
1981	First measurement of the hadronic structure function of the photon by PLUTO.
2011	The Higgs Boson will be produced through photon-photon fusion at TESLA?

Properties of the photon

Property	
Mass (m)	$0 \quad (m/m_{\mathrm{e}} < 4 \cdot 10^{-22}$, [1])
Charge (Q)	$0 \quad (Q/Q_{\mathrm{e}} < 5 \cdot 10^{-30}$, [2])
Velocity (c)	299792458 m/s
Spin parity ($\mathrm{J^{PC}}$)	1^{--}
Coupling (α)	$1/137.03599976(50)$
Task	Carrier of the electromagnetic interaction, no self-coupling

[1] Roderic Lakes, Phys. Rev. Lett. 80 (1998) 1826.

[2] Georg Raffelt, Phys. Rev. D50 (1994) 7792.

The 'first' photon – photon collider anno 1930

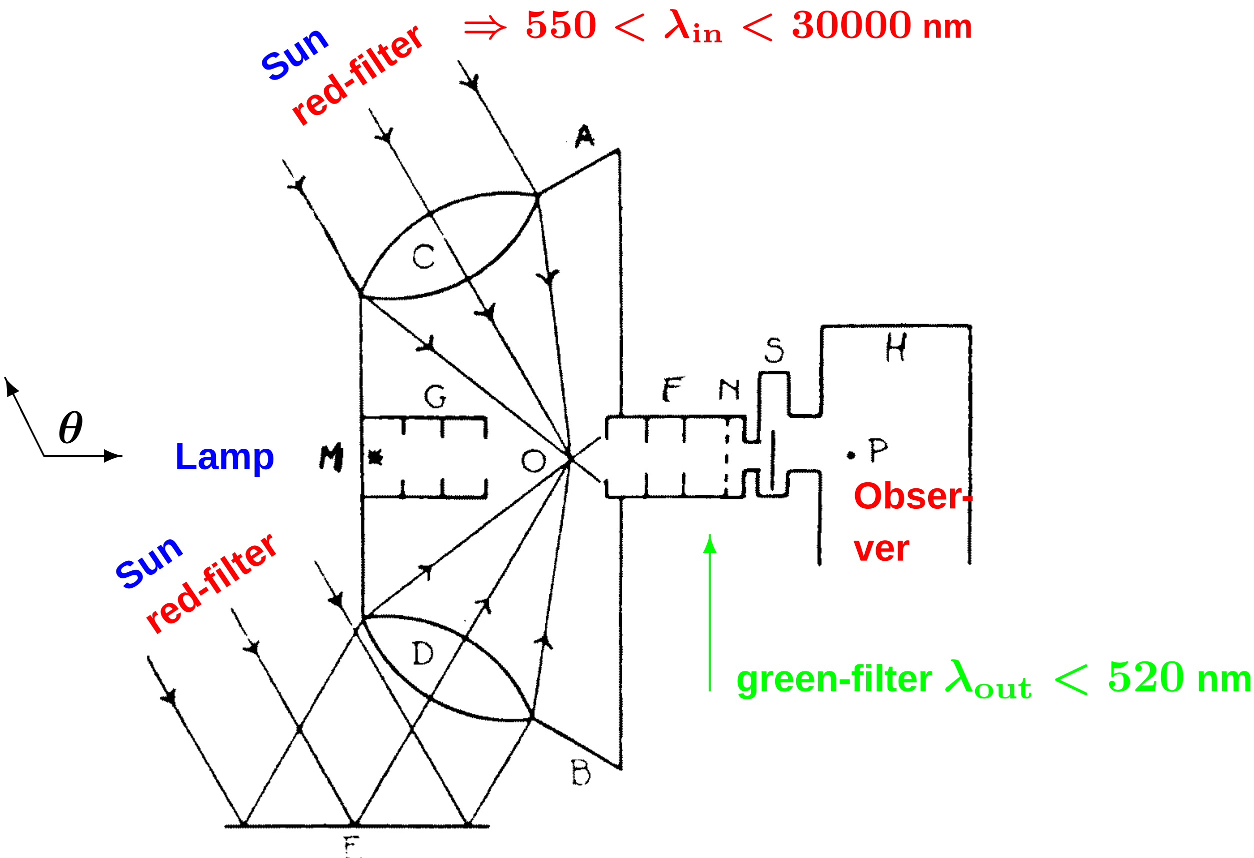

$$\gamma_1(\lambda_{in})\gamma_2(\lambda_{in}) \rightarrow \gamma_1'(\lambda_{out})\gamma_2'(\lambda_{out})$$

with:

$$\lambda_{out} = \lambda_{in}(1 + \cos\theta)$$

No light was observed.

$$\Rightarrow \sigma_{\gamma\gamma\to\gamma\gamma} < 3 \cdot 10^8 \text{ pb}$$

A.L. Hughes and G.E.M. Jauncey, Phys.Rev. 36 (1930) 773.

Why do we talk about photon structure?

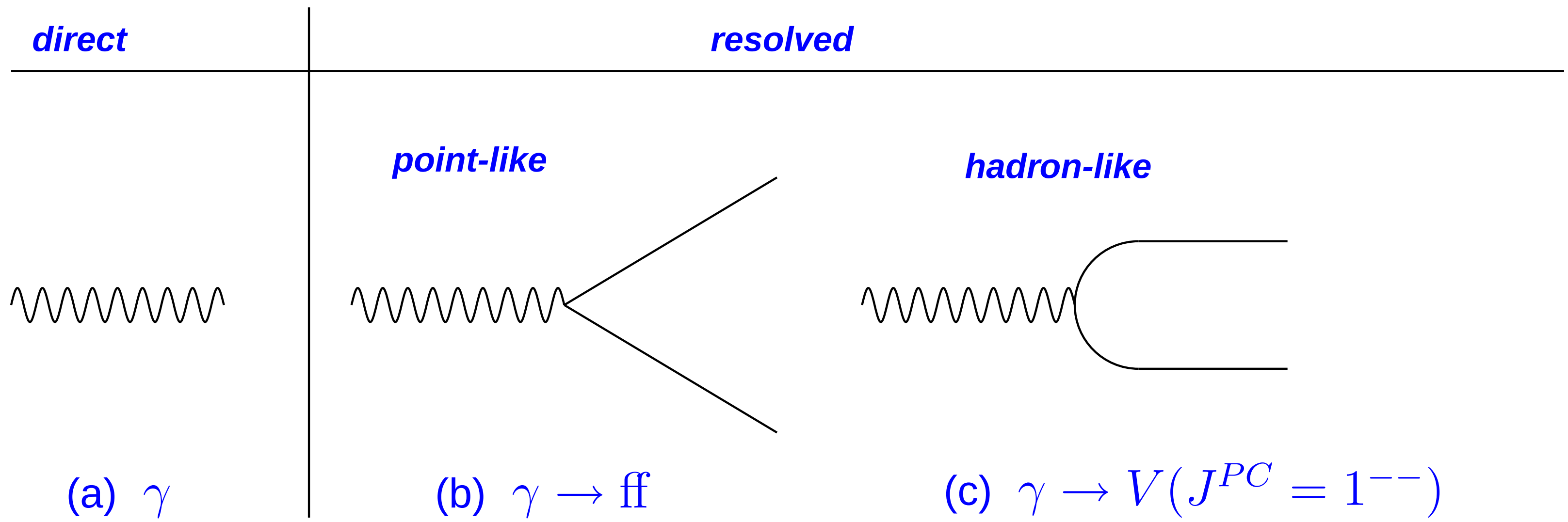

(a) γ (b) $\gamma \to \mathrm{f\bar{f}}$ (c) $\gamma \to V(J^{PC} = 1^{--})$

1) In (a) the whole photon interacts $\Rightarrow$ **NO structure.**

2) The fluctuations (b,c) exist due to the uncertainty principle $\Rightarrow$ **photon 'structure'.**

3) The typical lifetime of the fluctuations **increases** with the **photon energy** and **decreases** with the **photon virtuality.**

The reaction e e $\longrightarrow$ e e X

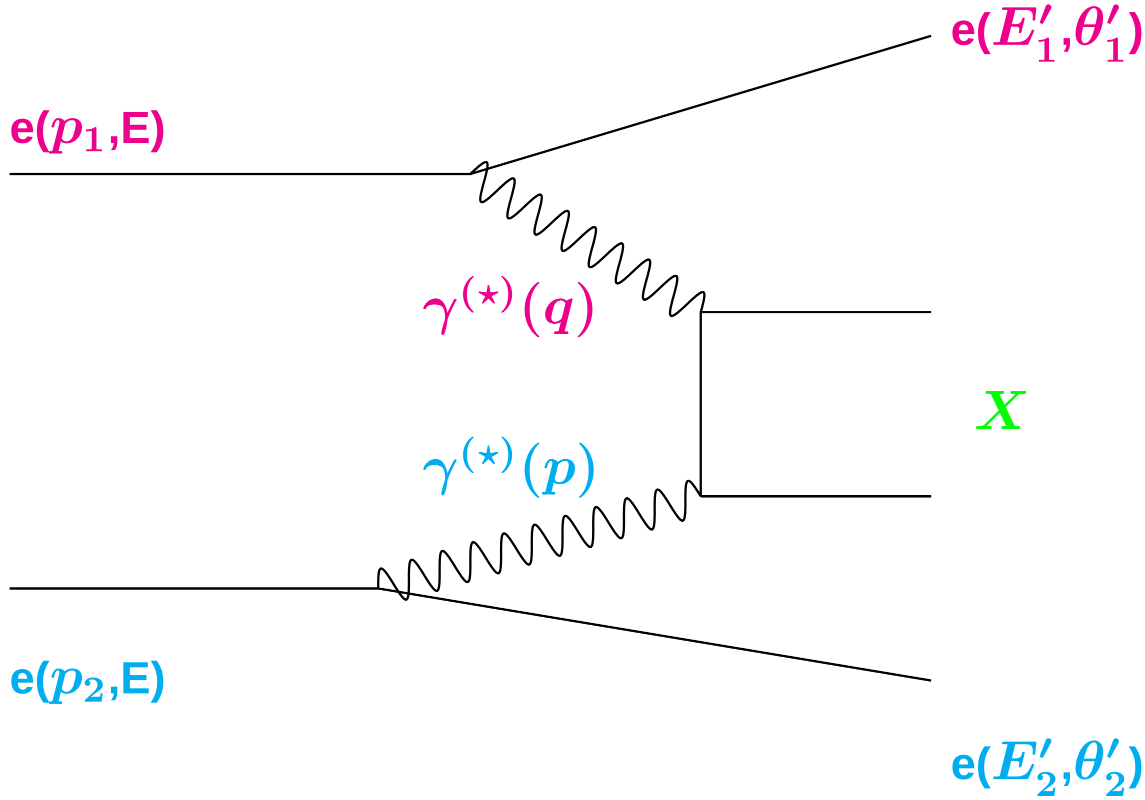

$$\mathrm{d}^6\sigma = \frac{\mathrm{d}^3 p_1' \mathrm{d}^3 p_2'}{E_1' E_2'} \frac{\alpha^2}{16\pi^4 Q^2 P^2} \left[\frac{(q\cdot p)^2 - Q^2 P^2}{(p_1 \cdot p_2)^2 - m_e^2 m_e^2} \right]^{1/2}$$
$$\Big(4\rho_1^{++}\rho_2^{++}\sigma_{\mathrm{TT}} + 2\rho_1^{++}\rho_2^{00}\sigma_{\mathrm{TL}}$$
$$+2\rho_1^{00}\rho_2^{++}\sigma_{\mathrm{LT}} + \rho_1^{00}\rho_2^{00}\sigma_{\mathrm{LL}} +$$
$$2|\rho_1^{+-}\rho_2^{+-}|\tau_{\mathrm{TT}}\cos 2\bar{\phi} - 8|\rho_1^{+0}\rho_2^{+0}|\tau_{\mathrm{TL}}\cos\bar{\phi} \Big)$$

$$Q^2 = -q^2 = 2\,E\,E_1'\,(1-\cos\theta_1')$$

$$P^2 = -p^2 = 2\,E\,E_2'\,(1-\cos\theta_2')$$

$$x = \frac{Q^2}{Q^2 + W^2 + P^2}$$

The LEP Accelerator

The integrated luminosities

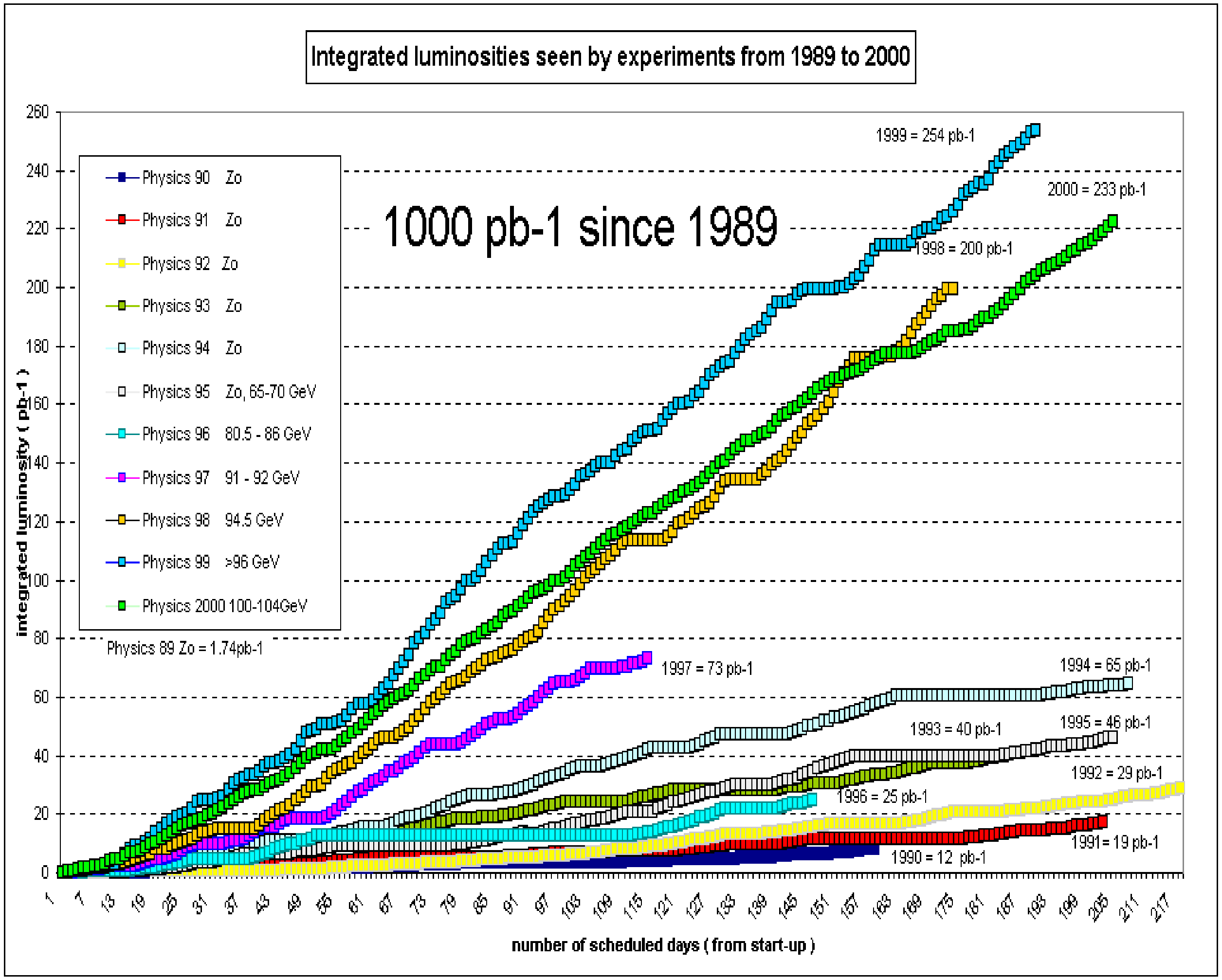

The integrated luminosity of the LEP programme exceeds 1000 pb^{-1}.

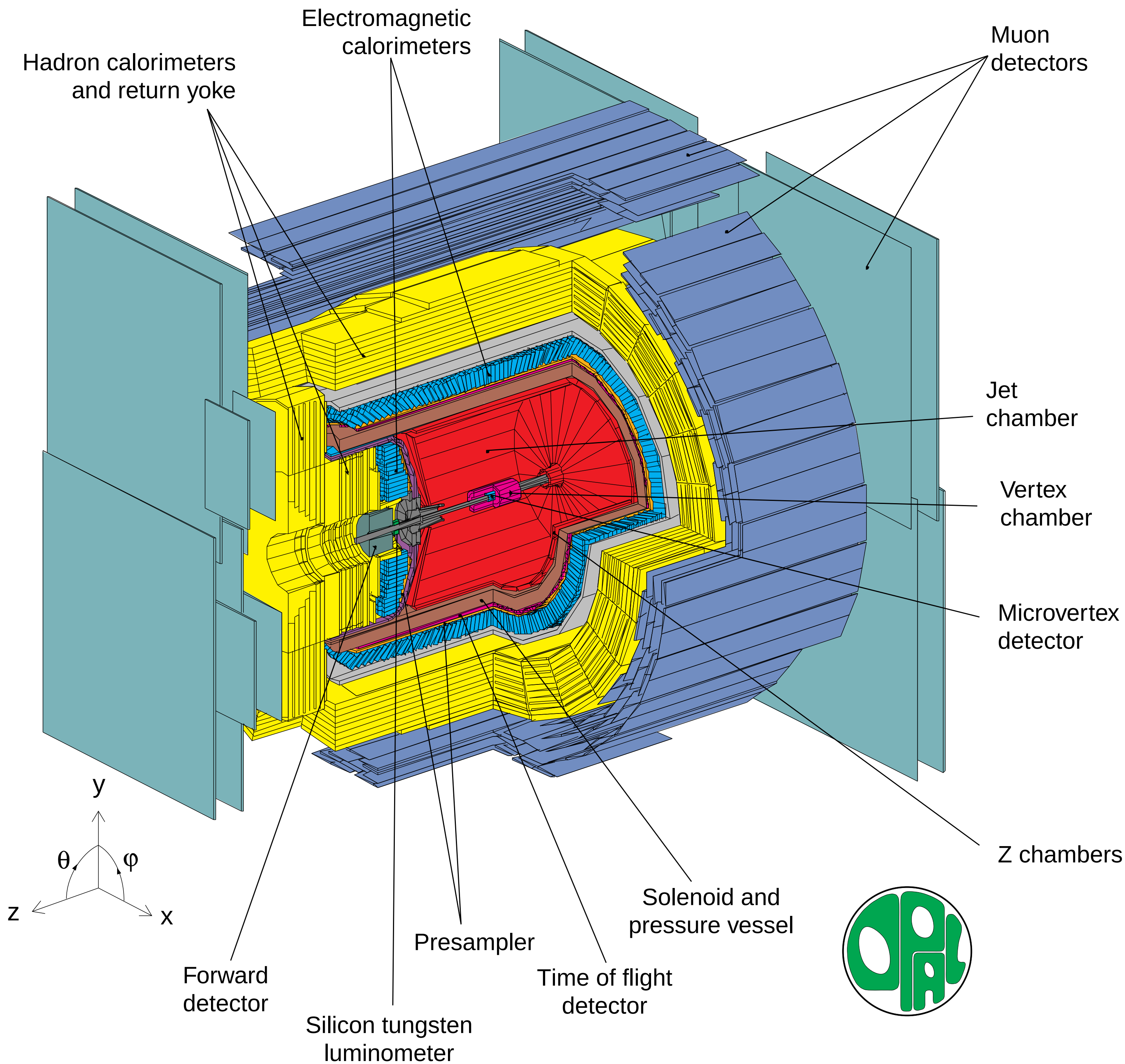

Hadron calorimeters and return yoke
Electromagnetic calorimeters
Muon detectors
Jet chamber
Vertex chamber
Microvertex detector
Z chambers
Solenoid and pressure vessel
Time of flight detector
Presampler
Silicon tungsten luminometer
Forward detector
y
z
x
θ
φ

Layout of a future Linear Collider

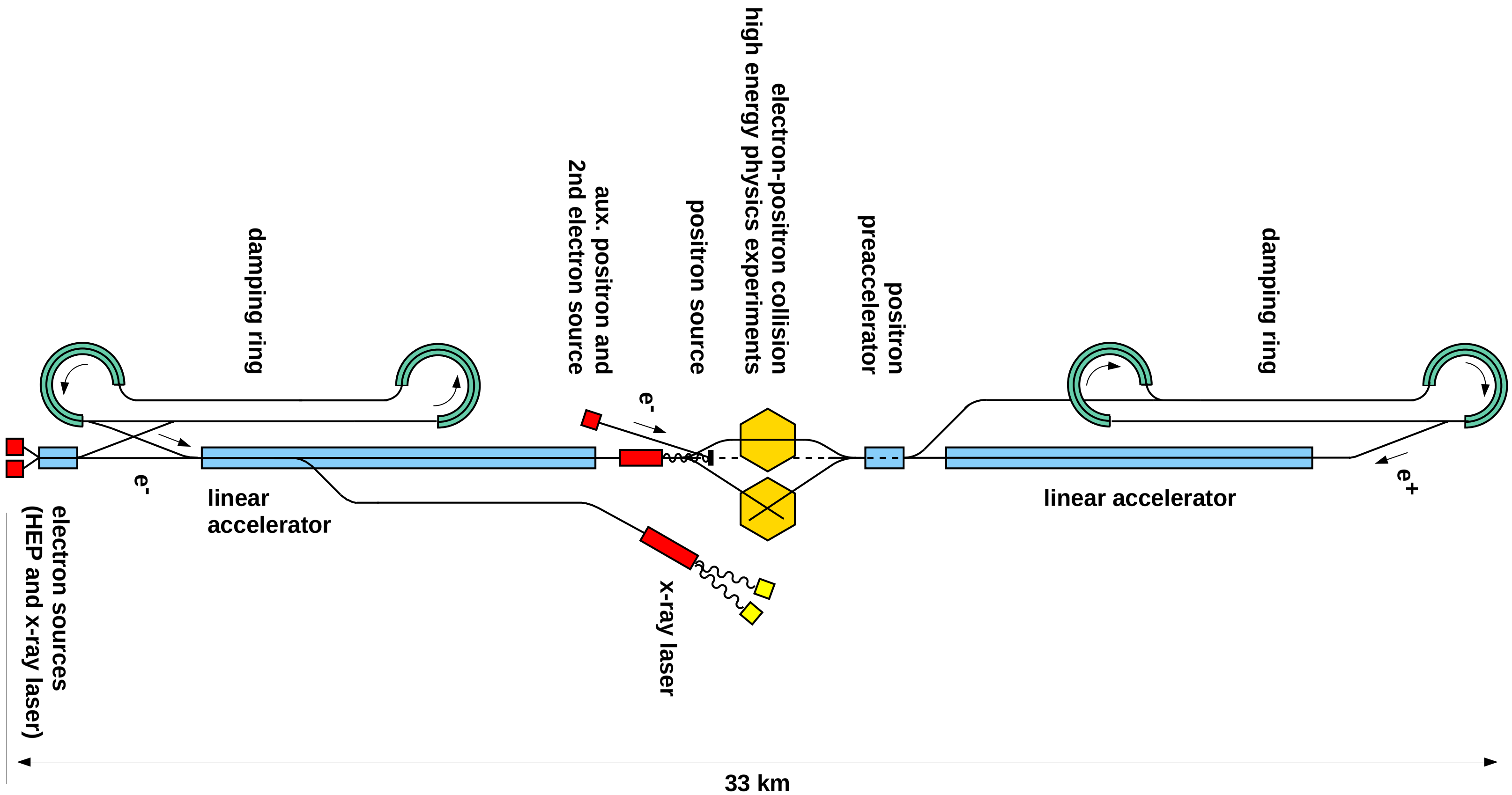

TESLA

From LEP/ SLC to TESLA

LEP

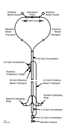

← SLC

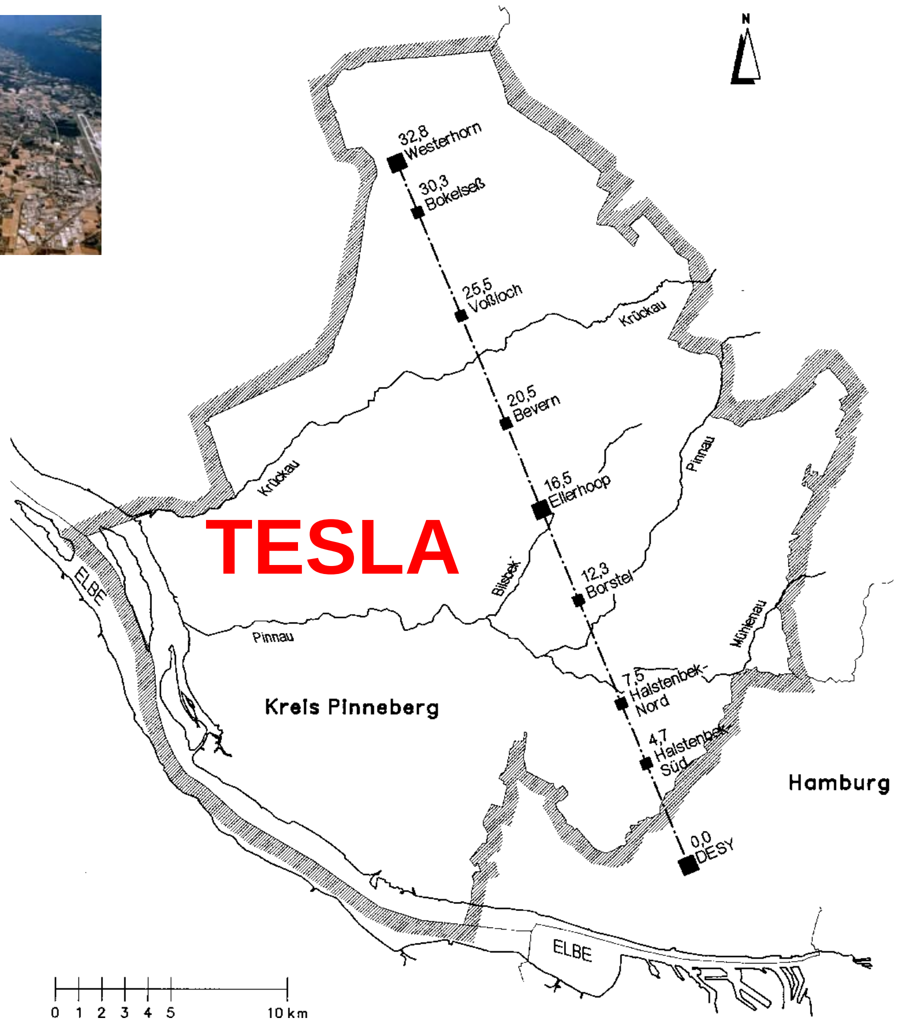

		LEP	SLC	TESLA
radius	[km]	8.5	∞	∞
length	[km]	26.7	4	33
gradient	[MV/m]	6	10	23.4
σ_x/σ_y	[μm/μm]	110 / 5	1.4 / 0.5	0.553/0.005
energy	[GeV]	100	50	250
lumi.	[10^{31}/cm^{2}s]	7.4	0.1	3400
$\mathcal{L}_{\rm int}$	[1/pb y]	250	15	10-100k

The expected cross-sections

assume: $\mathcal{L}_{\rm int} = 100$ fb$^{-1}/y$ $\Rightarrow$ Events/y

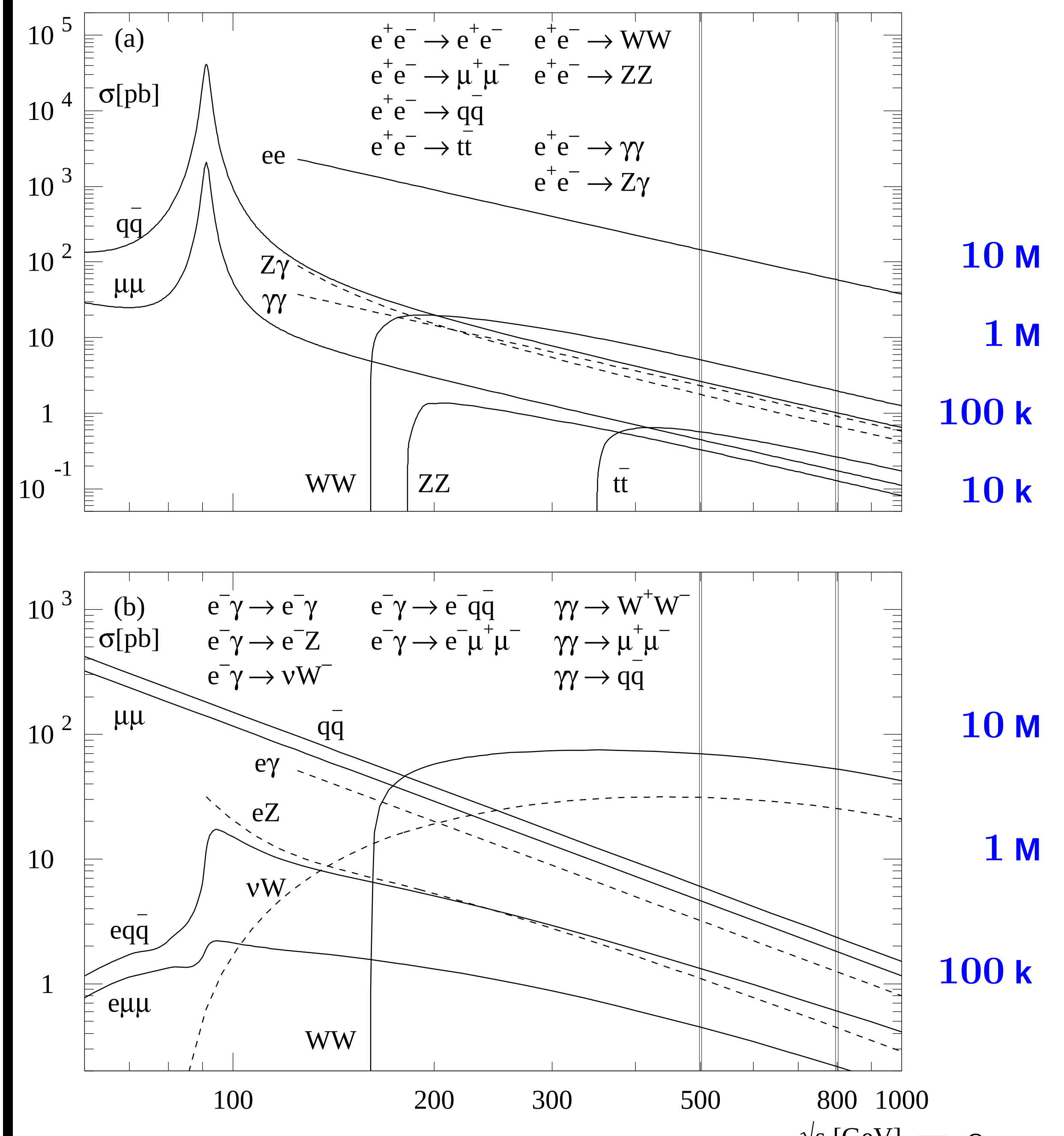

$= s_{\rm ee,e\gamma,\gamma\gamma}$

$10 < \theta_{\rm i} < 170$ deg, $M_{\mu^+\mu^-,q\bar{q}} > 50$ GeV

Charged particle pair production

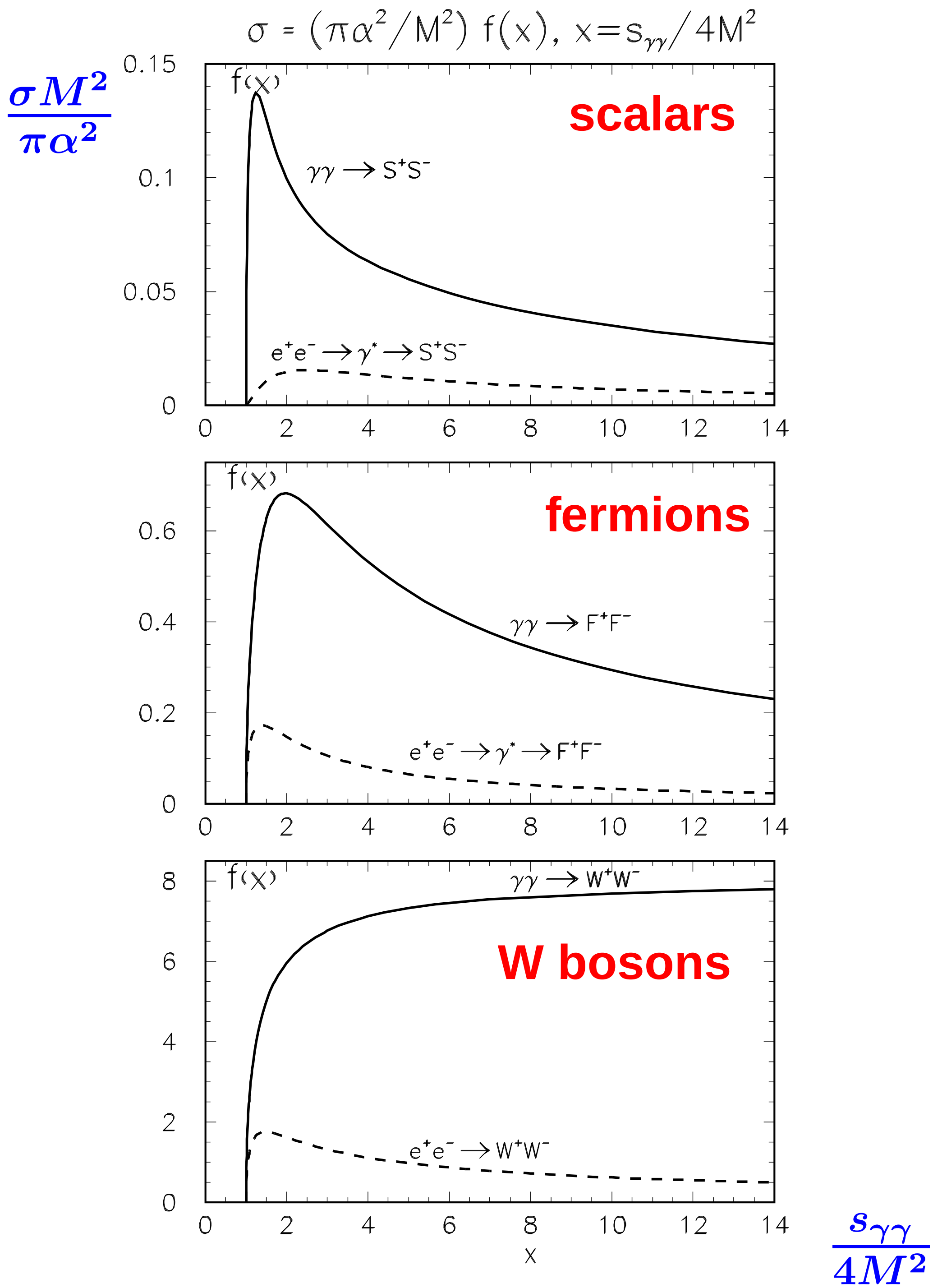

The photon collider has larger cross sections than the e^+e^- collider for several final states.

The creation of the photon beam

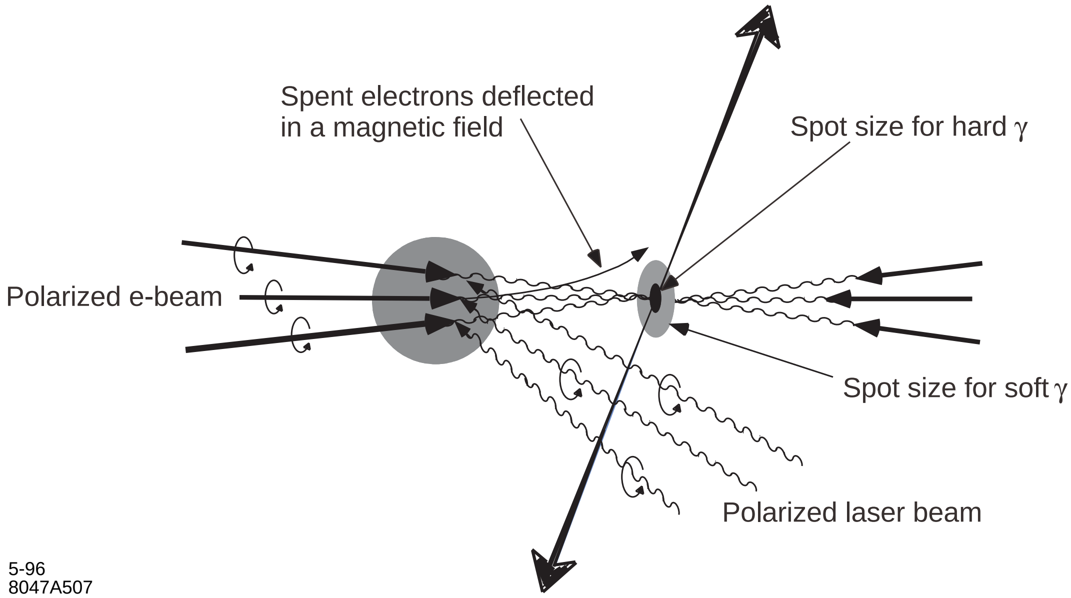

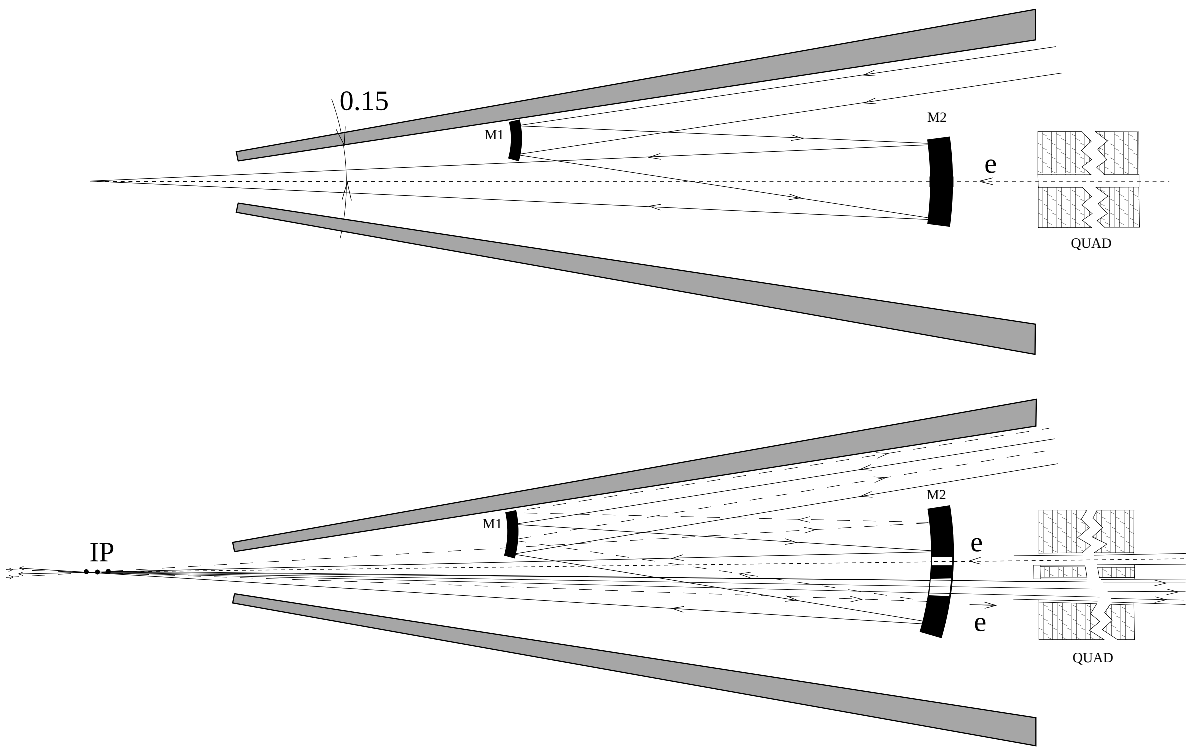

Some features of a Photon Collider

helicities

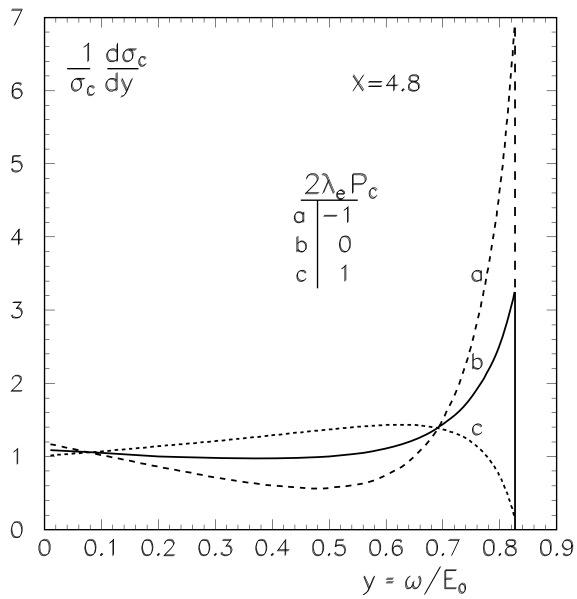

non-linear effects

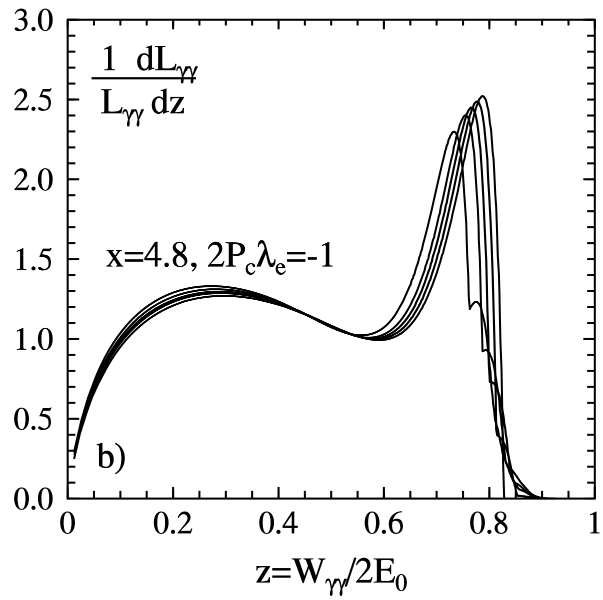

Photon energy spectra

TESLA(500)

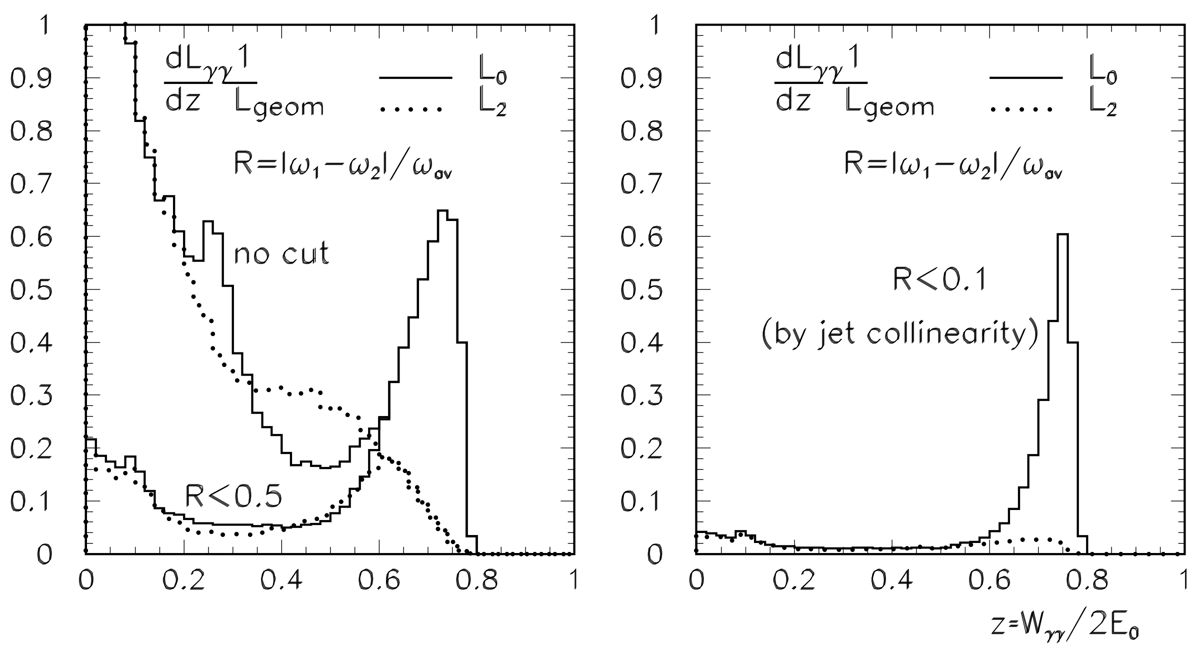

Luminosity spectra

From LEP to TESLA

the detector

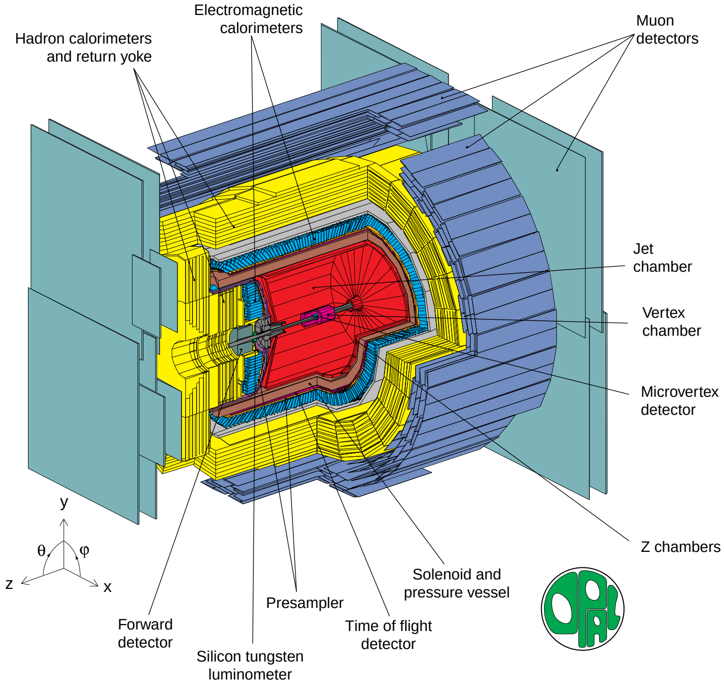

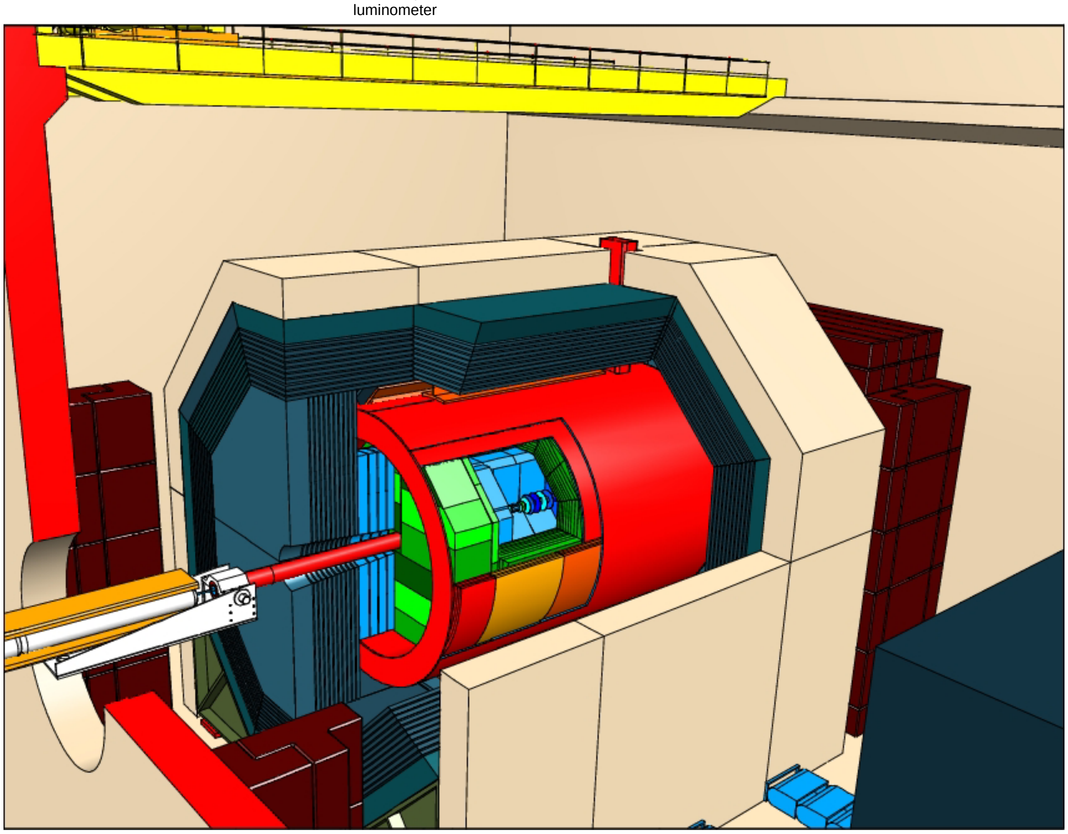

The general detector concept

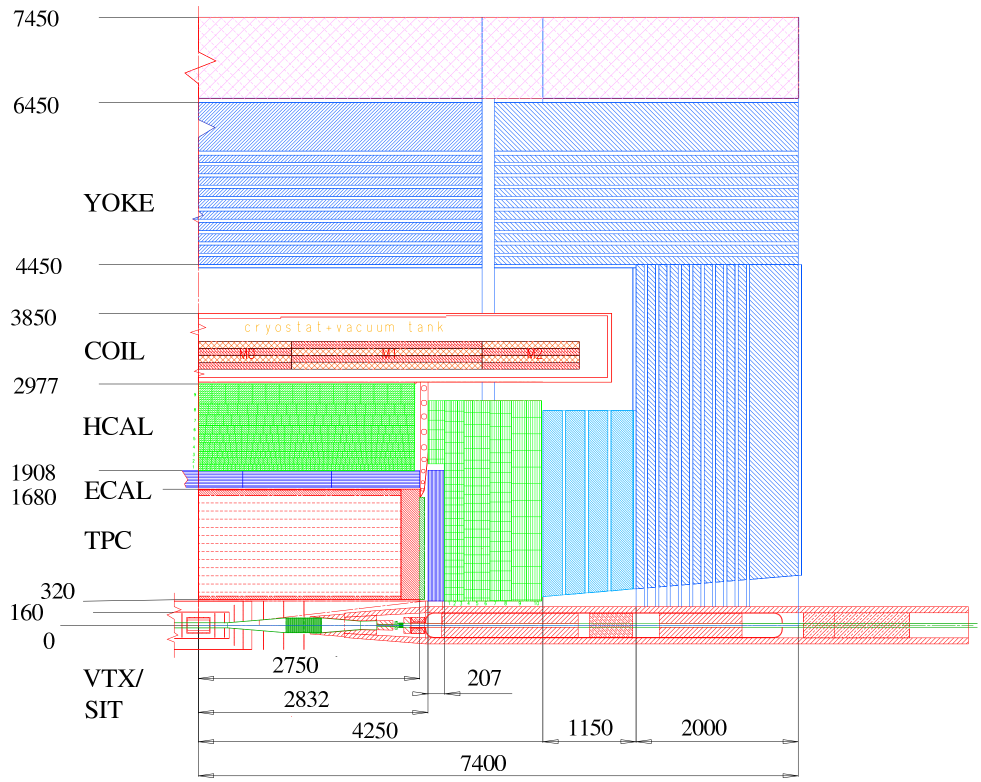

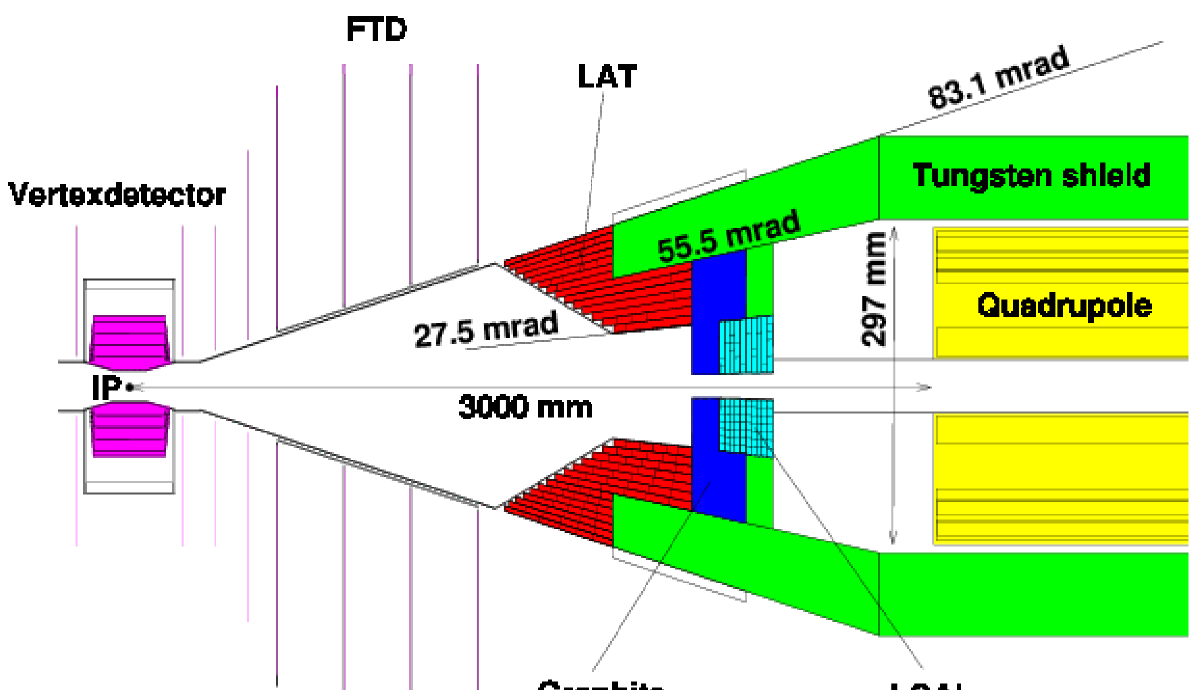

Some features of the background

$\gamma\gamma \rightarrow$ hadrons

Particle flow **Energy flow**

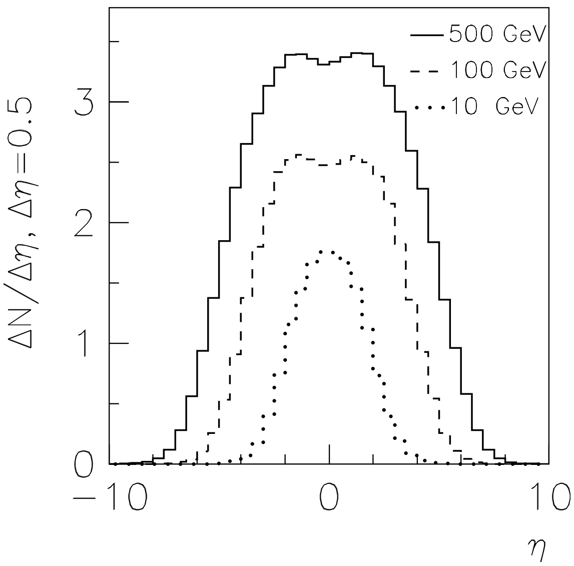

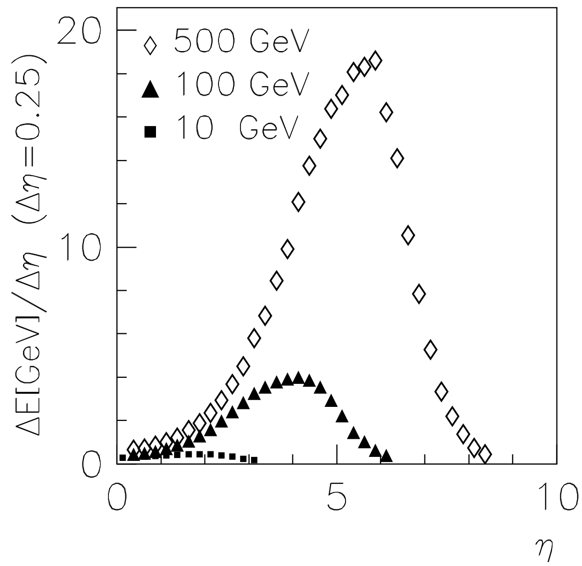

On average this yields 3.7 hadronic events per BX.

For $W_{\gamma\gamma} = 500\,\mathrm{GeV}$ one expects on average 25 particles within $-2 \leq \eta \leq 2$ and with $E_{\mathrm{tot}} \approx 15\,\mathrm{GeV}$.

Incoherent e^+e^- pair creation:

10^5 e^+e^- pairs per BX with $E_{\mathrm{tot}} = 1.5 \cdot 10^5\,\mathrm{GeV}$, and within the detector $E = 2 \cdot 10^4\,\mathrm{GeV}$ for $\theta_e > 10$ mrad and $p_e < 1\,\mathrm{GeV}$

The background from 10 e^+e^- pairs

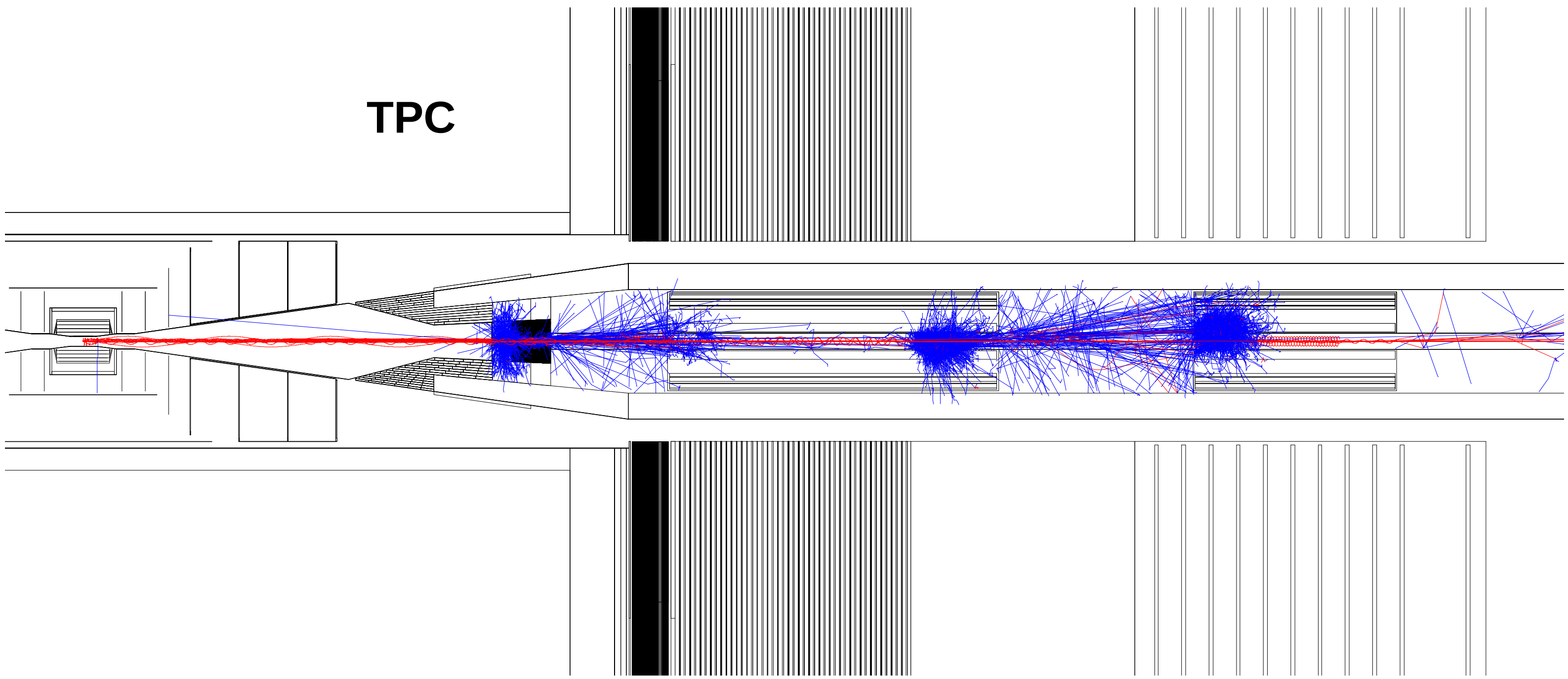

A very unfriendly environment for the Low Angle Tagger (LAT) and especially for the Luminosity Calorimeter (LCAL)

Photon — photon scattering

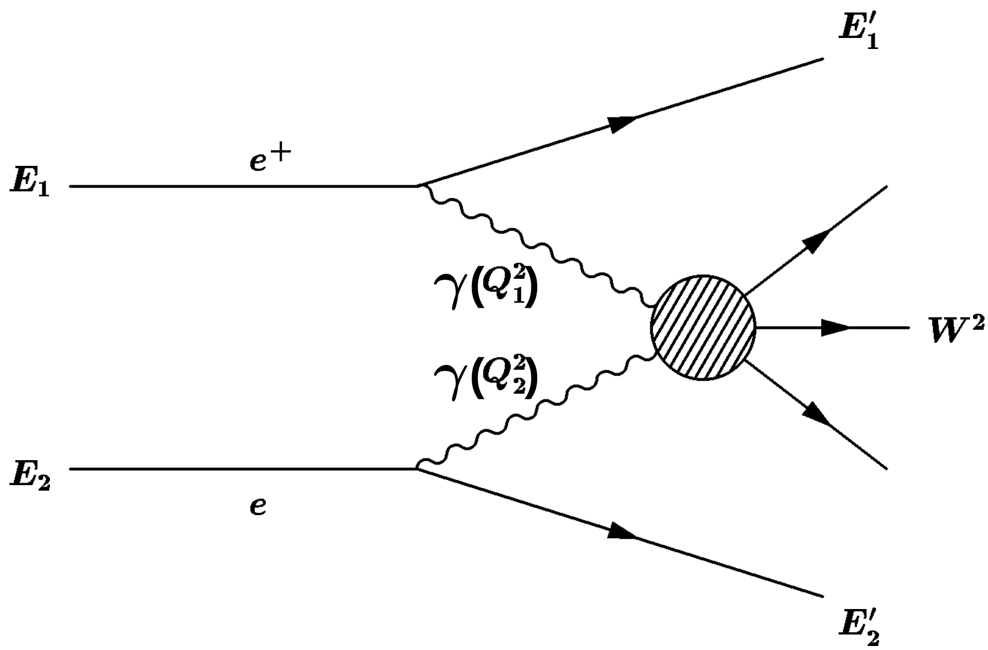

Interaction of two quasi-real photons

$$\gamma\gamma \longrightarrow X$$

e.g. $X(s_{\gamma\gamma}) = \ell^+\ell^-, \mathrm{q\bar{q}}, \mathrm{Q\bar{Q}}, \mathrm{z^0z^0}, \mathrm{W^+W^-}, H$

$$Q_i^2 = 2E_iE_i'(1-\cos\theta_i) \approx 0$$

$$W^2 = s_{\gamma\gamma} = \left(\sum_h E_h\right)^2 - \left(\sum_h \vec{p}_h\right)^2$$

Leading order diagrams

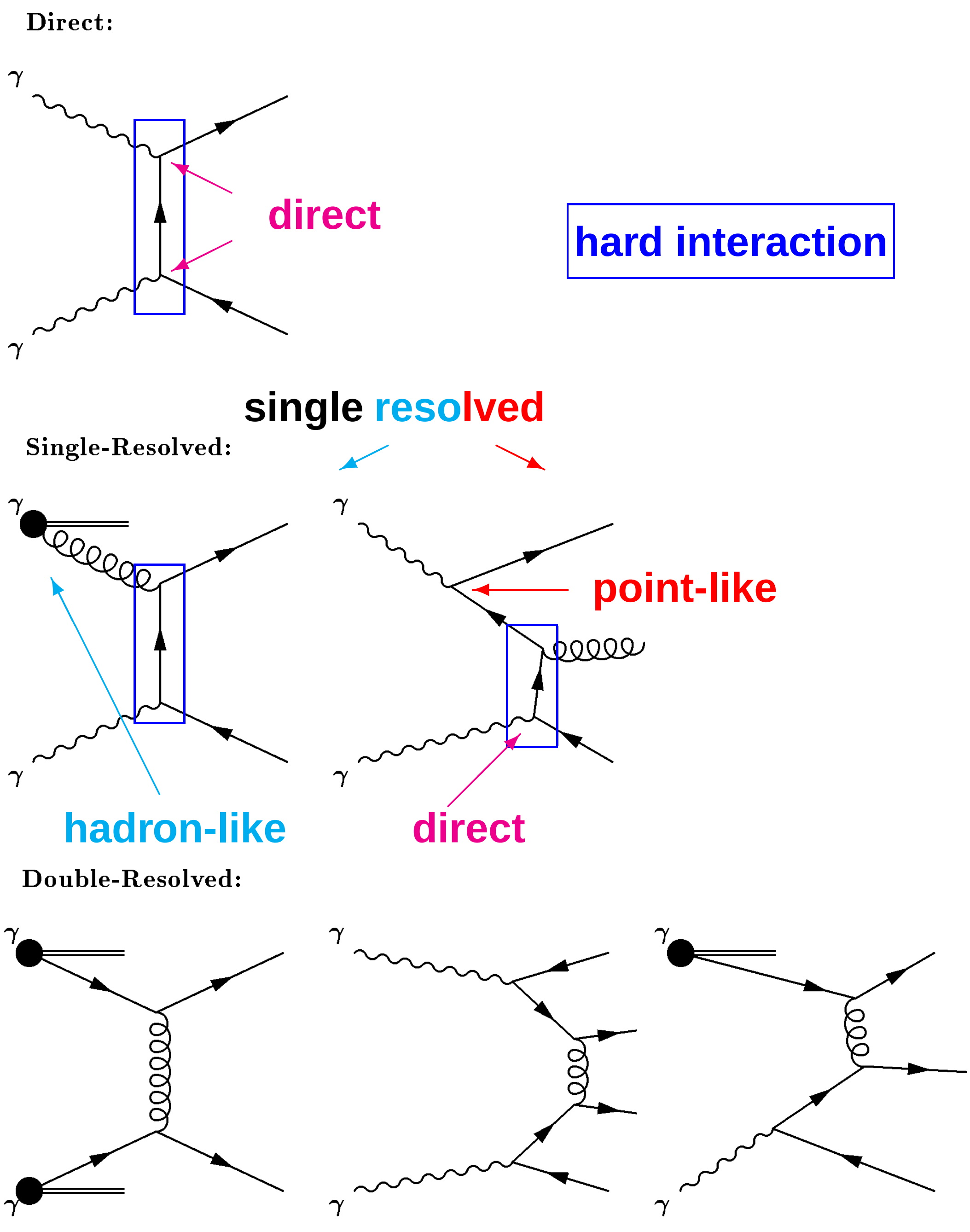

W distributions for anti-tagged events

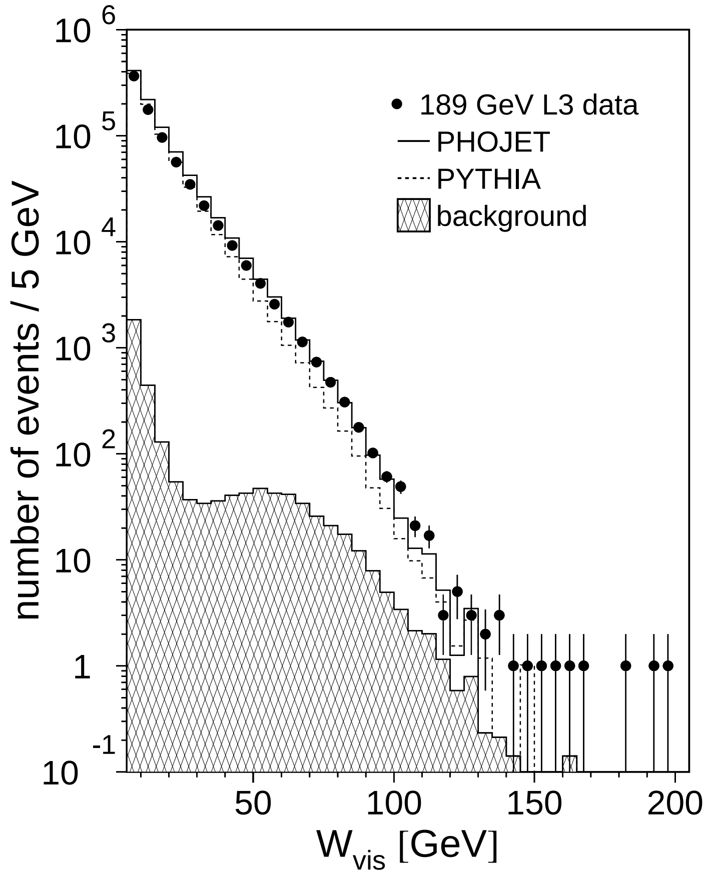

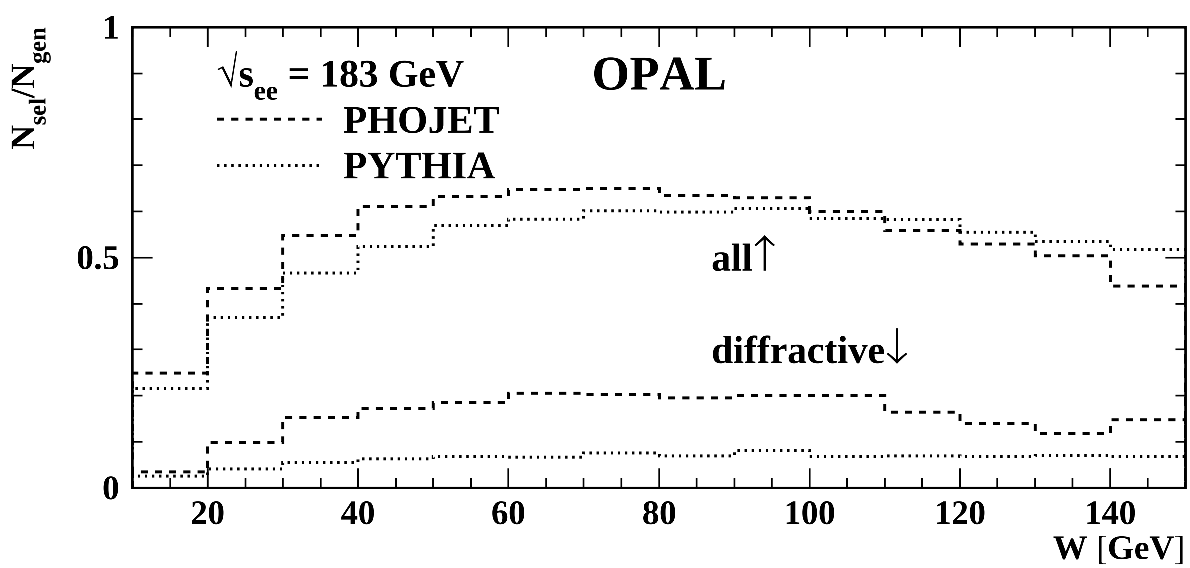

The acceptance for diffractive events is very different for the PHOJET and PYTHIA models.

The total hadronic cross-section $\sigma_{\gamma\gamma}$ from PDG(00)

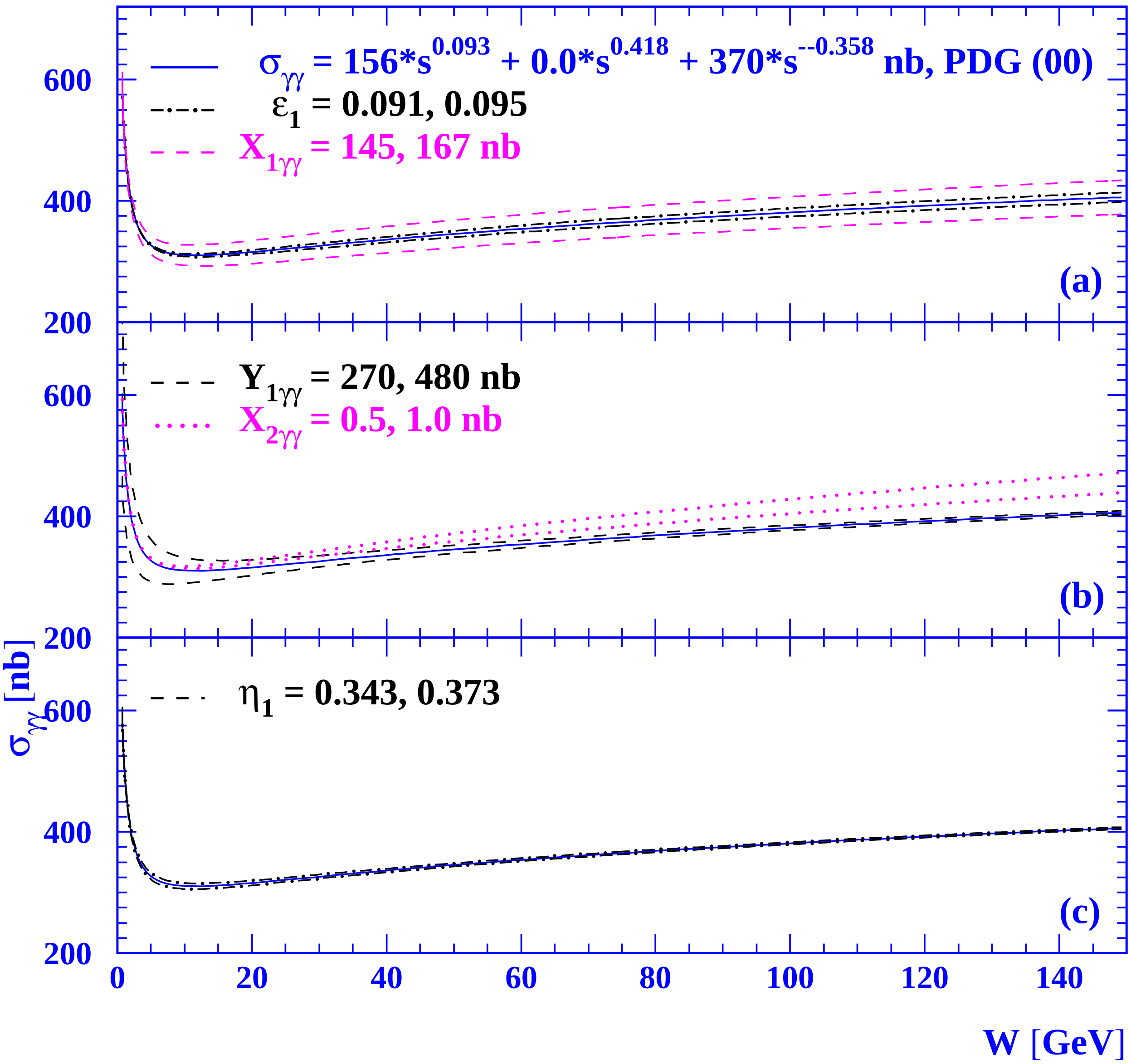

The parameters are strongly correlated.

The total hadronic cross-section $\sigma_{\gamma\gamma}$

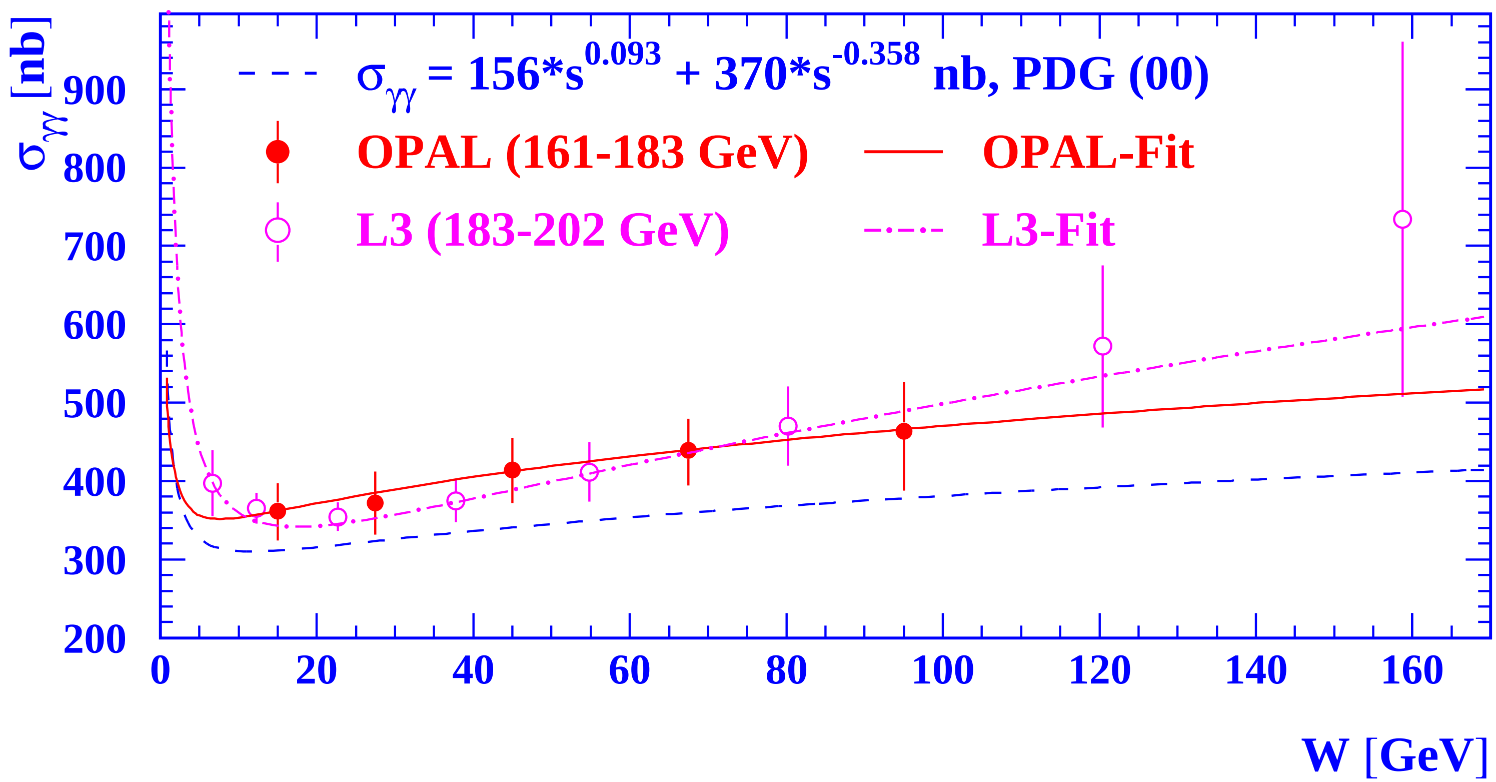

A clear rise of the total cross-section is observed in the data.

Predictions for the cross-section $\sigma_{\gamma\gamma}$

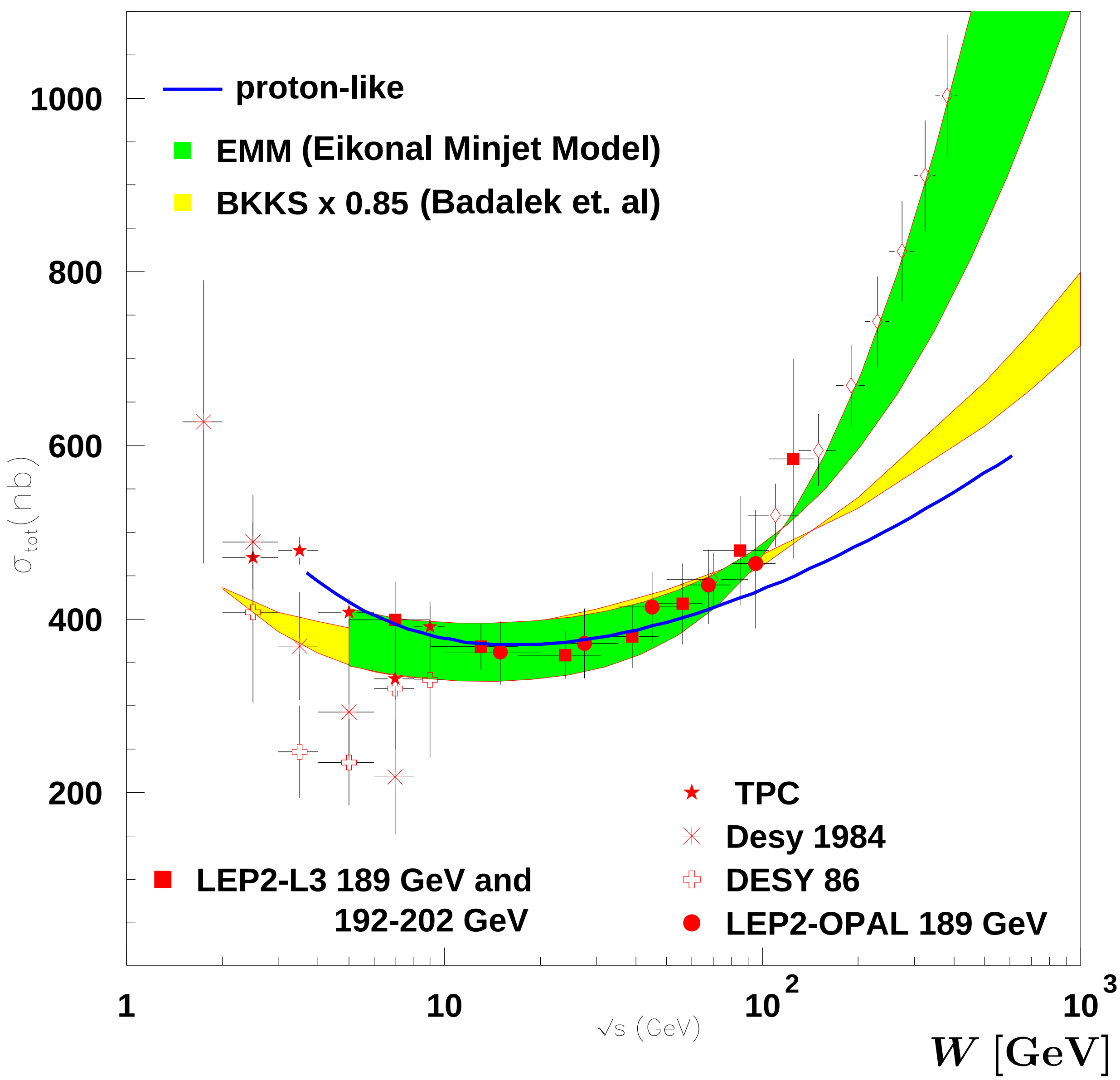

To achieve a 5-10% precision on W a Photon Collider is needed to avoid the reconstruction of W from the hadronic final state.

The rise of the charm cross-section as a function of W

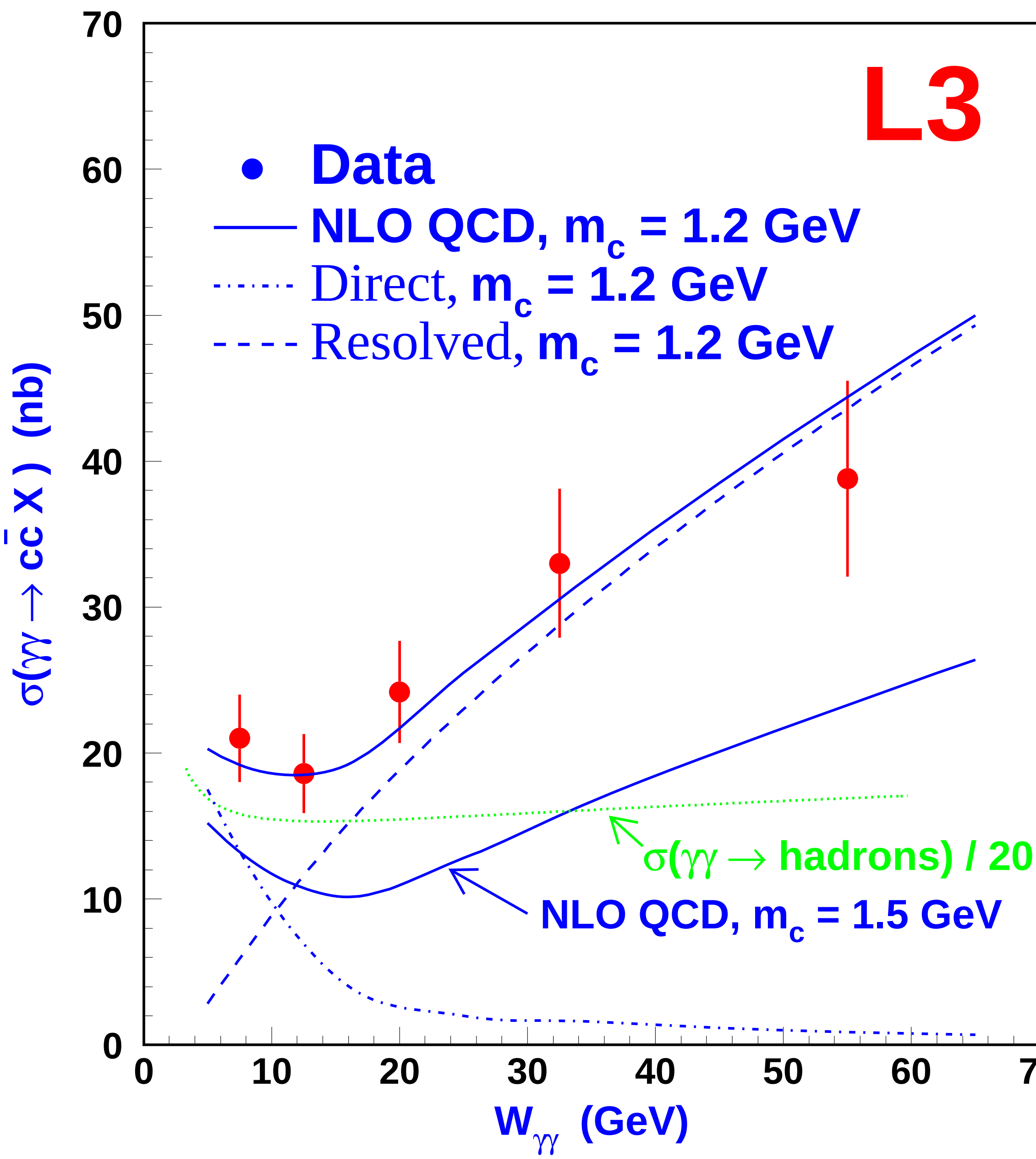

The charm cross-section rises faster than the total hadronic cross-section.

The inclusive jet cross-sections

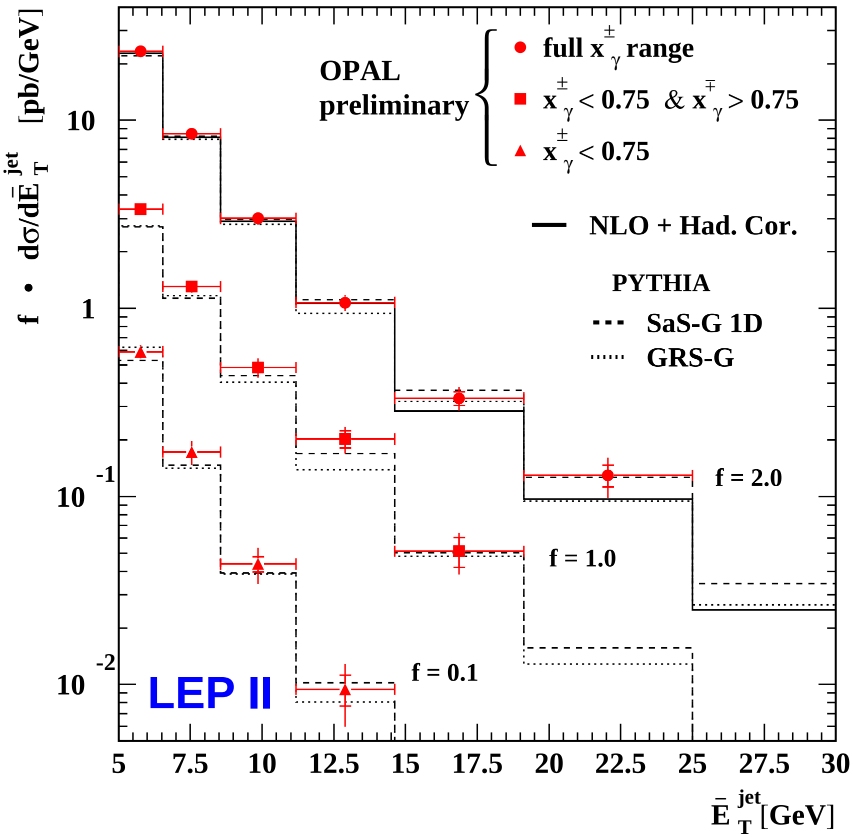

$$x_\gamma^\pm = \frac{\sum_{\text{jets}}(E \pm p_z)}{\sum_{\text{had}}(E \pm p_z)}$$

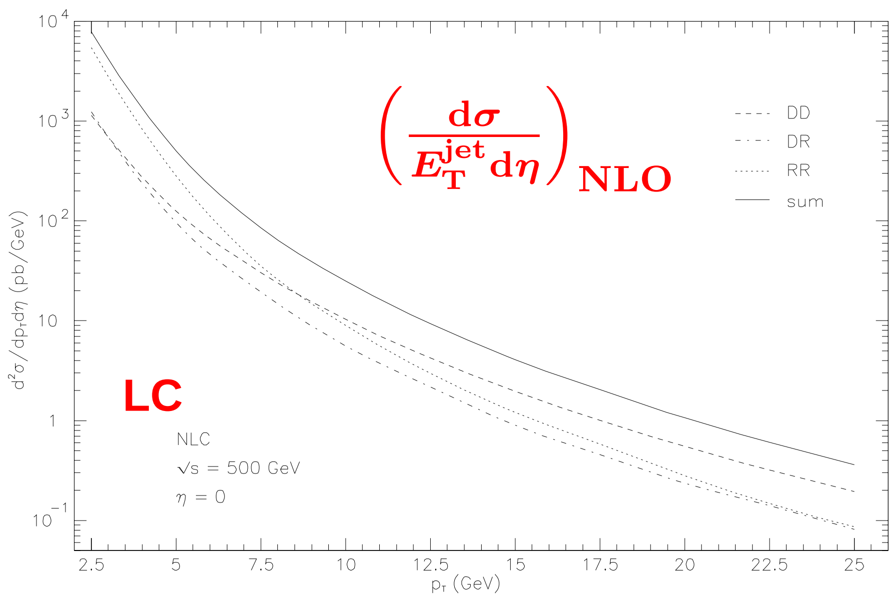

The measurement will be extended to larger E_T^{jet}

The sensitivity to parton densities

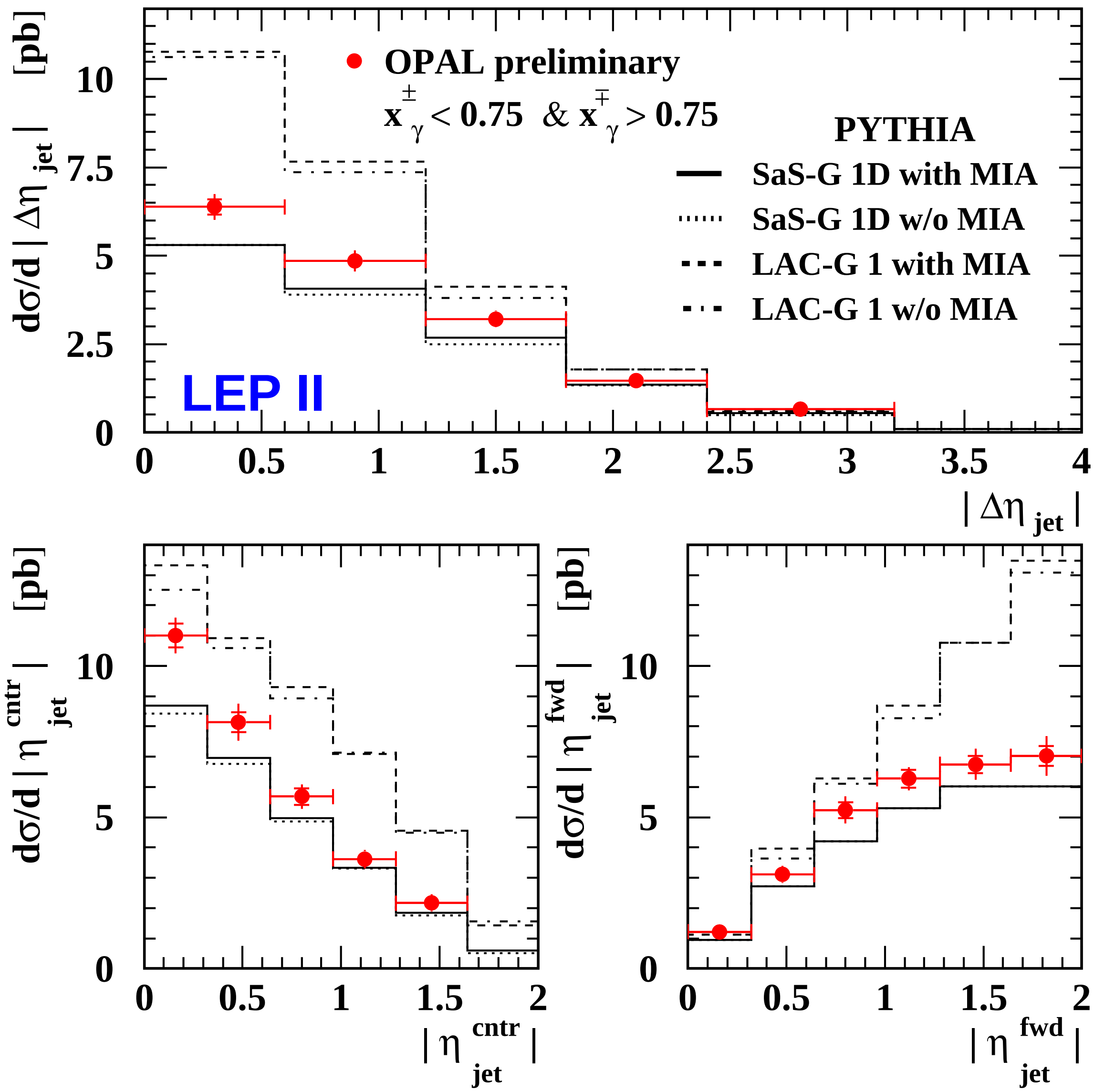

1) The gluon density $f_{g/\gamma}$ in the photon can be constrained.

2) The simulation of hadronic final states must be improved.

Inclusive charm production

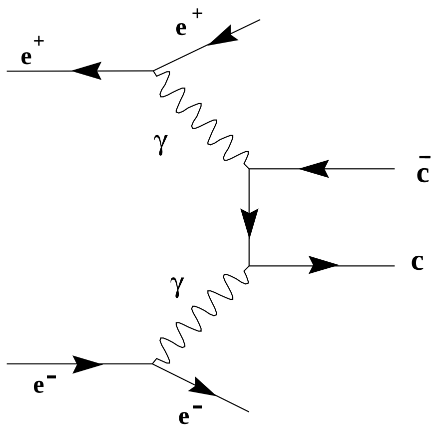

Direct

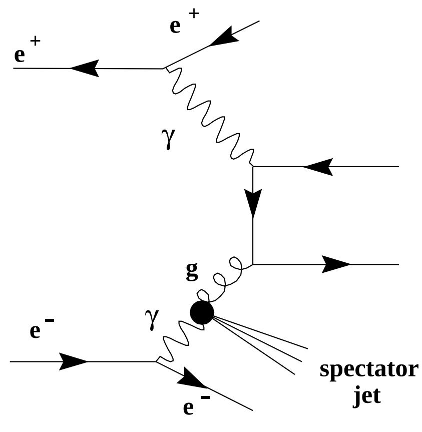

Single Resolved

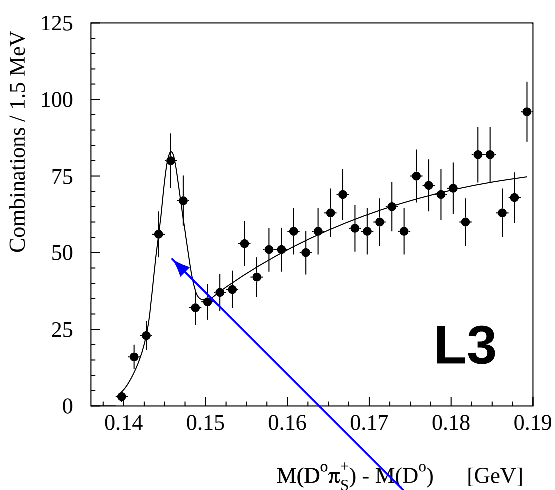

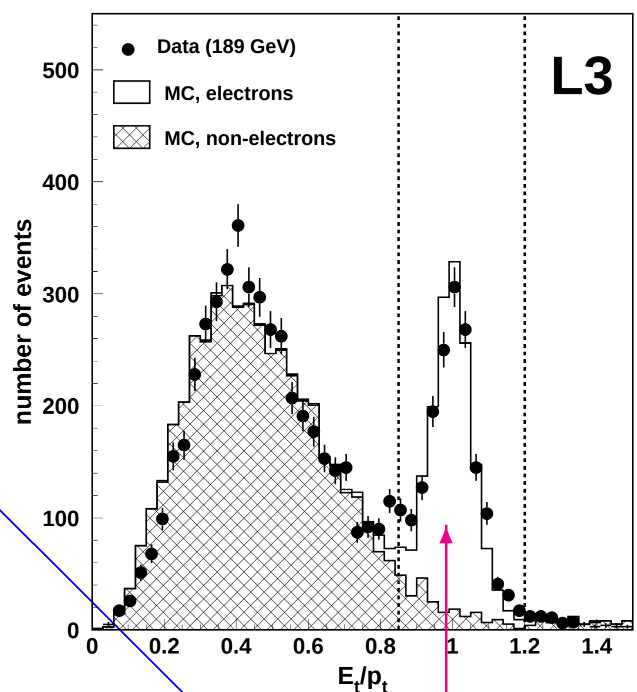

$$\mathrm{D}^\star \longrightarrow \mathrm{D}^0\,\pi$$

$$\mathrm{D}^0 \longrightarrow K\pi, K\pi^0, K\pi\pi\pi$$

Clean charm tags can be obtained using leptons from the semileptonic decays or $D^\star$ mesons.

Differential D* cross-section

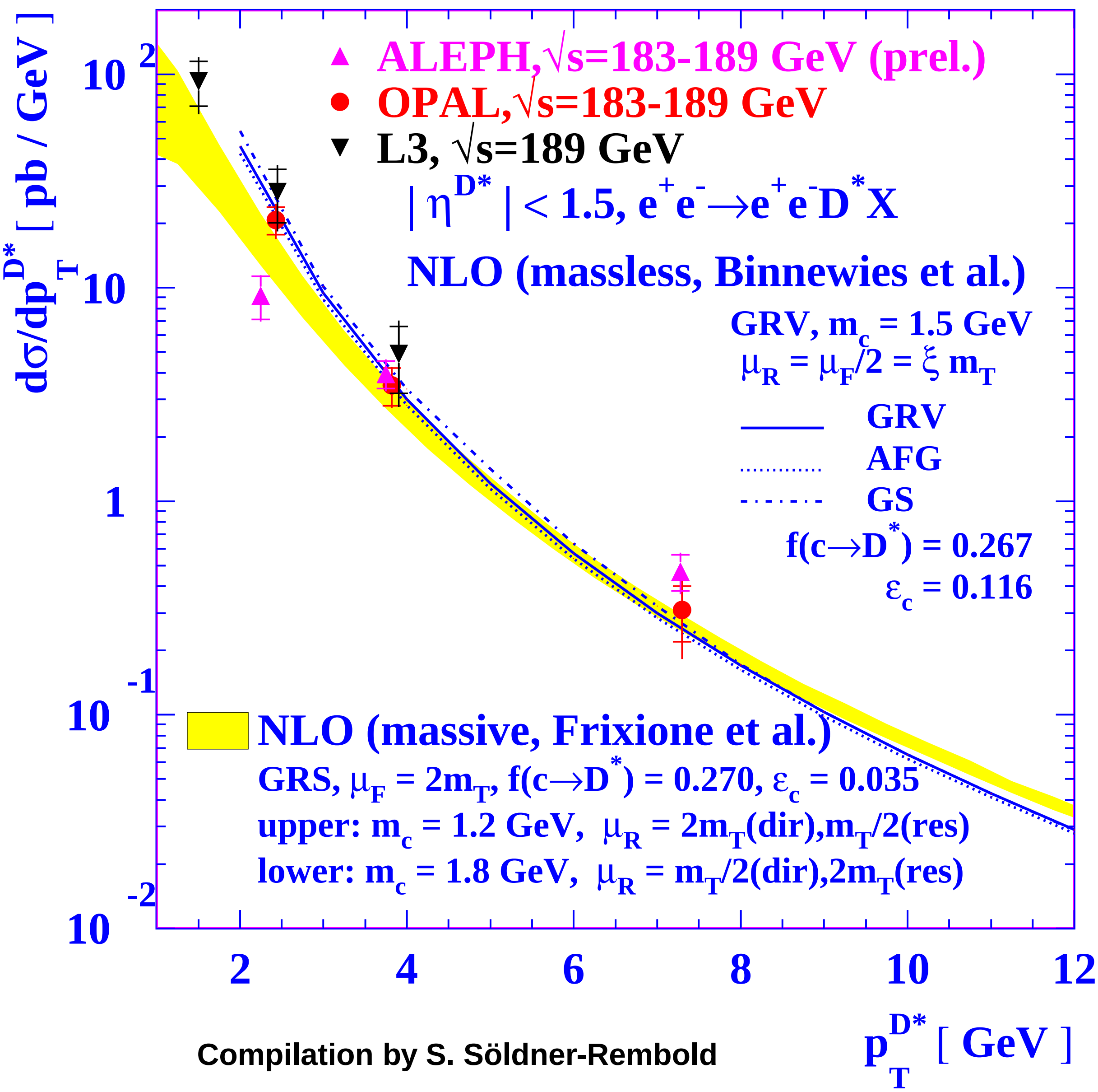

For $p_{\mathrm{T}}^{D^\star} \geq 3\,\mathrm{GeV}$ the data agree well and they are satisfactorily described by he NLO QCD calculations.

The heavy quark cross-sections

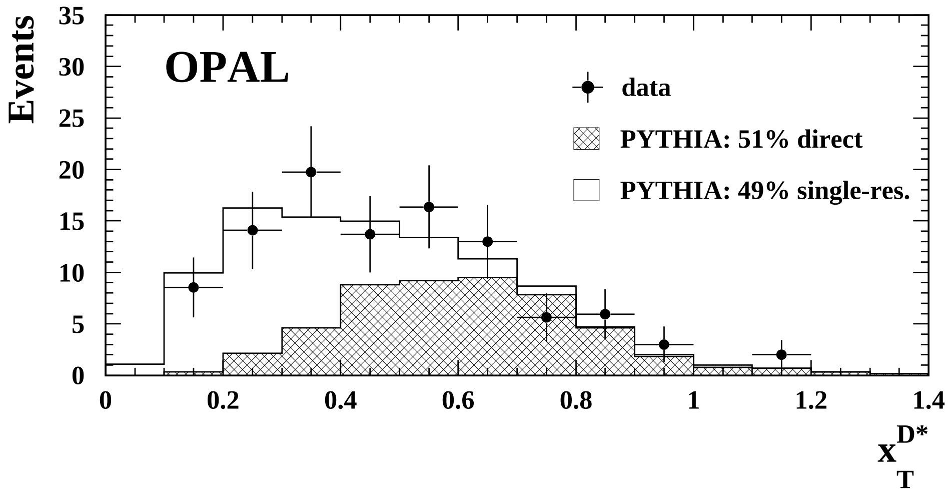

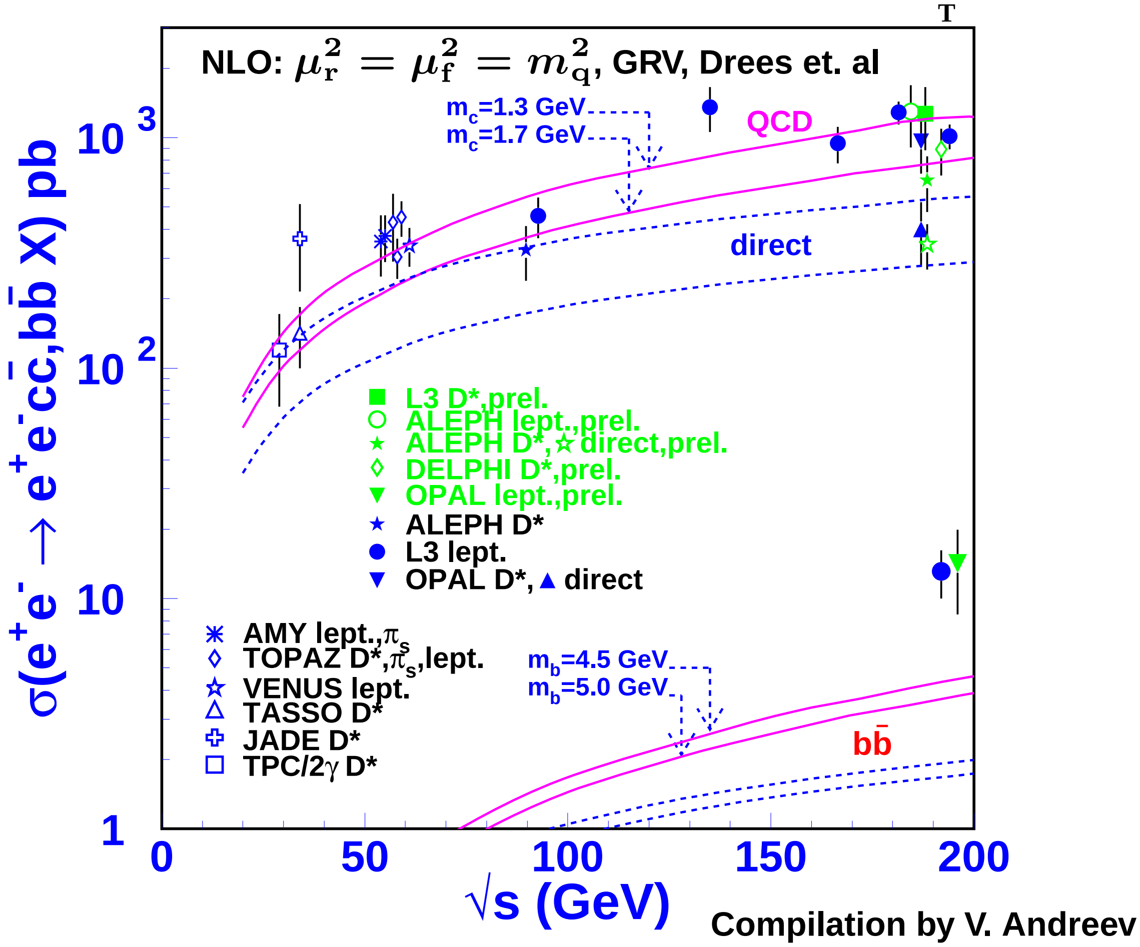

The direct production of charm quarks is insufficient.

Charm cross-section in $\gamma\gamma$

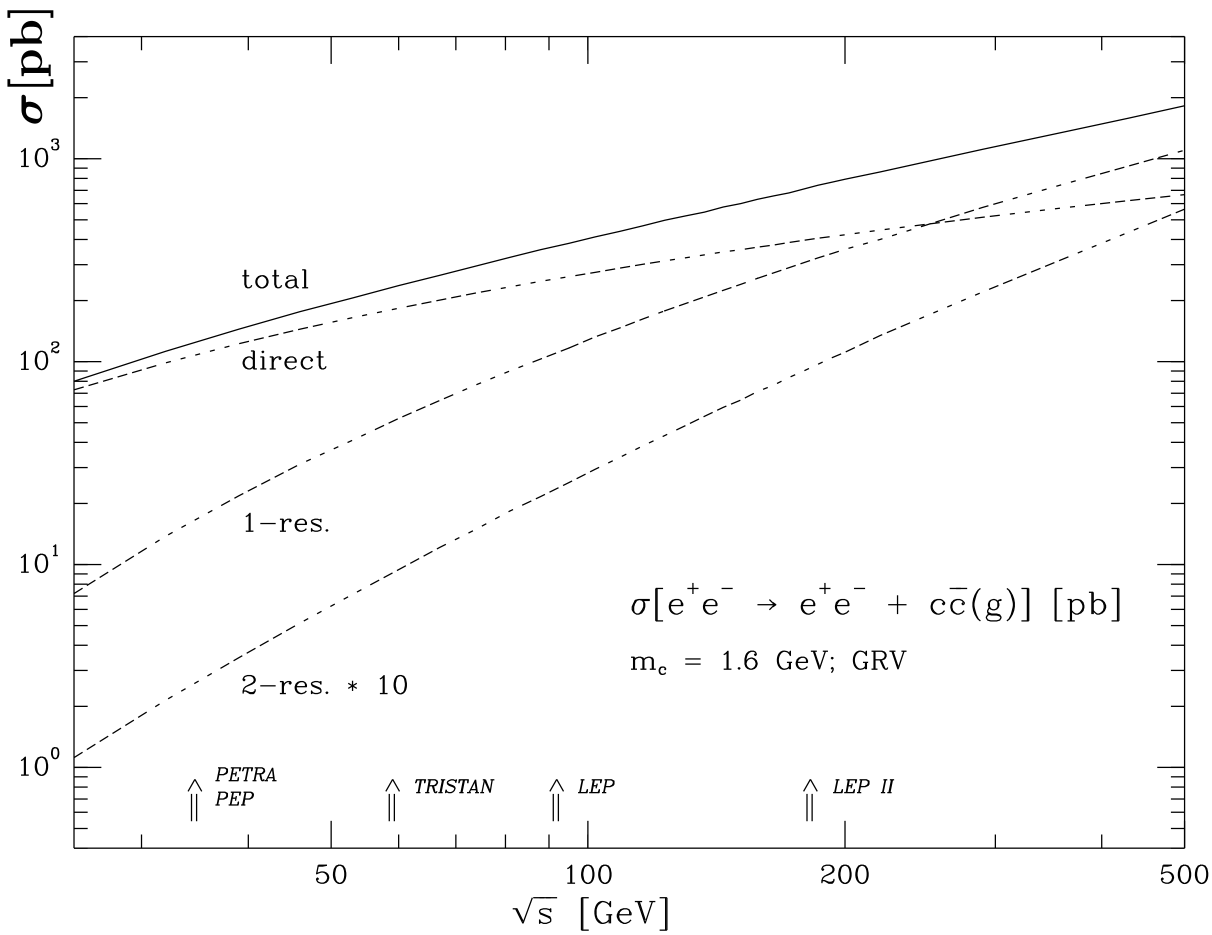

1. The calculation for the direct, 1-res (NLO) and 2-res (LO) contributions are based on the EPA.
2. $\mu^2 = m_c^2/2, m_c = 1.6\,\mathrm{GeV}, W > 3.8\,\mathrm{GeV}.$
3. One expects about 10^7 $c\bar{c}$ events/year.
4. The direct process is a pure QCD prediction with $\sigma = f(m_c, \alpha_s)$.

Charm production in $\gamma\gamma$

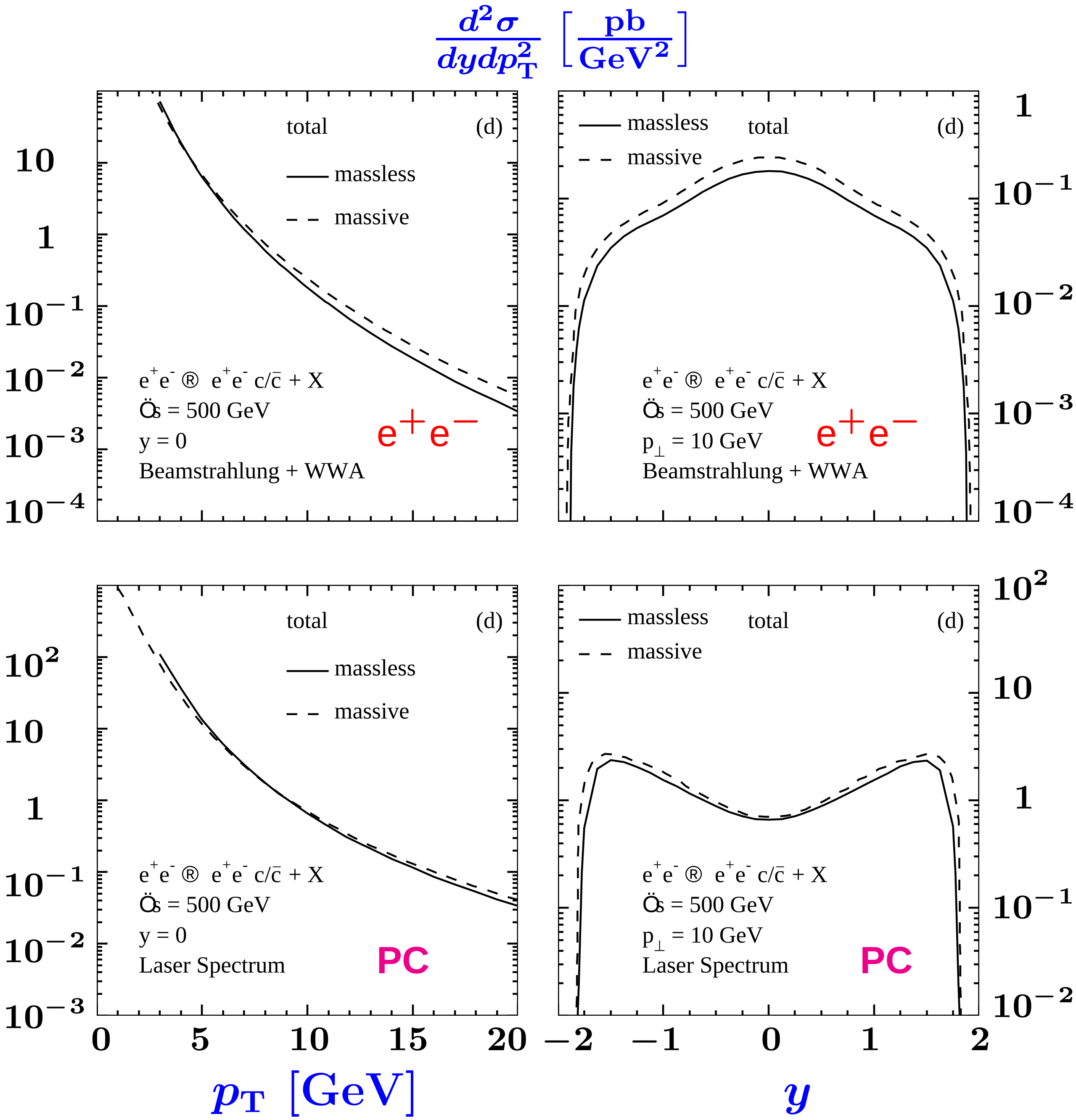

The NLO calculation uses the EPA integrated up to $\theta_{tag} = 175$ mrad and $m_c = 1.5$ GeV.

Search for bottom production

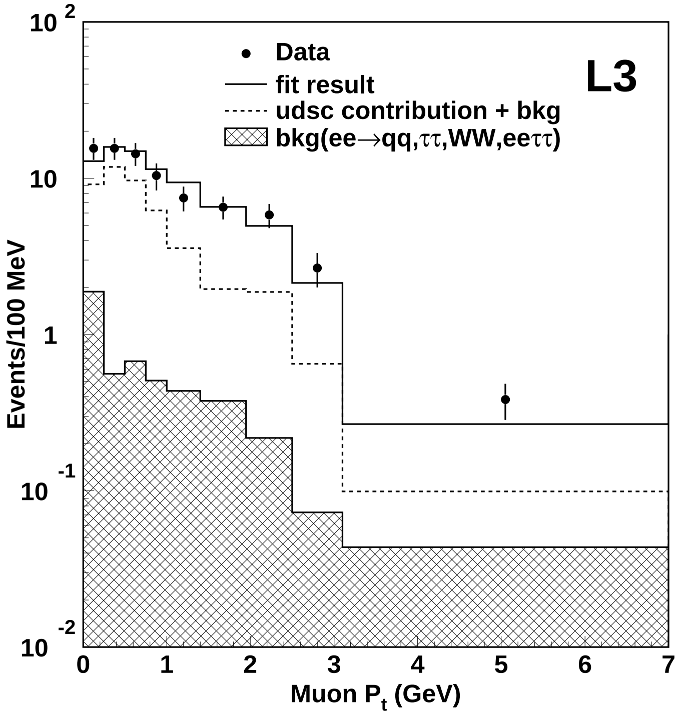

$p_\mu > 2.0$ GeV

$|\theta_\mu| < 0.8$

$N_{\mathrm{ev}} = 269$

$\epsilon_{\mathrm{b}} = 2.2\%$

$f_{\mathrm{b}} = 52 \pm 10\%$

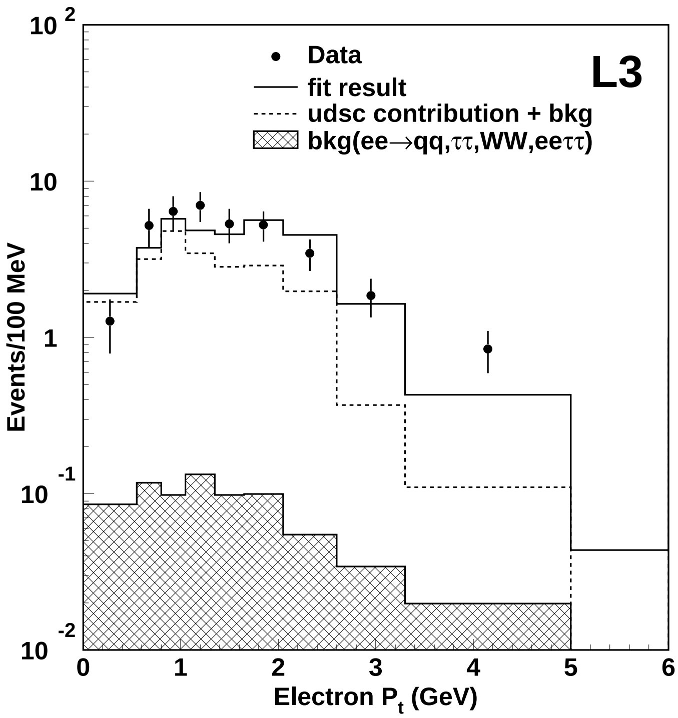

$p_{\mathrm{e}} > 2$ GeV,

$|\theta_{\mathrm{e}}| < 0.725$

$N_{\mathrm{ev}} = 137$

$\epsilon_{\mathrm{b}} = 1.25\%$

$f_{\mathrm{b}} = 42 \pm 11\%$

Look at p_{t} of the lepton with respect to the nearest jet to tag bottom production.

The LEP results on bottom production

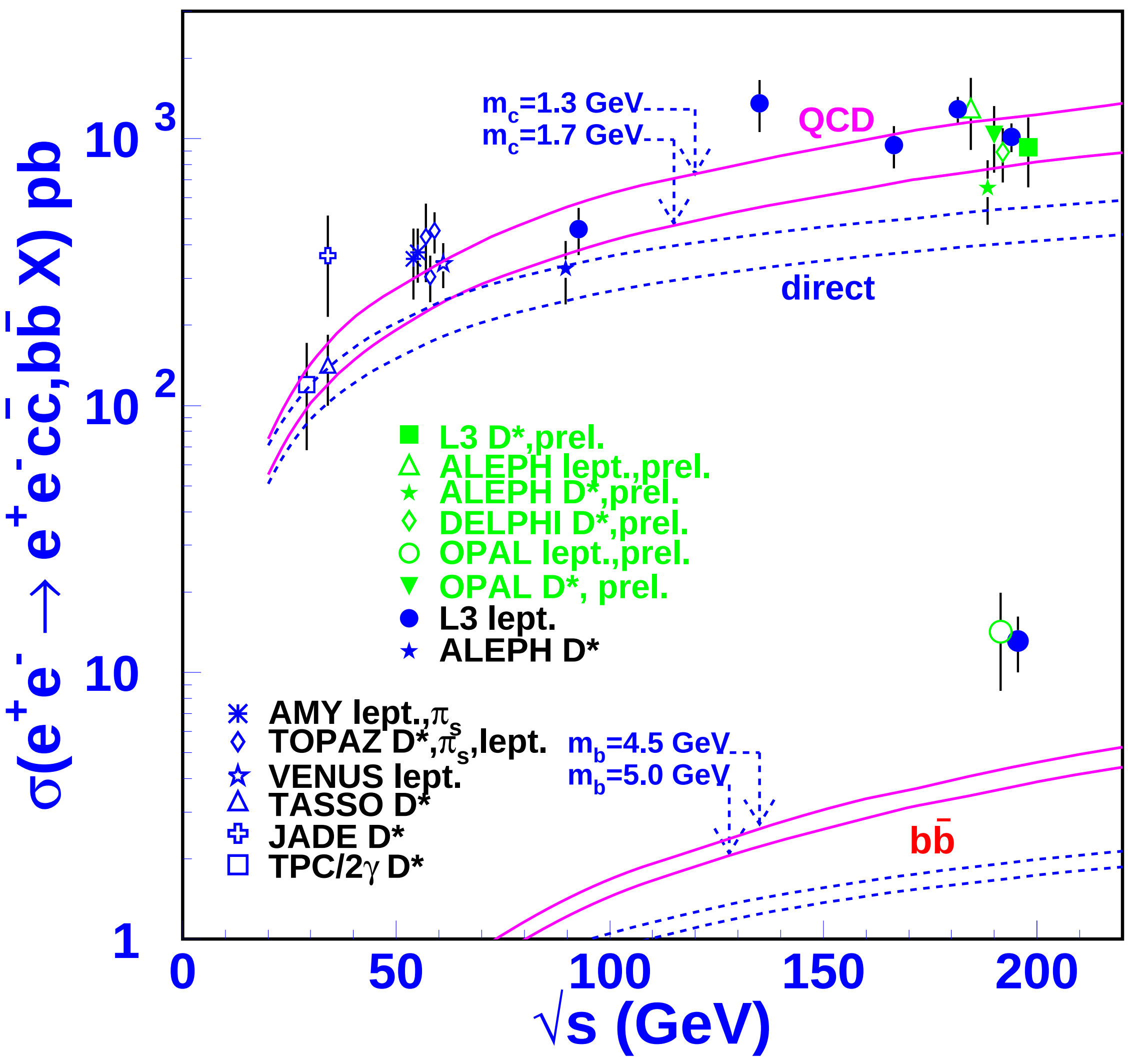

μ tag: $\sigma^{\mu}_{b\bar{b}} = 14.9 \pm 2.8(\mathrm{stat}) \pm 2.6(\mathrm{sys})$ pb

e tag: $\sigma^{e}_{b\bar{b}} = 10.9 \pm 2.9(\mathrm{stat}) \pm 2.0(\mathrm{sys})$ pb

---

L3: $\sigma_{b\bar{b}} = 13.1 \pm 2.0(\mathrm{stat}) \pm 2.4(\mathrm{sys})$ pb

OPAL(μ) prel.: $\sigma_{b\bar{b}} = 14.2 \pm 2.5(\mathrm{stat})\ {}^{+5.3}_{-4.8}(\mathrm{sys})$ pb

The NLO QCD prediction falls short by 4σ!

The limit of deep inelastic electron-photon scattering

Using:

$$\begin{aligned} 2xF_{\mathrm{T}}^{\gamma} &= \frac{Q^2}{4\pi^2\alpha}\,\sigma_{\mathrm{TT}}(x,Q^2) \\ F_{\mathrm{L}}^{\gamma} &= \frac{Q^2}{4\pi^2\alpha}\,\sigma_{\mathrm{LT}}(x,Q^2) \\ F_2^{\gamma} &= 2xF_{\mathrm{T}}^{\gamma} + F_{\mathrm{L}}^{\gamma} \end{aligned}$$

and the limit $(p\cdot q)^2 - Q^2P^2 \approx (p\cdot q)^2$ the cross section reduces to:

$$\begin{aligned} \frac{\mathrm{d}^4\sigma}{\mathrm{d}x\,\mathrm{d}Q^2\,\mathrm{d}z\,\mathrm{d}P^2} &= \frac{\mathrm{d}^2 N_{\gamma}^{\mathrm{T}}}{\mathrm{d}z\mathrm{d}P^2}\cdot\frac{2\pi\alpha^2}{x\,Q^4}\cdot\left[1+(1-y)^2\right]\cdot \\ &\quad \underbrace{\left[2xF_{\mathrm{T}}^{\gamma}(x,Q^2) + \frac{2(1-y)}{1+(1-y)^2}F_{\mathrm{L}}^{\gamma}(x,Q^2)\right]}_{\to F_2^{\gamma}\ \text{for}\ y\ll 1} \end{aligned}$$

$$\text{with:}\quad \frac{\mathrm{d}^2 N_{\gamma}^{\mathrm{T}}}{\mathrm{d}z\mathrm{d}P^2} = \frac{\alpha}{2\pi}\left[\frac{1+(1-z)^2}{z}\frac{1}{P^2} - \frac{2\,m_{\mathrm{e}}^2\,z}{P^4}\right]$$

Electron-photon scattering

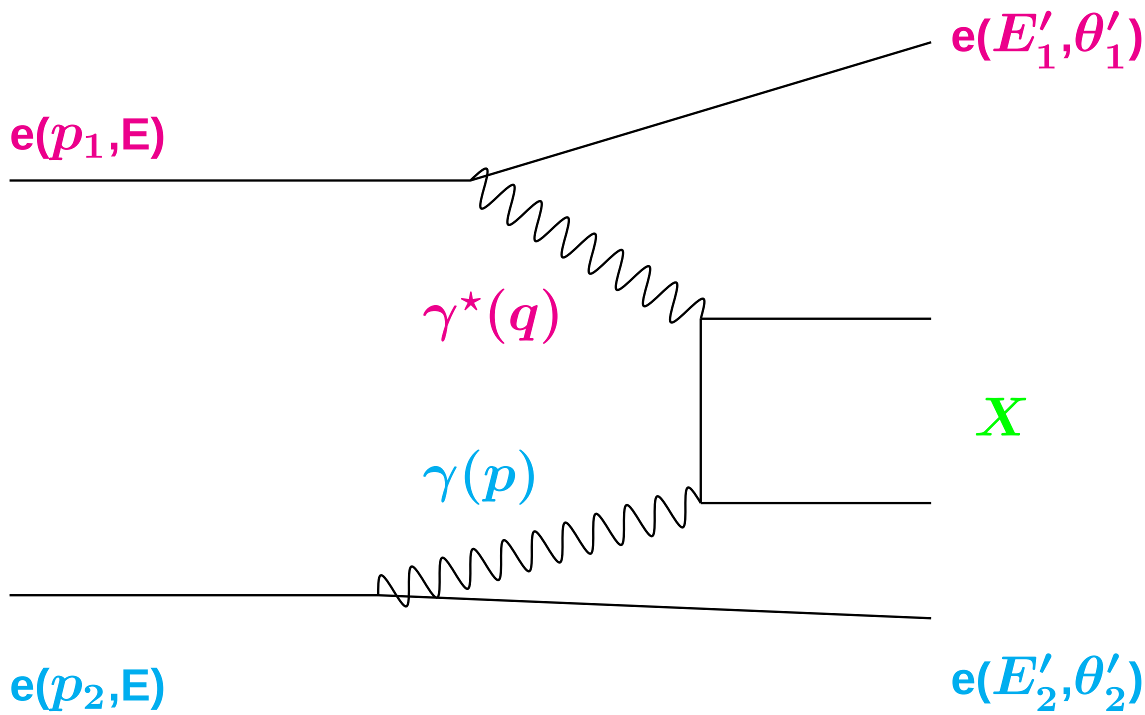

$$\frac{\mathrm{d}^4\sigma}{\mathrm{d}x\mathrm{d}Q^2\mathrm{d}z\mathrm{d}P^2} \propto \frac{\mathrm{d}^2N_\gamma^{\mathrm{T}}}{\mathrm{d}z\mathrm{d}P^2}\cdot\frac{2\pi\alpha^2}{x\,Q^4}\cdot f_y\cdot F_2^\gamma(x,Q^2)$$

with:

$$f_y = 1+(1-y)^2$$

$$Q^2 = -q^2 = 2\,E\,E'_1\,(1-\cos\theta'_1)$$

$$x = \frac{Q^2}{Q^2+W^2+P^2}$$

$$P^2 = -p^2 = 2\,E\,E'_2\,(1-\cos\theta'_2) \ll Q^2$$

$$\frac{\mathrm{d}^2N_\gamma^{\mathrm{T}}}{\mathrm{d}z\mathrm{d}P^2} = \frac{\alpha}{2\pi}\left[\frac{1+(1-z)^2}{z}\frac{1}{P^2} - \frac{2\,m_e^2\,z}{P^4}\right]$$

The muon pair final state

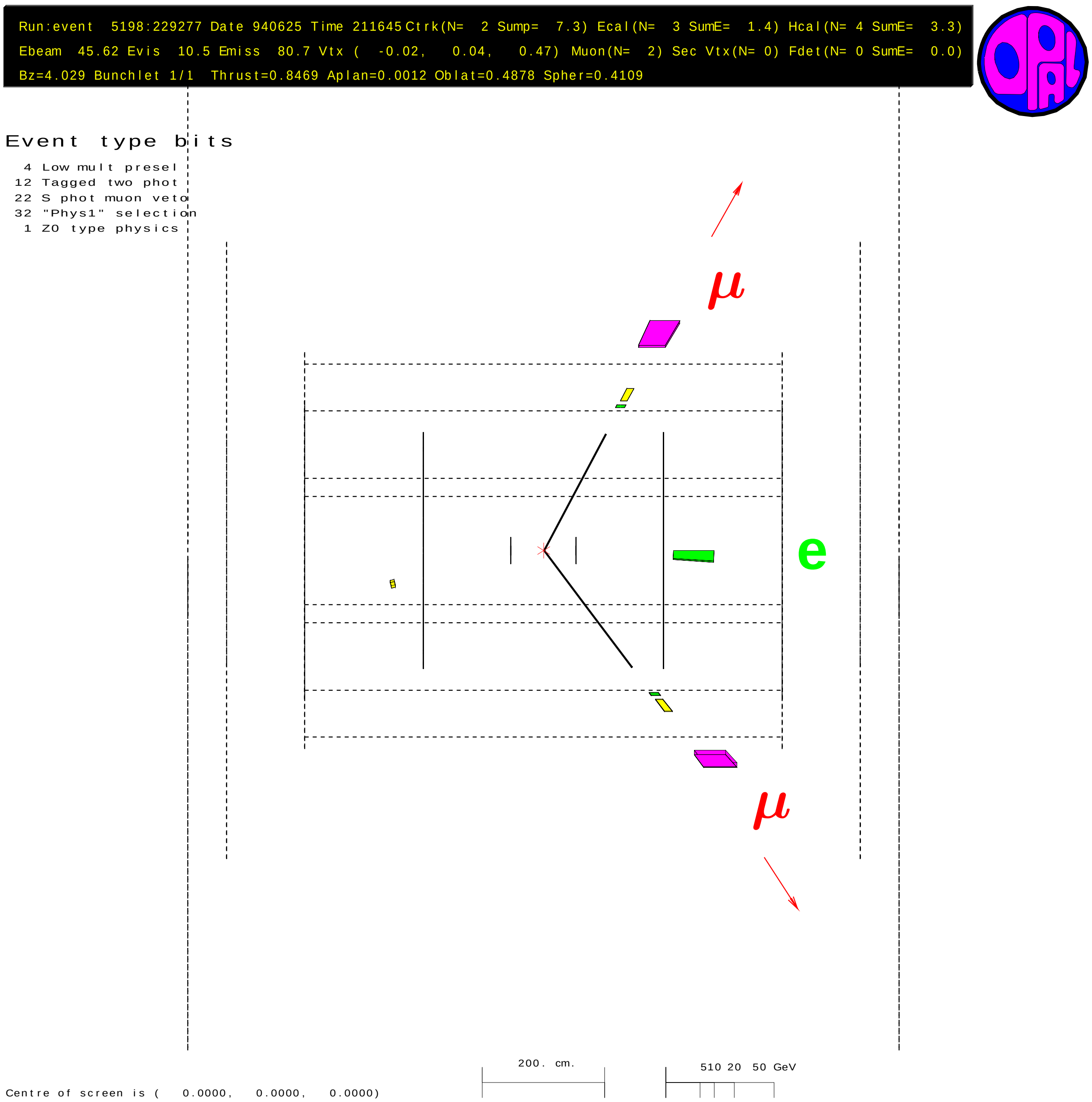

The muon pair final state is a clear topology with good mass resolution.

The world data on $F_{2,\mathrm{QED}}^{\gamma}$

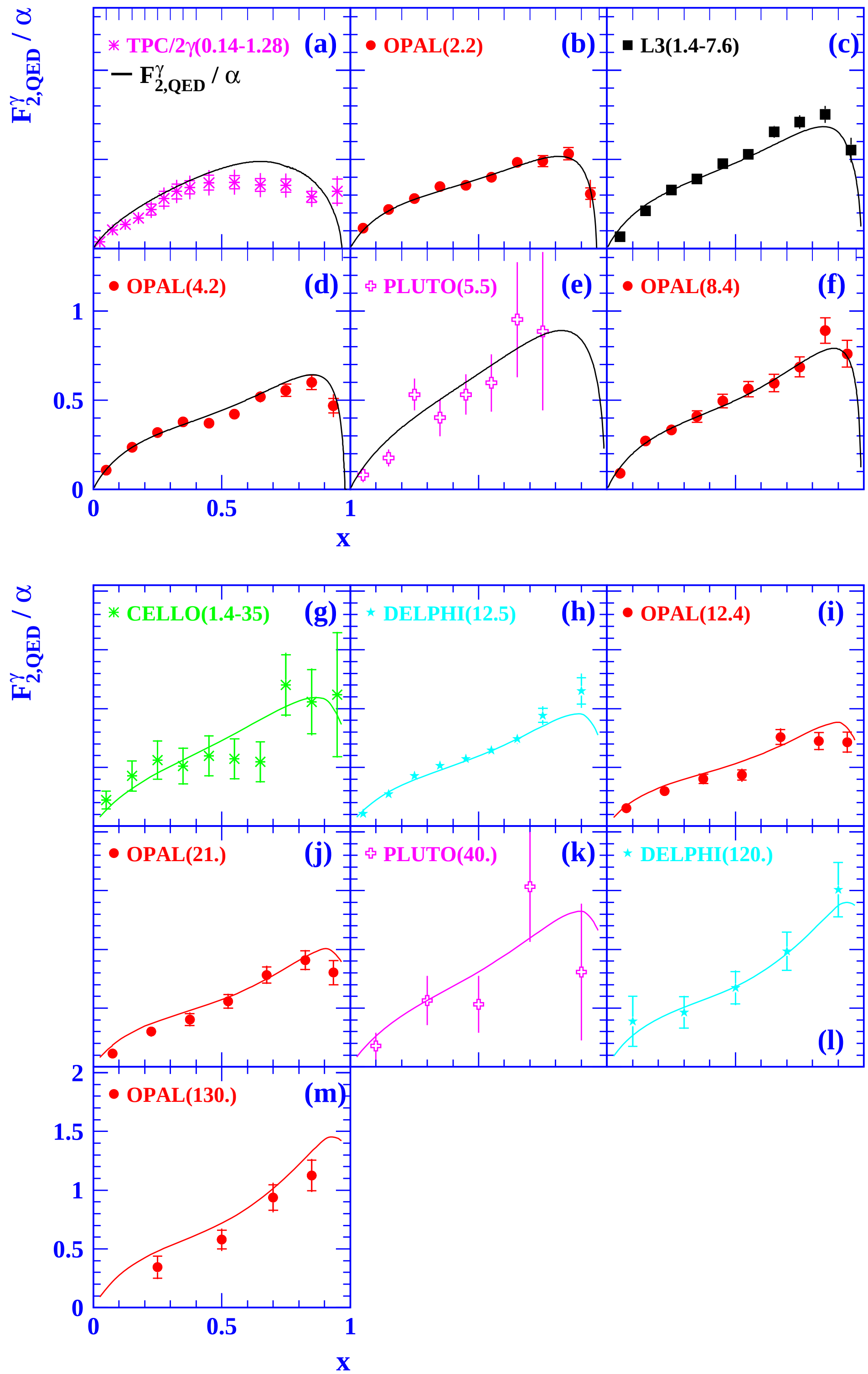

The P^2 dependence of F_2^γ

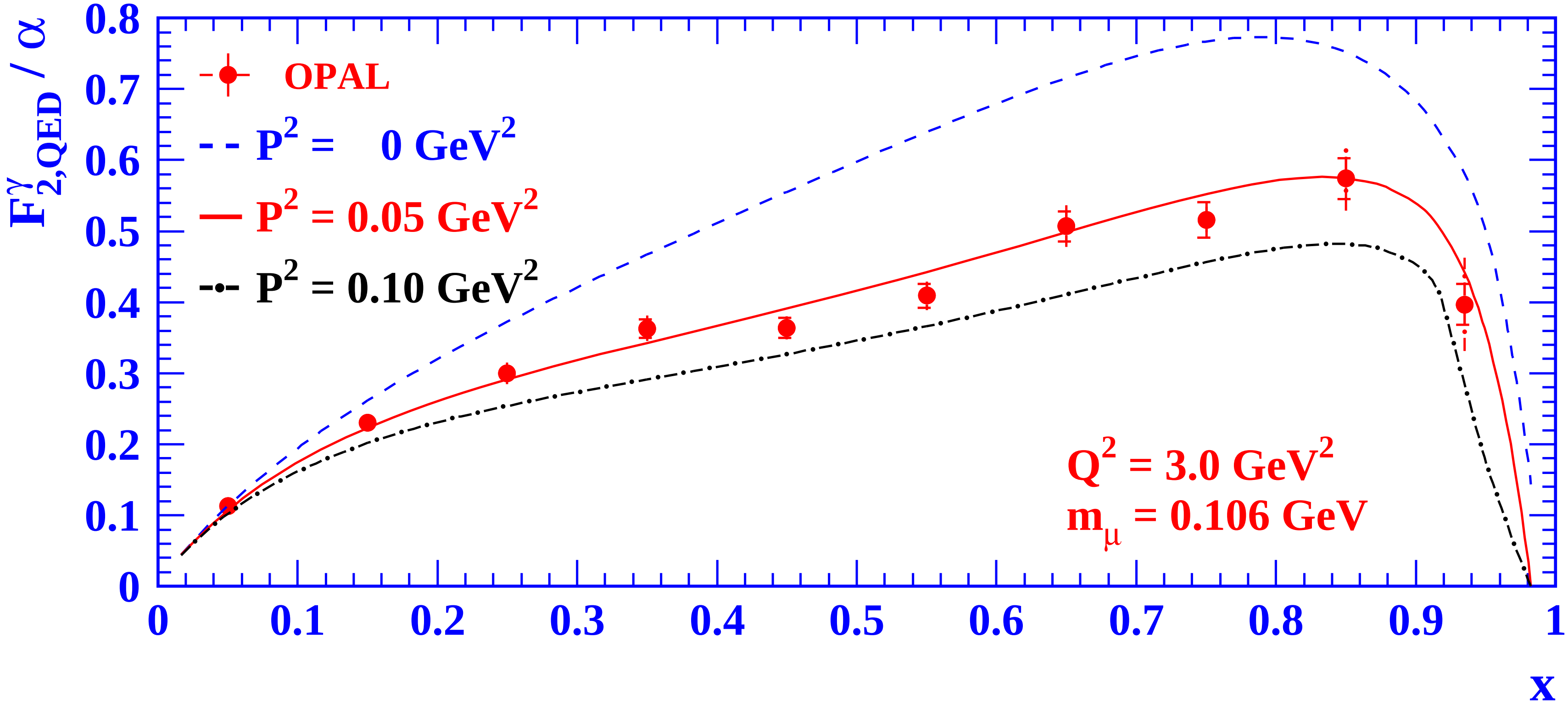

The suppression of the photon structure with the photon virtuality P^2 is clearly observed in the data.

Azimuthal correlations

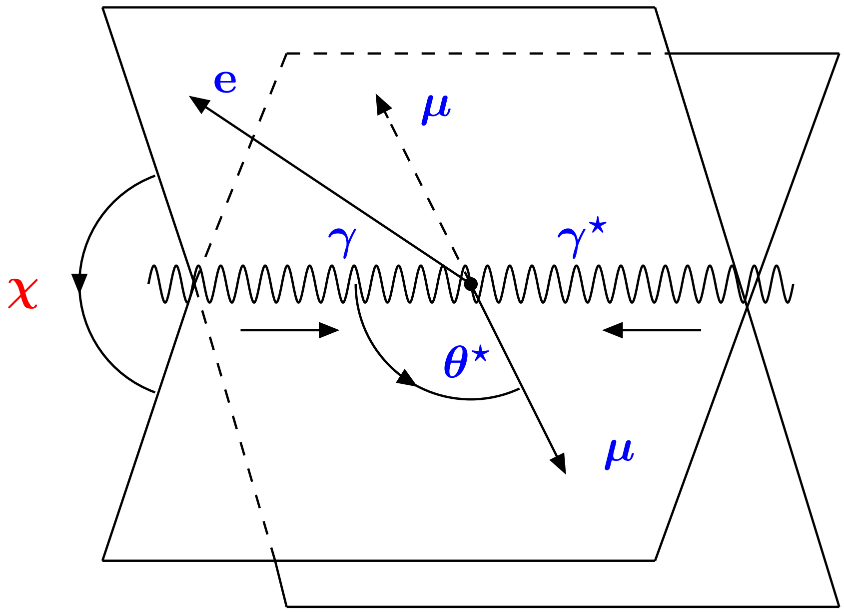

$$\mathrm{e}\gamma \longrightarrow \mathrm{e}\mu\mu$$

$$\mathrm{d}\sigma \quad \propto \quad 1 - \rho(y) F_{\mathrm{A}}^{\gamma}/F_2^{\gamma} \cos\chi + \frac{1}{2}\epsilon(y) F_{\mathrm{B}}^{\gamma}/F_2^{\gamma} \cos 2\chi$$

$$\epsilon(y) = \frac{2(1-y)}{1+(1-y)^2} \approx 1, \;\; \rho(y) = \frac{(2-y)\sqrt{1-y}}{1+(1-y)^2} \approx 1$$

Helicity structure:

F_{A}^{γ}: **transverse–longitudinal interference**

F_{B}^{γ}: **transverse–transverse interference**

The χ dependence gives access to other structure functions besides F_2^{γ}.

The structure functions F_A^γ and F_B^γ

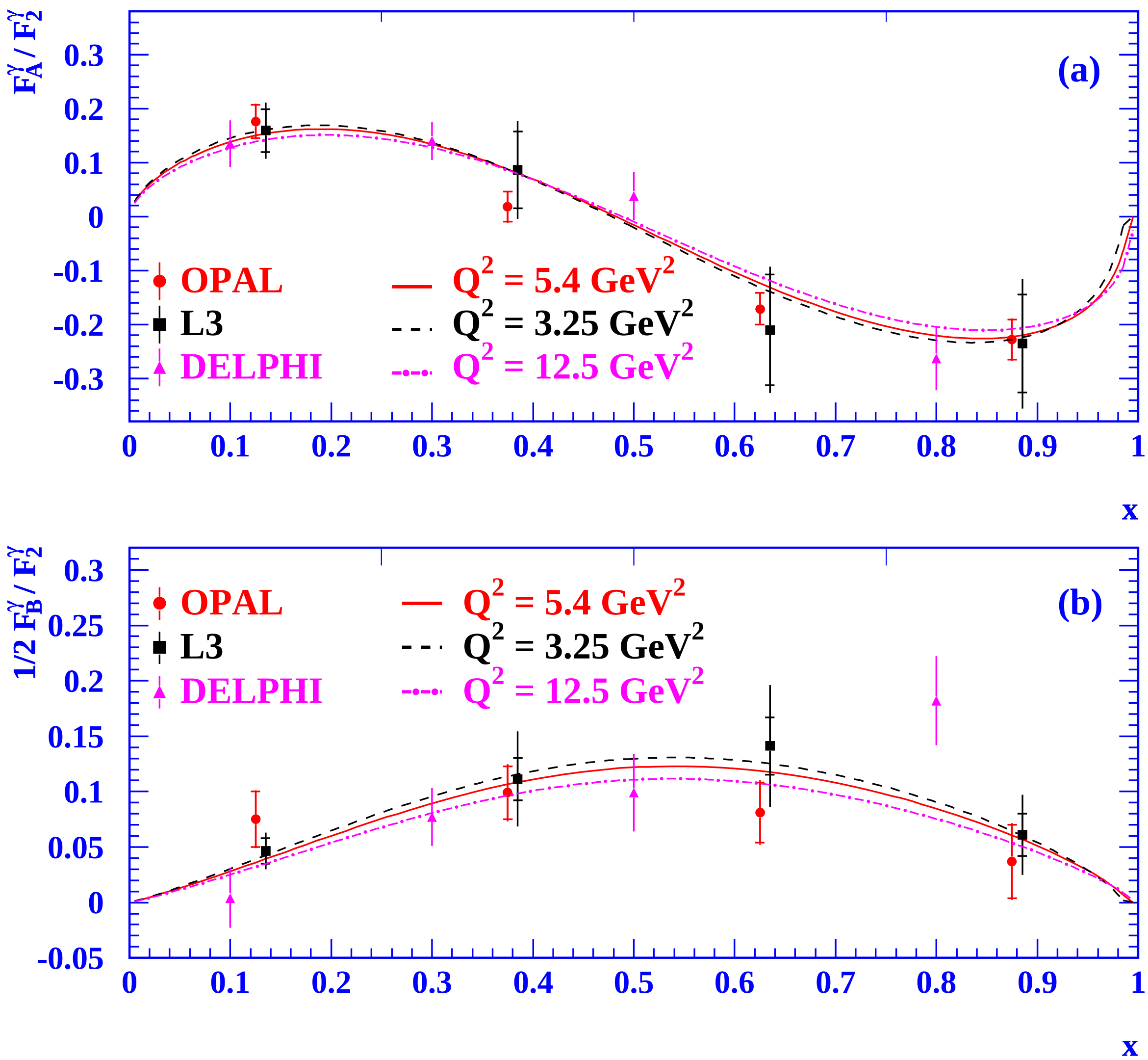

First measurement that goes further than measuring the differential cross-section and gives more information on the helicity structure of the interaction.

Production of tau pairs at LEP

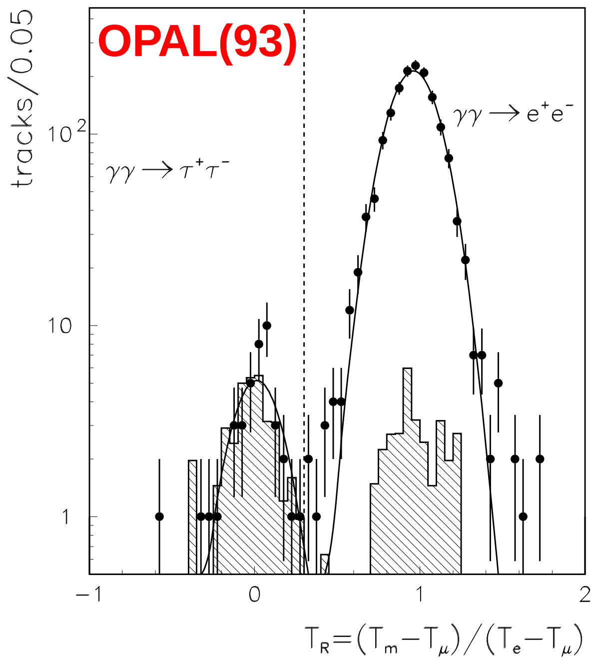

First seen in $\gamma\gamma^\star \longrightarrow \tau\tau$

$\tau\tau \longrightarrow (\mathrm{e}\,\bar{\nu}_\mathrm{e}\nu_\tau)(\mu\,\bar{\nu}_\mu\nu_\tau)$

Leptons identified by $\mathrm{d}E/\mathrm{d}x$

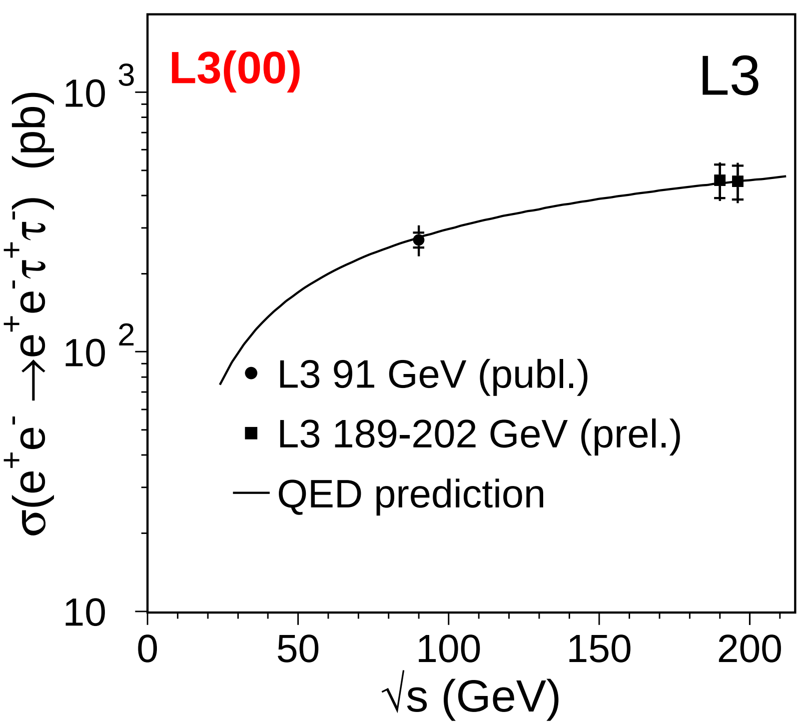

Cross-section for $\gamma\gamma \longrightarrow \tau\tau$ using $\tau\tau$ decays into $(\mathrm{e}\,\bar{\nu}_\mathrm{e}\nu_\tau)(\pi\pi^0\nu_\tau)$

Tau pair production has been measured at LEP.

The hadronic final state

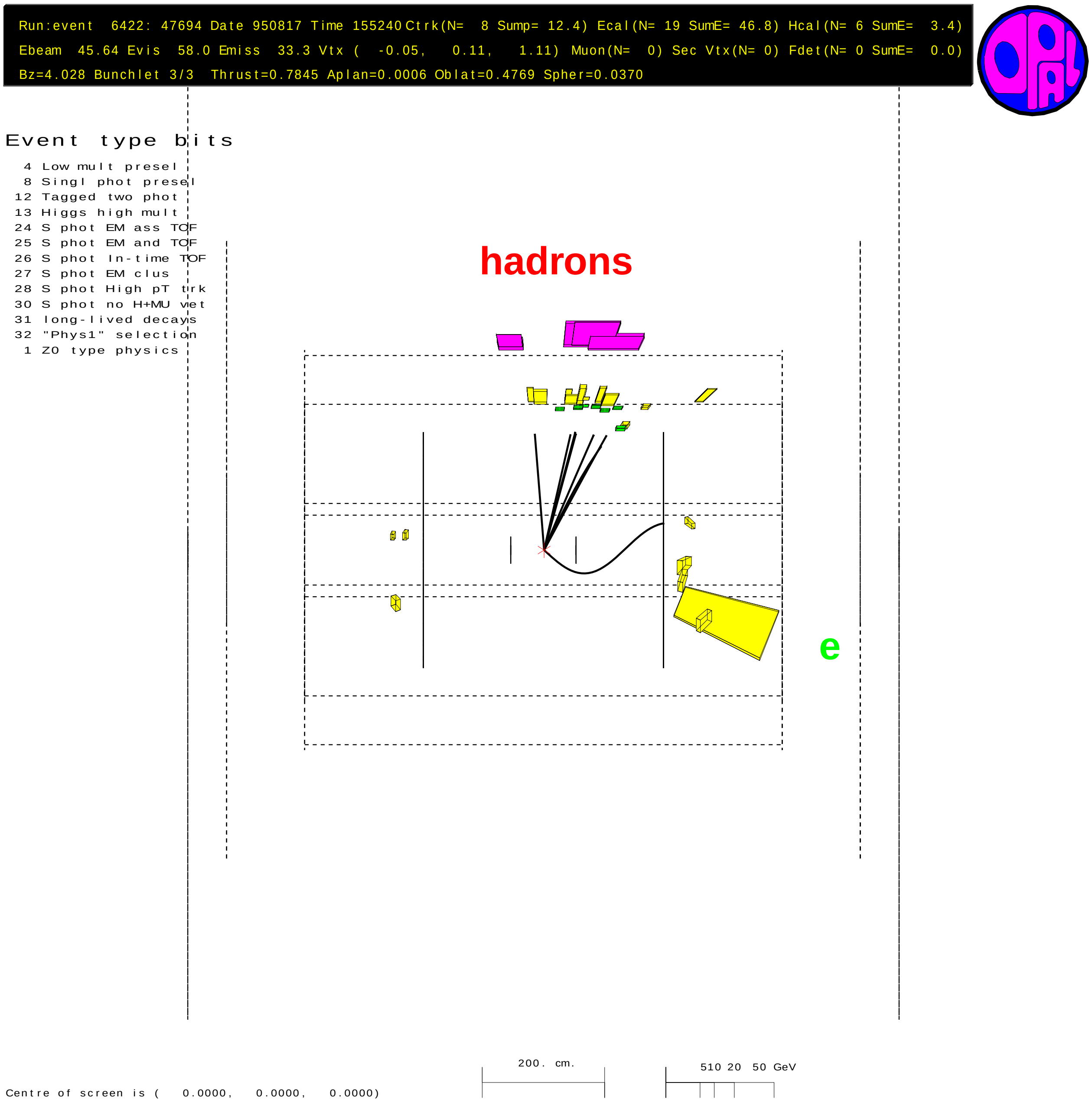

The scattered electron is clearly visible.
However, the hadronic final state may partly disappear along the beam axis.

The description of the hadronic final state

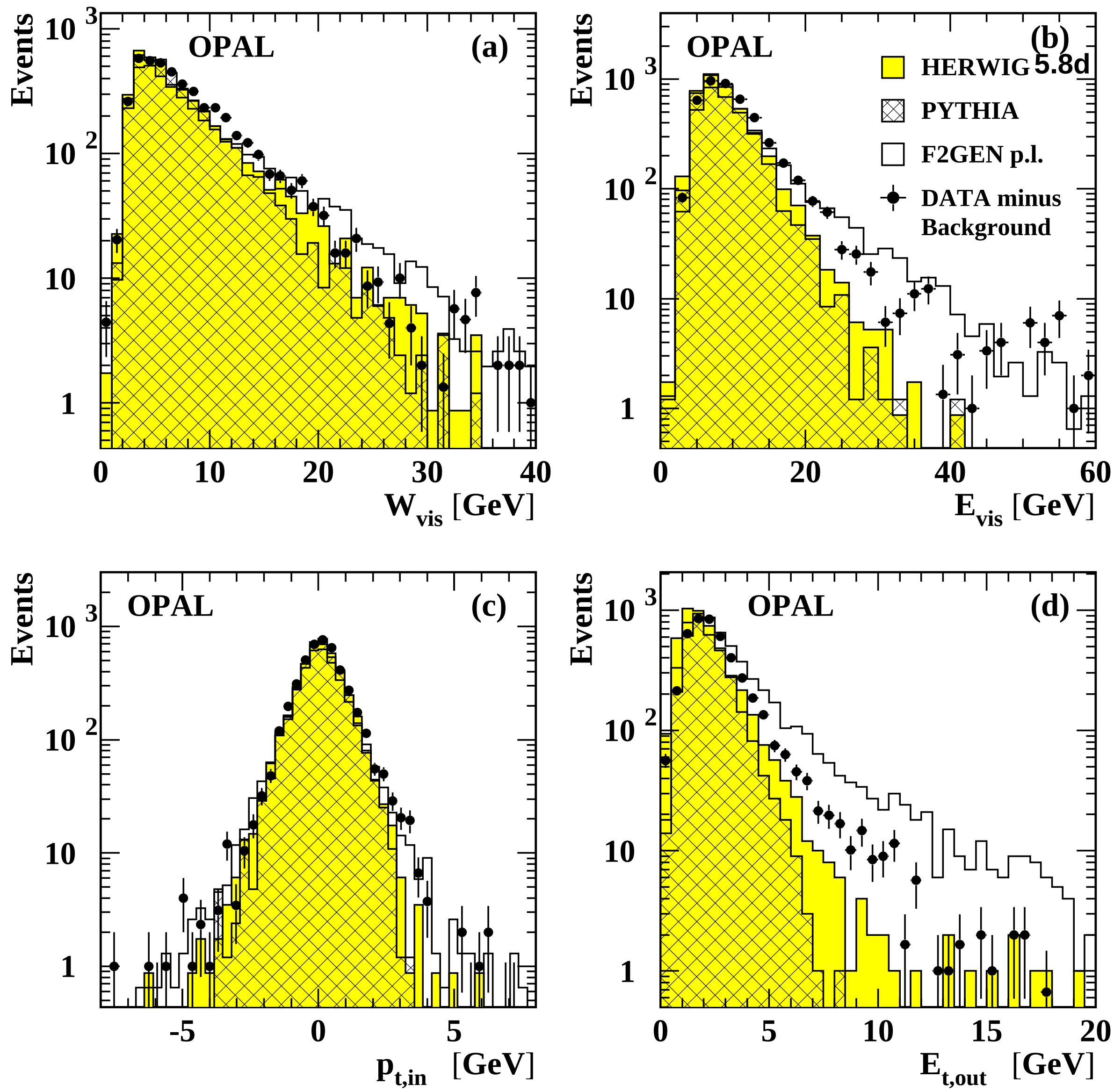

There are significant differences between the data and the Monte Carlo predictions (OPAL '96)

Comparison to LEP combined data

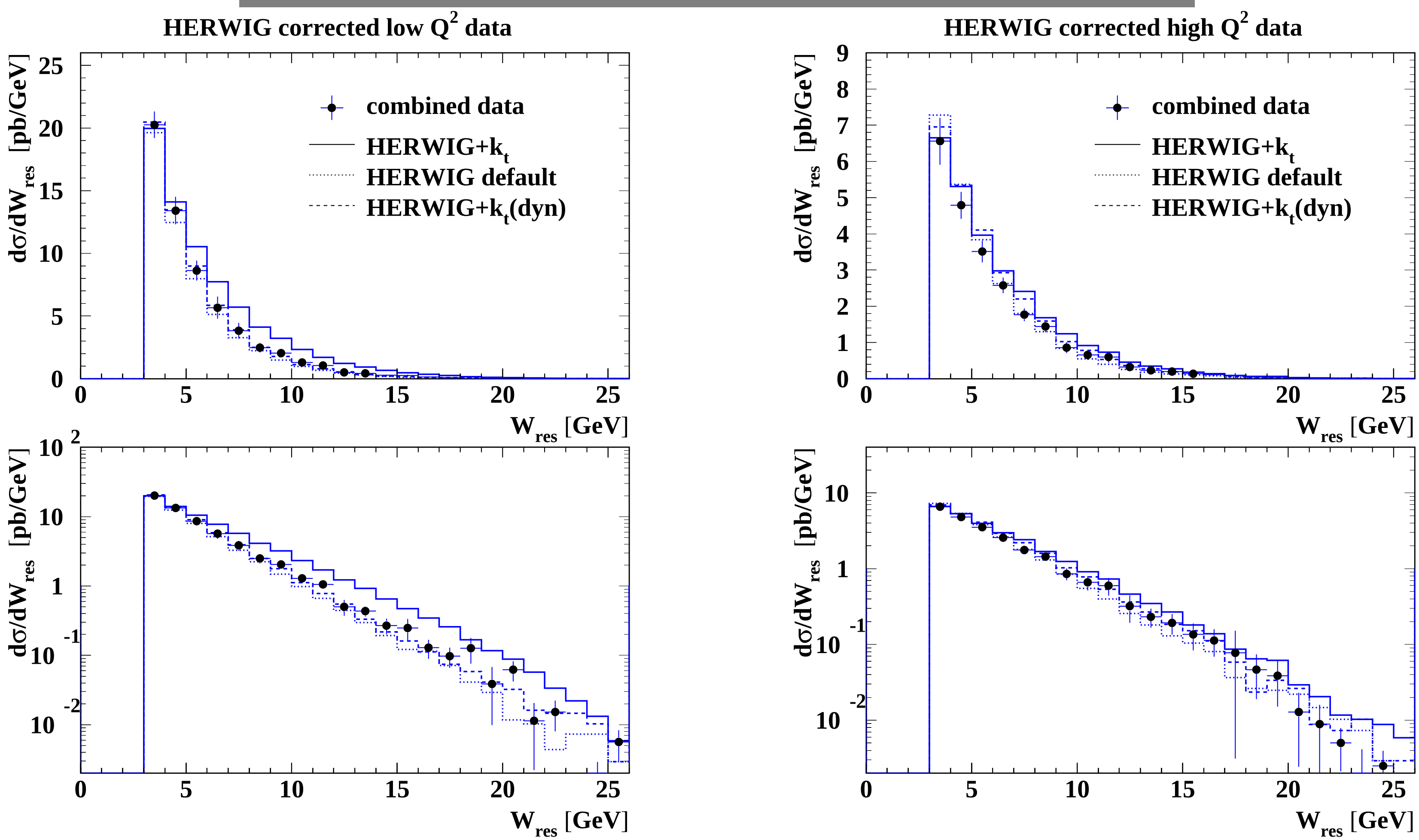

The combined data are a valuable input to constrain the Monte Carlo models (LEP Two-Photon WG CERN-EP-2000-109)

The contributions to $F_2^\gamma(x,Q^2)$

$$F_2^\gamma(x,Q^2) = x\sum_{c,f} e_q^2\, f_{q,\gamma}(x,Q^2)$$

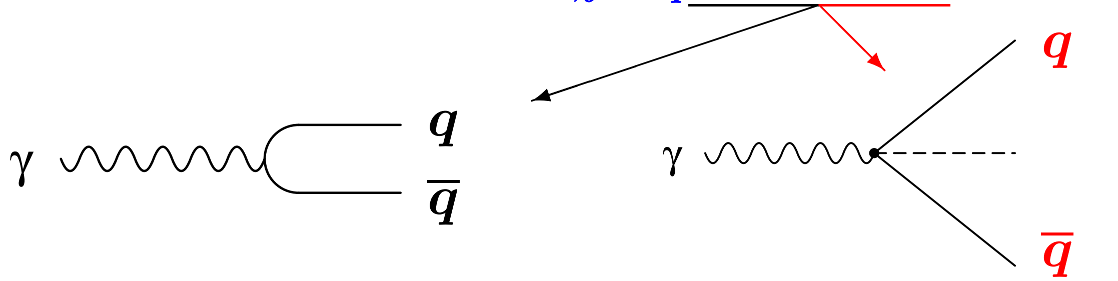

hadron-like, *non–perturbative* — **e.g. VMD(ρ,ω,ϕ), low-x**

point-like, *perturbative* — **high-x**

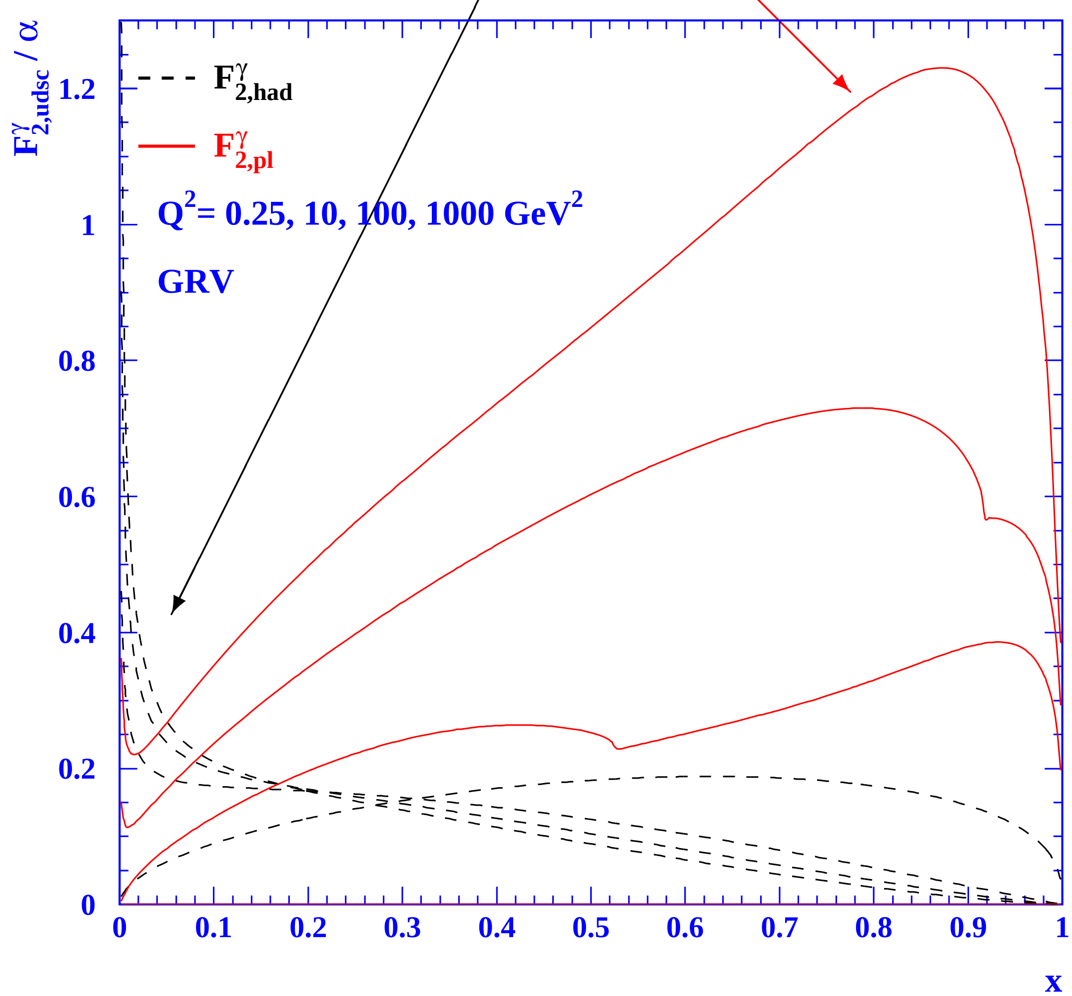

Charm production tagged by D*s

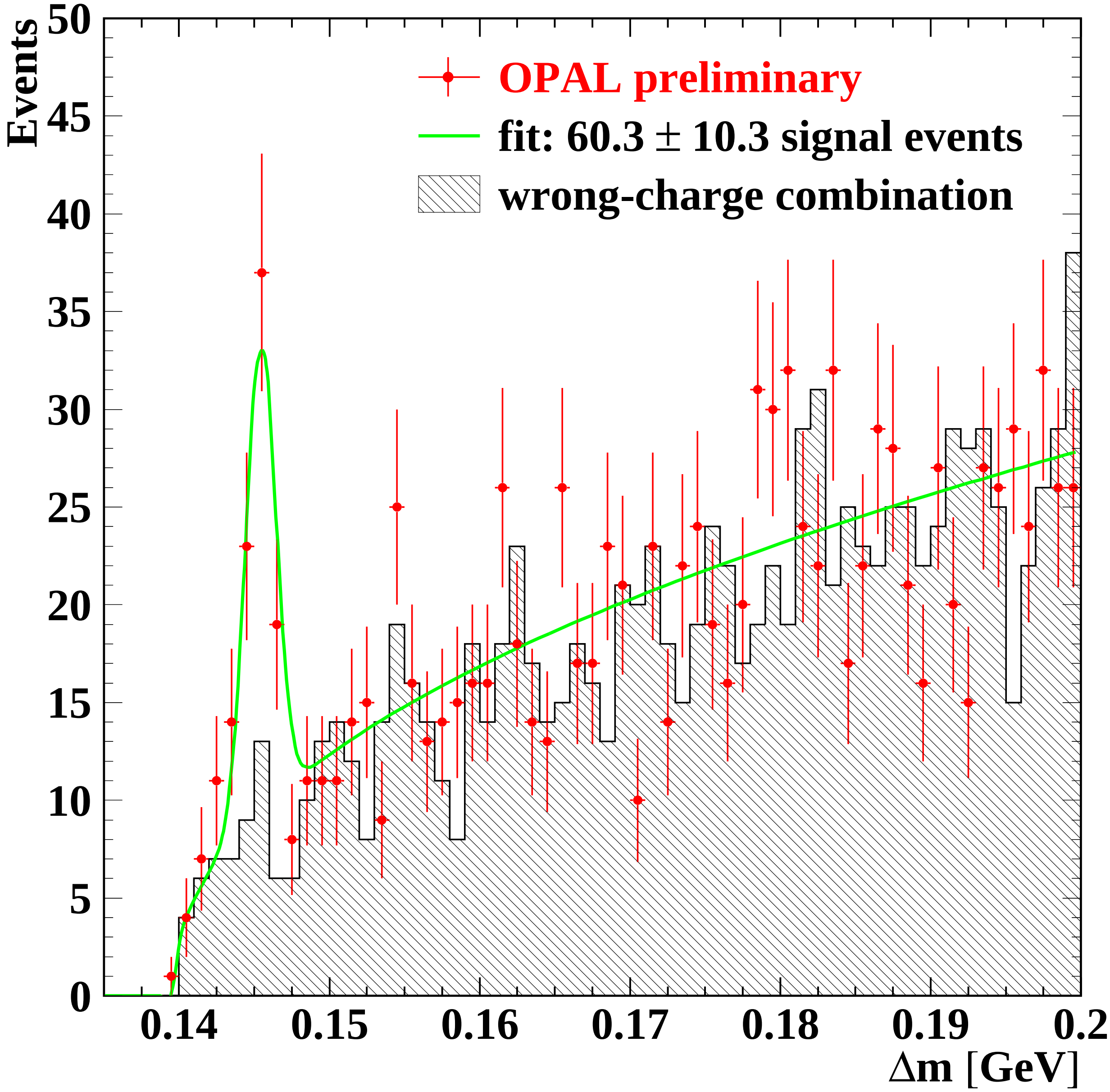

A clear signal in the $\Delta m = M(D^\star) - M(D^0)$ mass spectrum is seen.

The first measurement of $F_{2,c}^{\gamma}$

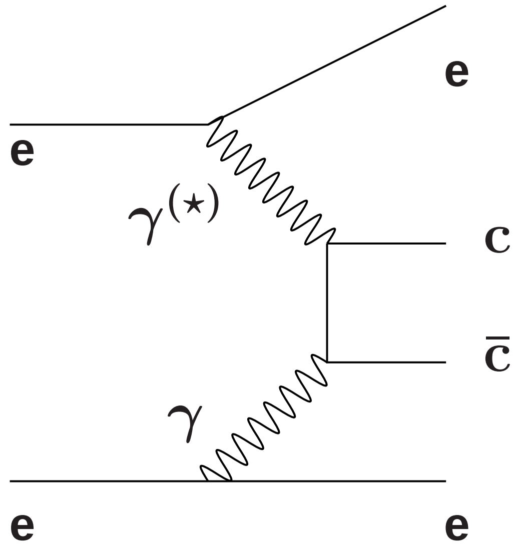

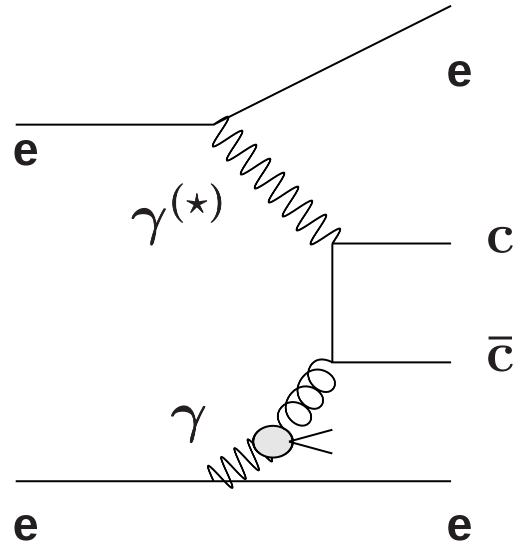

point-like, purely perturbative QCD prediction, dominates at high-x

hadron-like, depends on f_g^{γ}, dominates at low-x

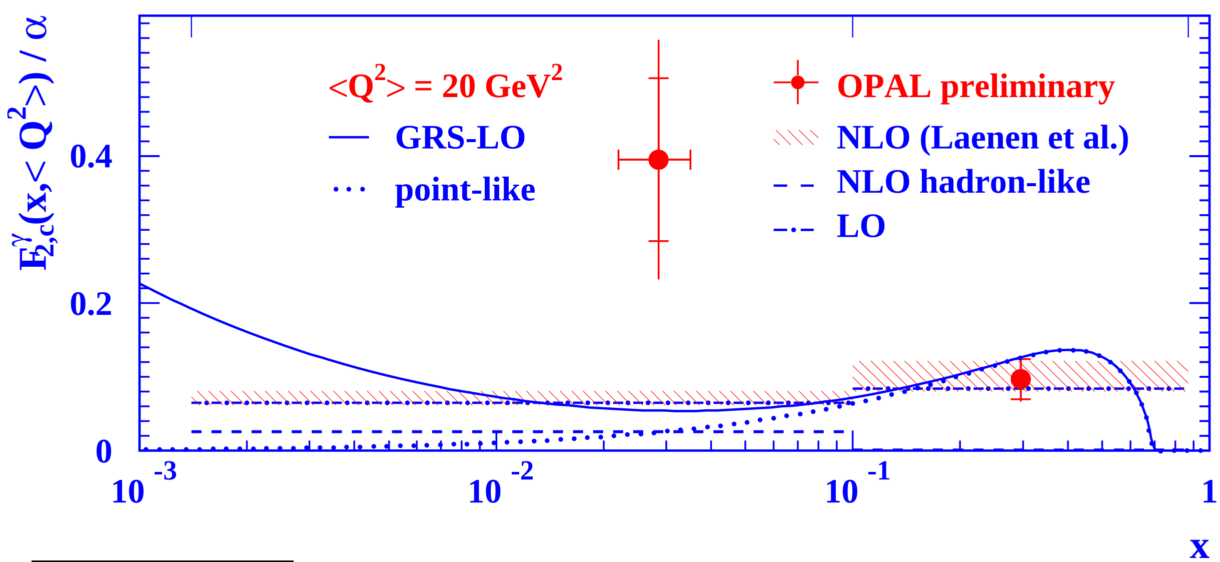

OPAL Collab., Eur. Phys. J. C16 (2000) 579. (updated)

$F_{2,c}^{\gamma}$ at the Linear Collider

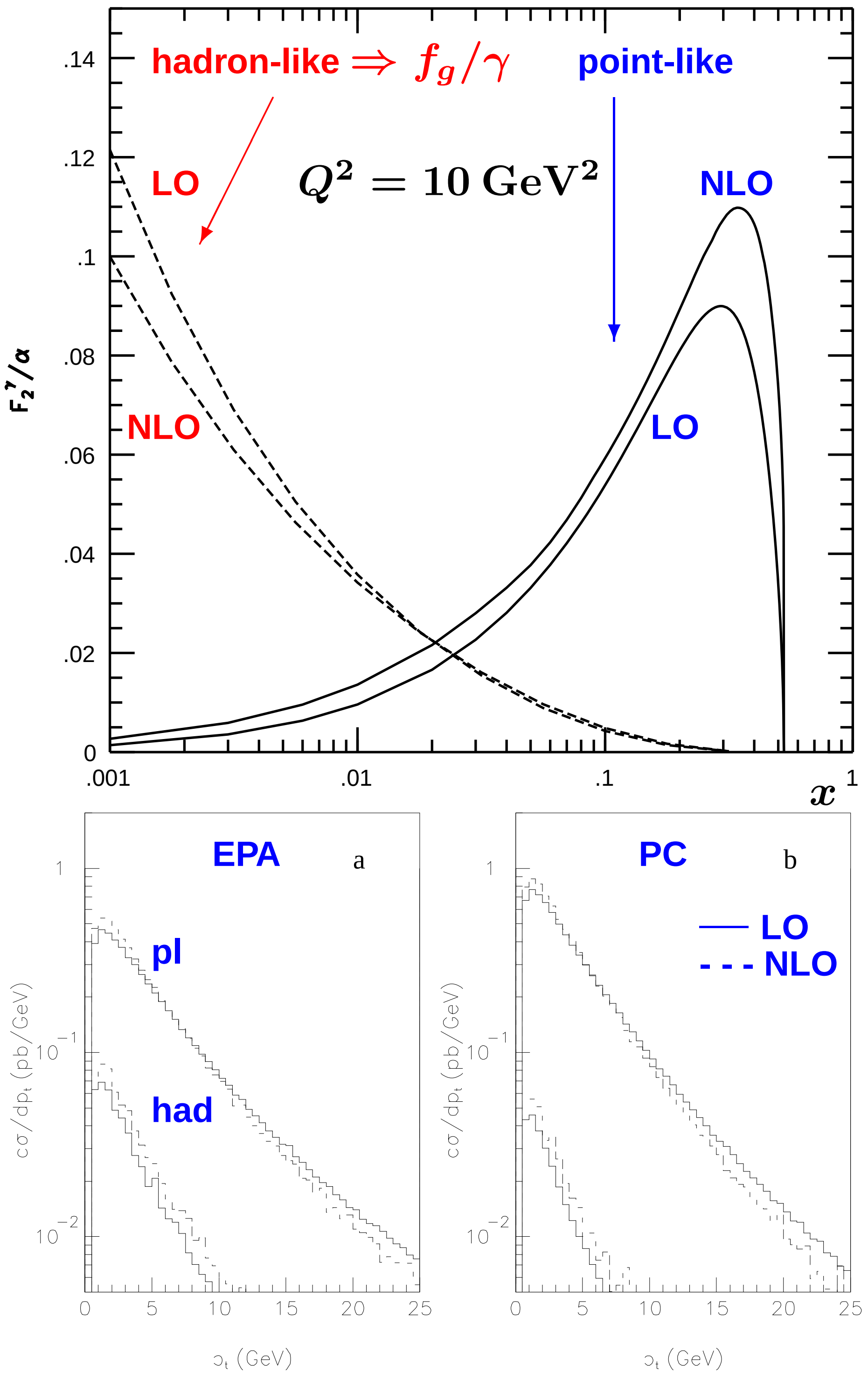

$E_{\mathrm{tag}}/E_{\mathrm{b}} > 0.5, \theta_{\mathrm{tag}} > 40$ mrad, $m_c = 1.5$ GeV, $\mu = Q$

The pointlike contribution to $F_{2,\mathrm{h}}^{\gamma}$

charm versus bottom

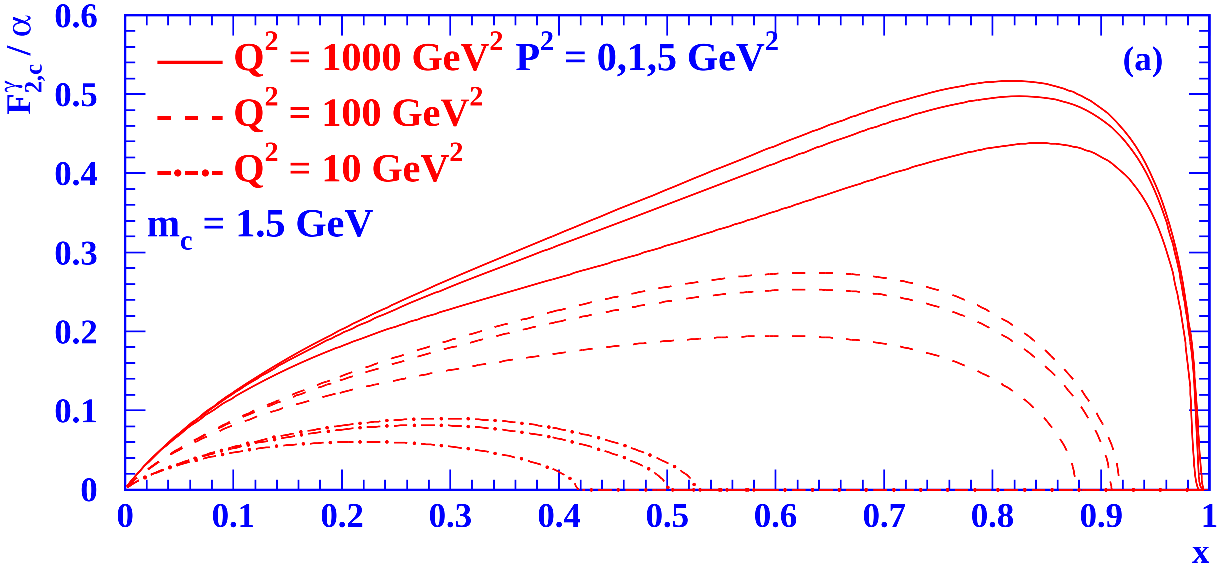

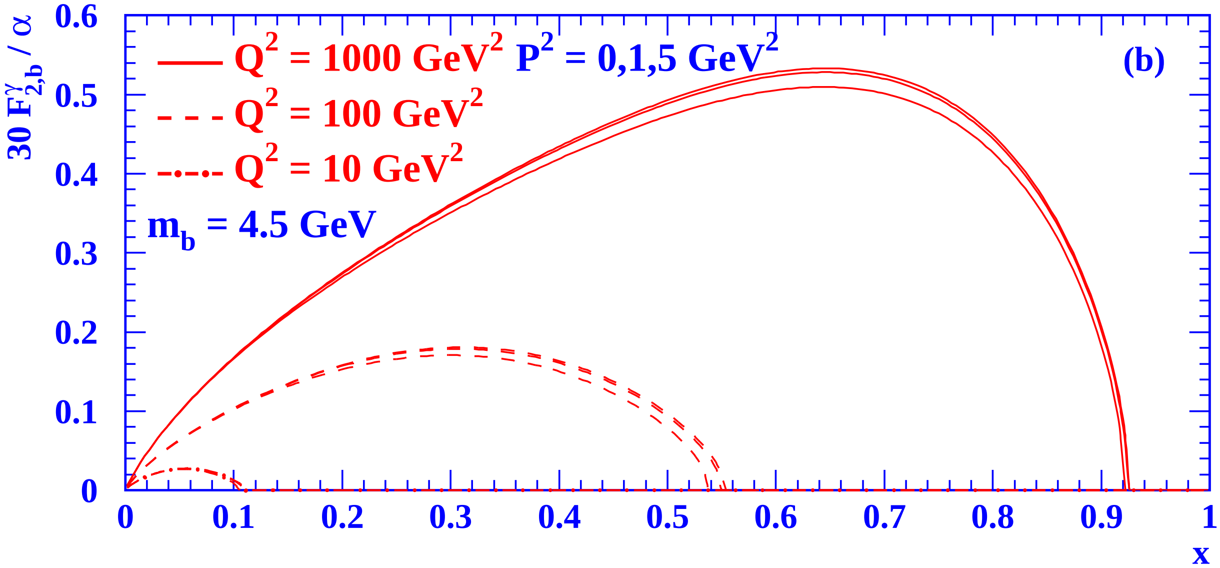

Bottom is heavier and also disfavoured by the charge.
It may still be possible to measure $F_{2,\mathrm{b}}^{\gamma}$ at a Photon Collider.

Single bottom production at the LC

1) The method

DIS: $e\gamma \xrightarrow{Z^0/\gamma} ebX$

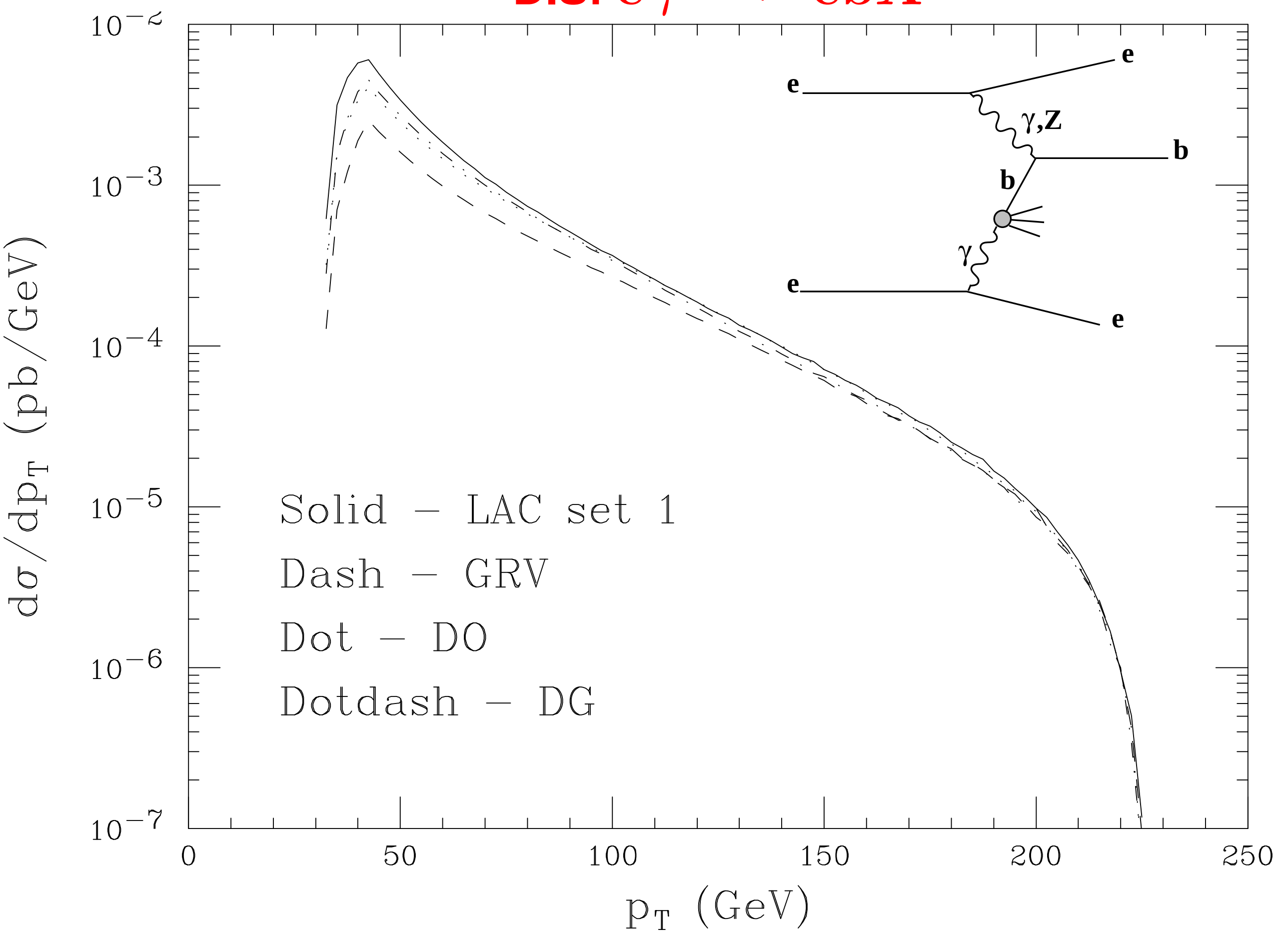

By virtue of the hard scale $p_{t,b} > 40\ \mathrm{GeV} \gg m_b$, bottom is treated as a massless quark distribution function of the photon.

Single bottom production at the LC

2) Event rates

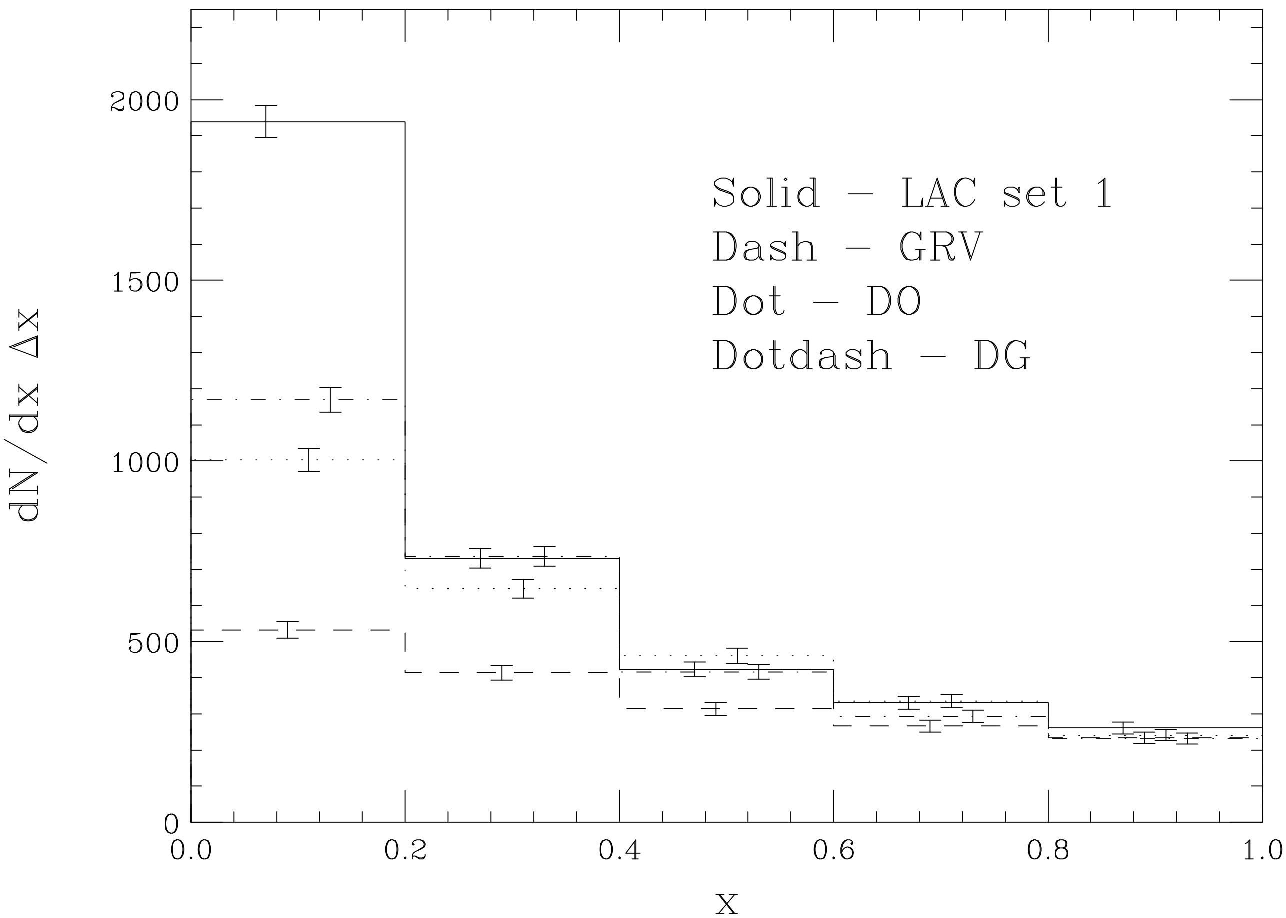

Assuming $\epsilon_{\mathrm{b}}^{\mu} = 50\%$ for $|\theta_{\mathrm{b}}| < 0.85$ a distinction between several predictions of bottom distribution functions should be possible at a Photon Collider.

The world data on F_2^γ

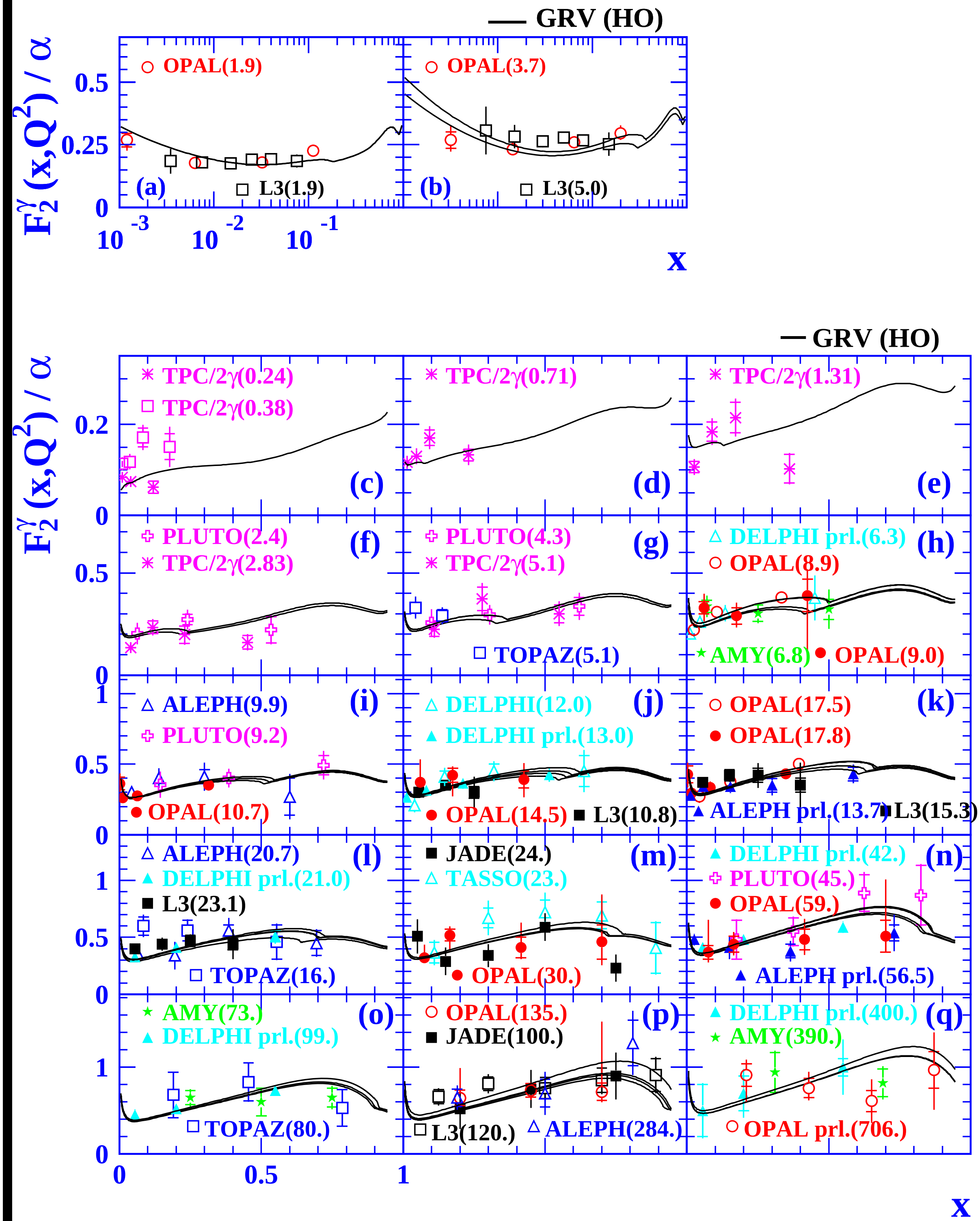

The high Q^2 reach of F_2^γ at LEP

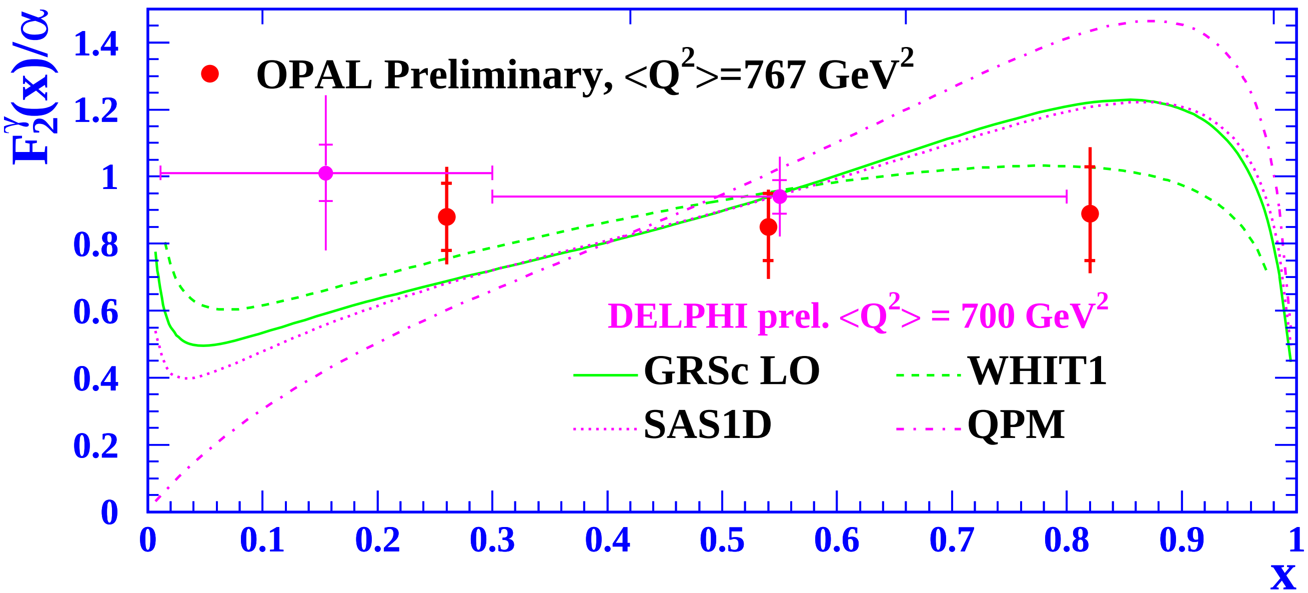

1) We start to look at factorisation scales of about 1000 GeV^2.

2) F_2^γ is measured with 15-20% precision at $Q^2 \approx 750\ \mathrm{GeV}^2$.

3) For $x > 0.1$ the precision of the measurement is mainly limited by the statistical error. Get ADOL together to improve on the statistical error.

Measurements at low Q^2 and x

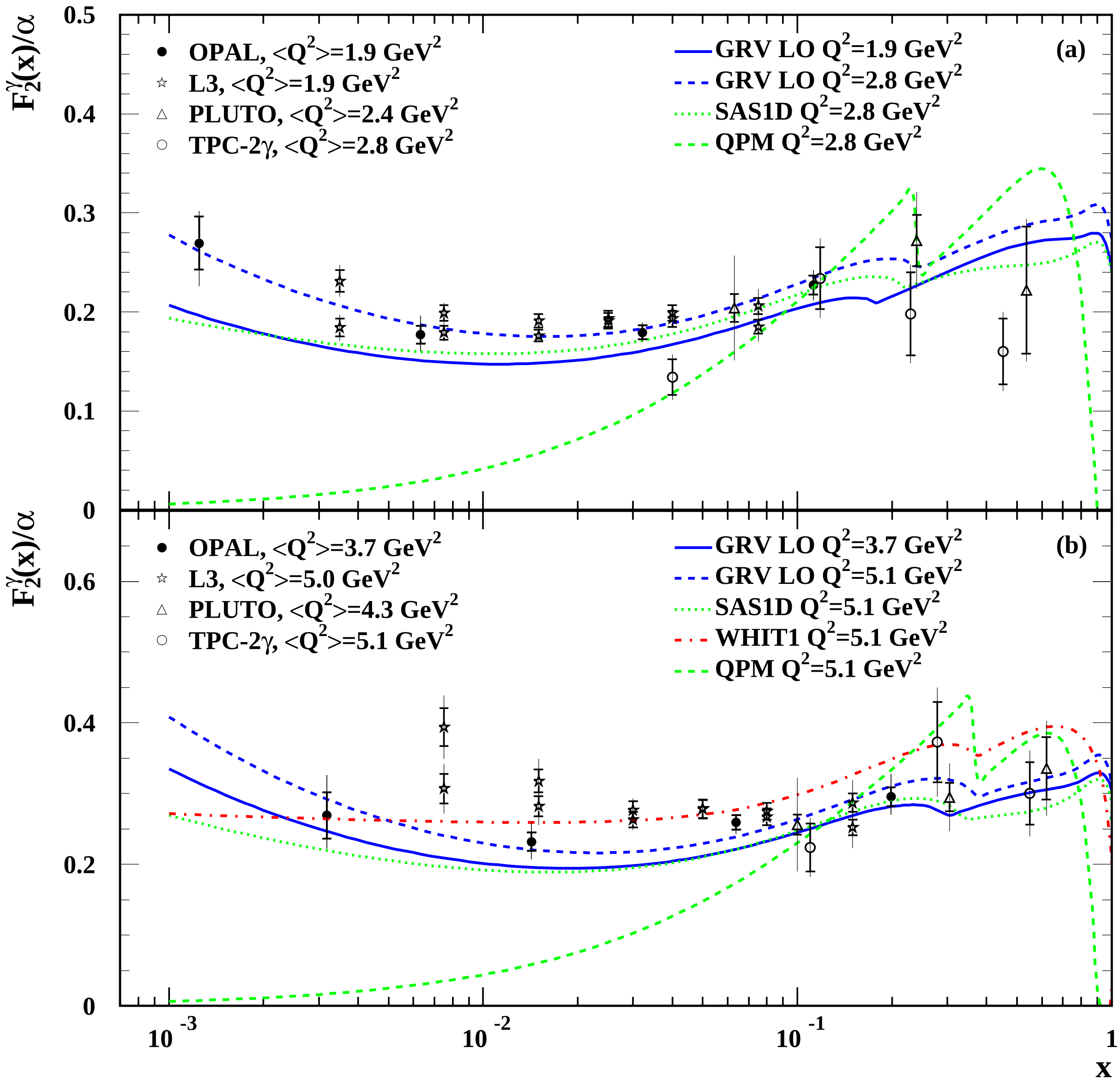

GRV(LO) and SaS1D are slightly too low compared to the data.

OPAL Collab., Eur. Phys. J. C18 (2000) 15.

The Q^2 evolution of F_2^γ for $n_f = 4$

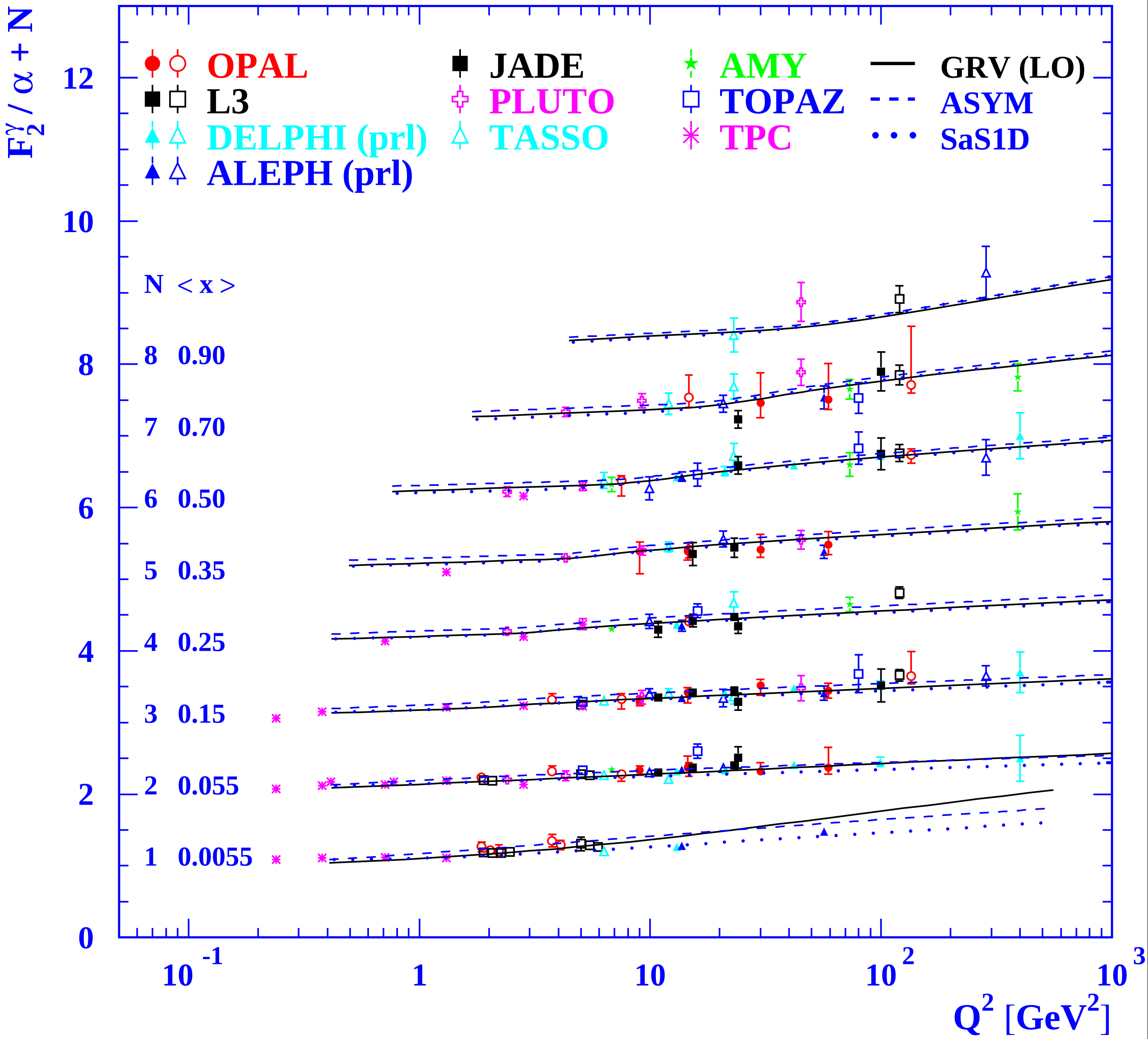

The general trend of the data is followed by the parametrisations.

Q^2 evolution compared to linear fits

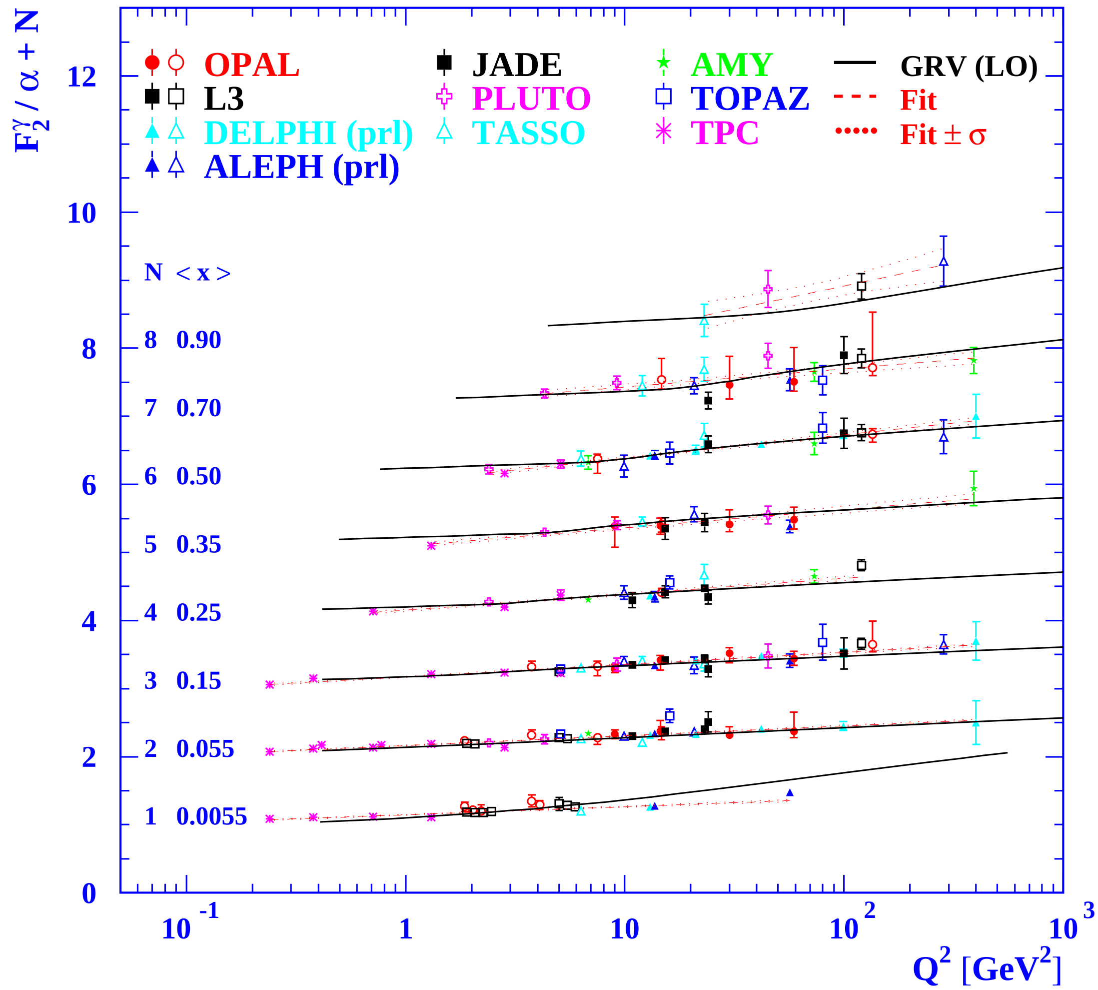

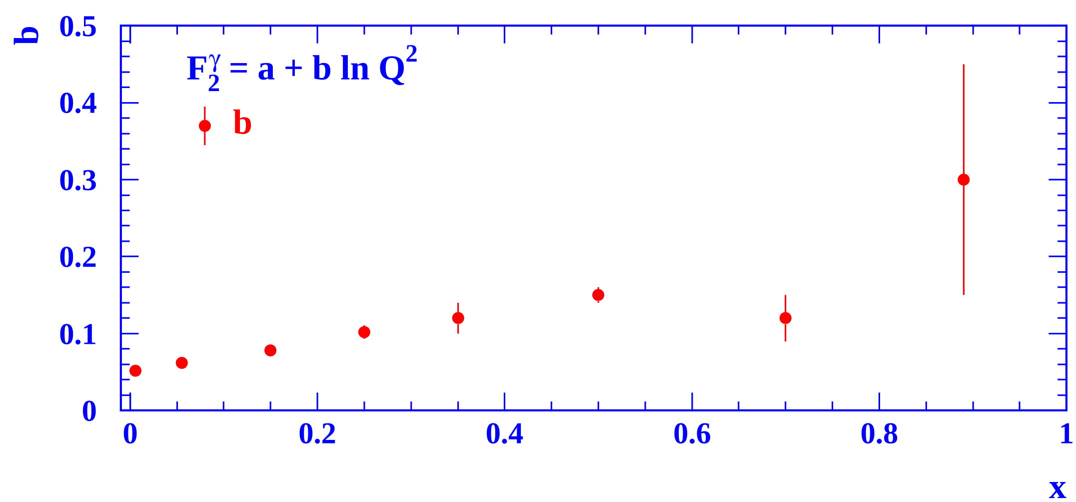

An increasing slope as a function of x is observed.

Latest news on the Q^2 evolution of F_2^γ

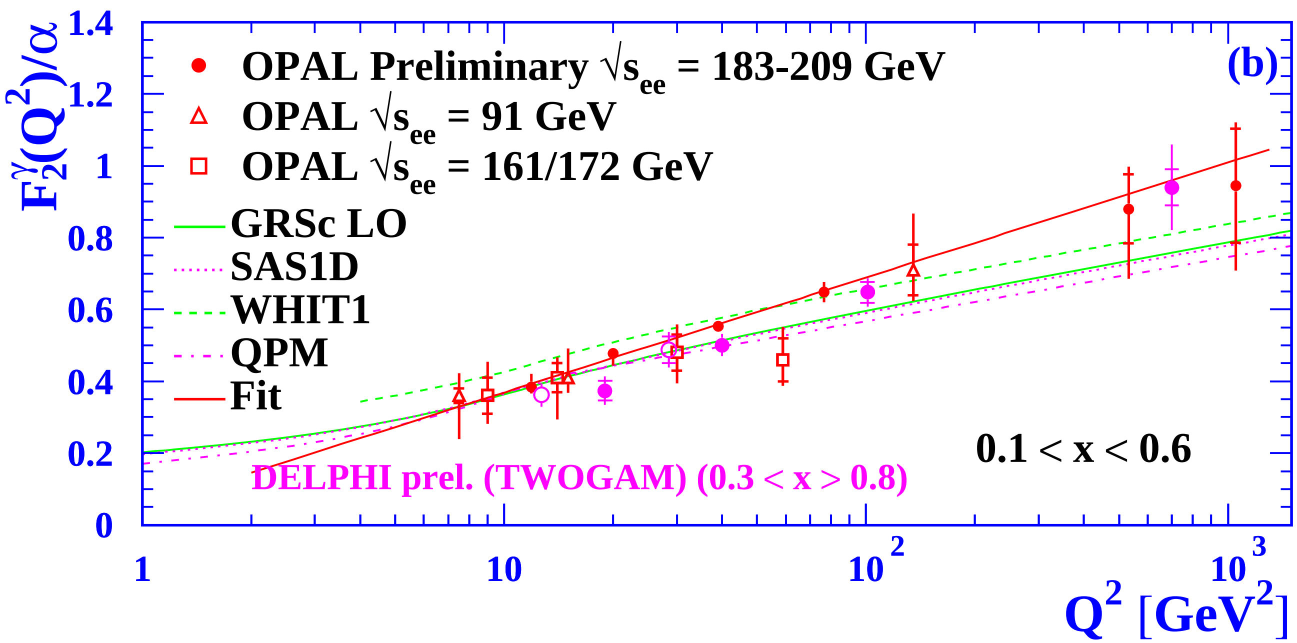

1) The errors have been reduced to about 5-10% at Q^2 around 10-100 GeV^2.

2) The measurements start to challenge theoretical predictions.

3) We need to worry more about the virtuality suppression of $F_2^\gamma(x, Q^2, P^2)$ and radiative corrections.

The future of the F_2^γ measurement

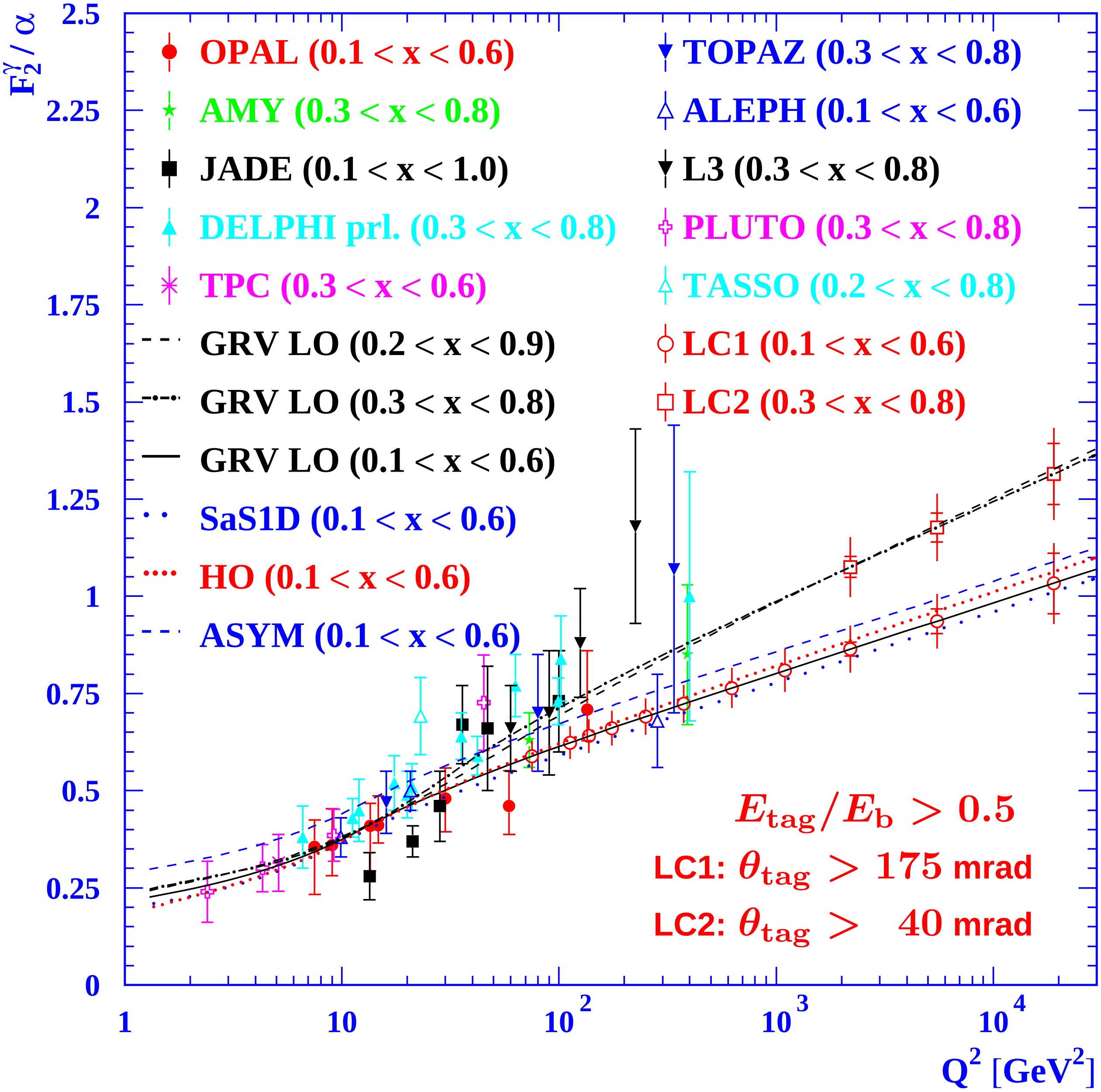

The Linear Collider will play an important role in testing this fundamental prediction of perturbative QCD.

Photon spectra for F_2^γ measurements

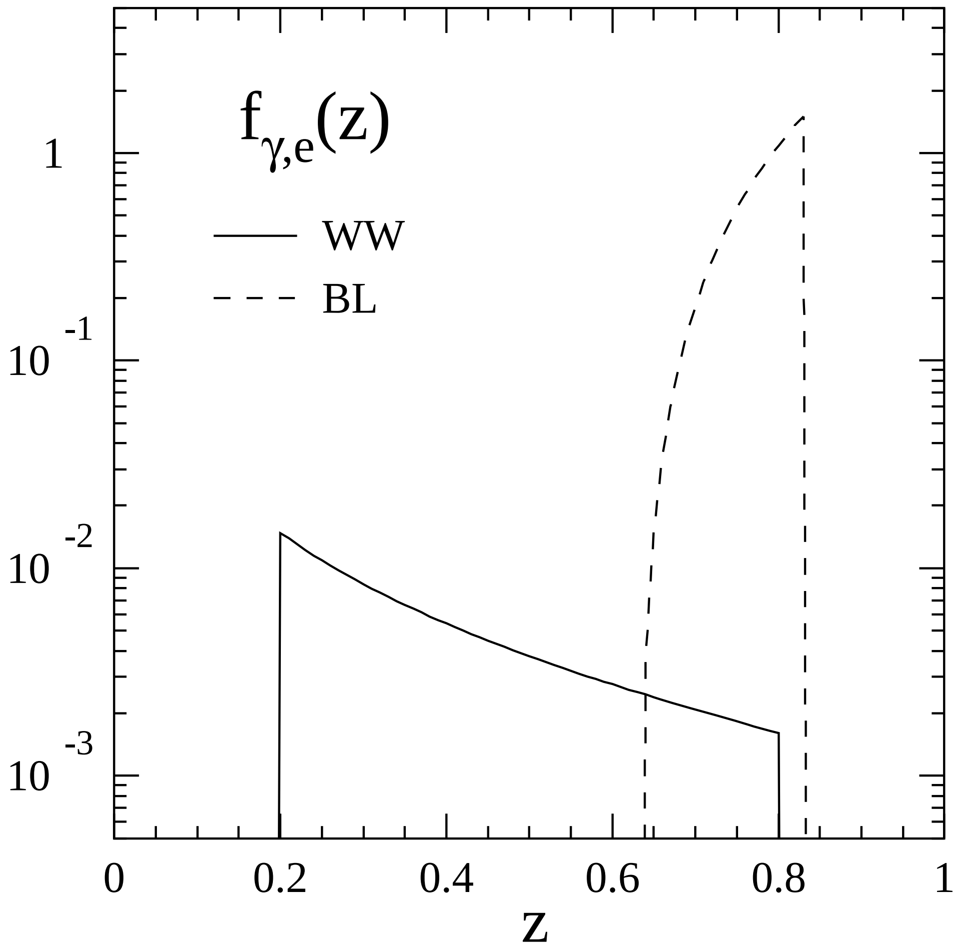

Used parameters:

LC(WW): $\epsilon = 10\%$ **for tagging the electron that radiated the quasi-real photon**

PC(BL): $E_\gamma \approx 0.8 E_{\mathrm{b}}$ **and** $\Delta E_\gamma \approx 0.1 E_\gamma$

Further assumptions:

$E_{\mathrm{tag}} > 50\,\mathrm{GeV}$ **and** $\sigma_{\mathrm{sys}} = \max(3\%, \sigma_{\mathrm{stat}})$

The W reconstruction

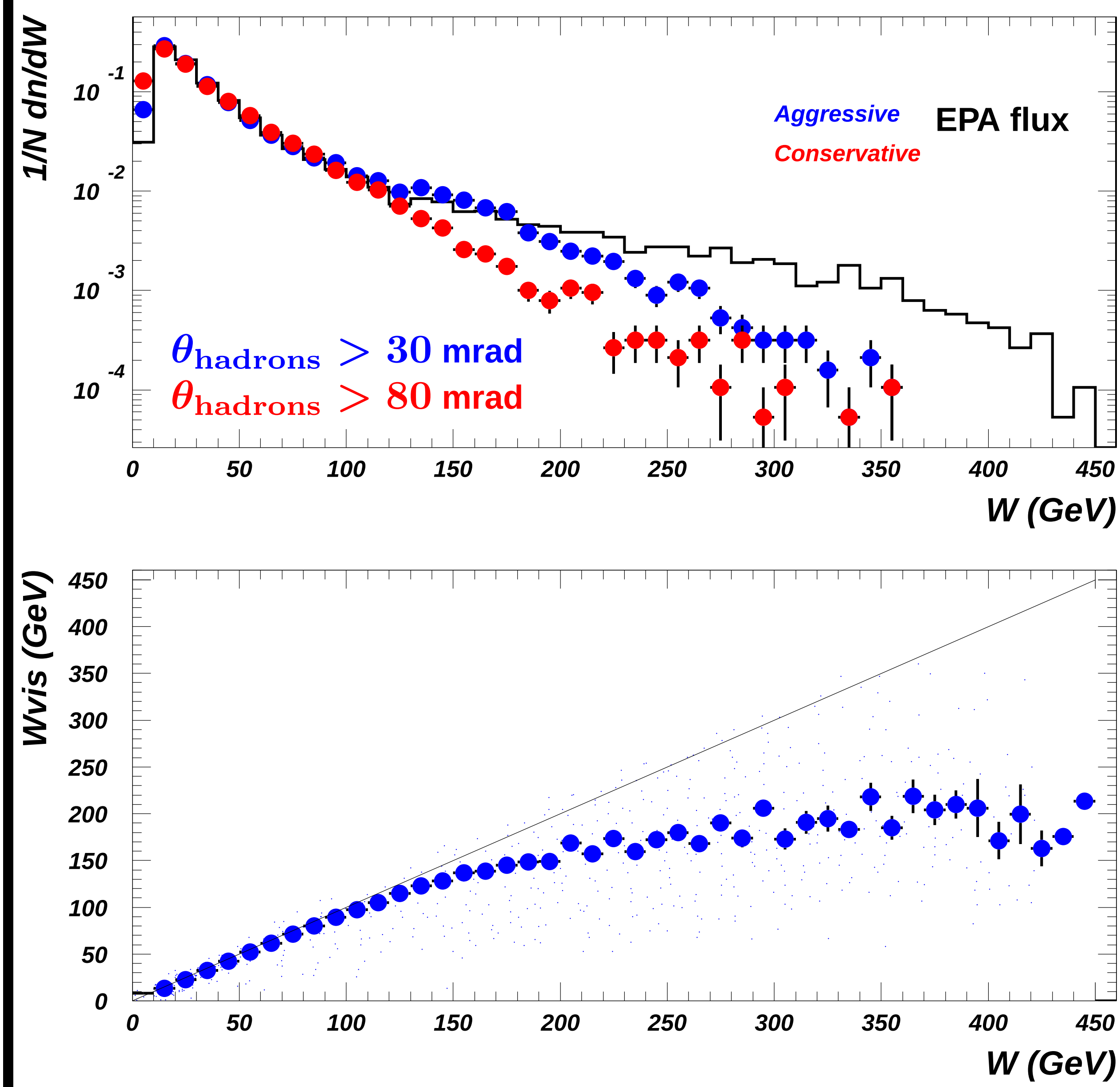

As usual, the forward region is vital for good W reconstruction.

The x reconstruction

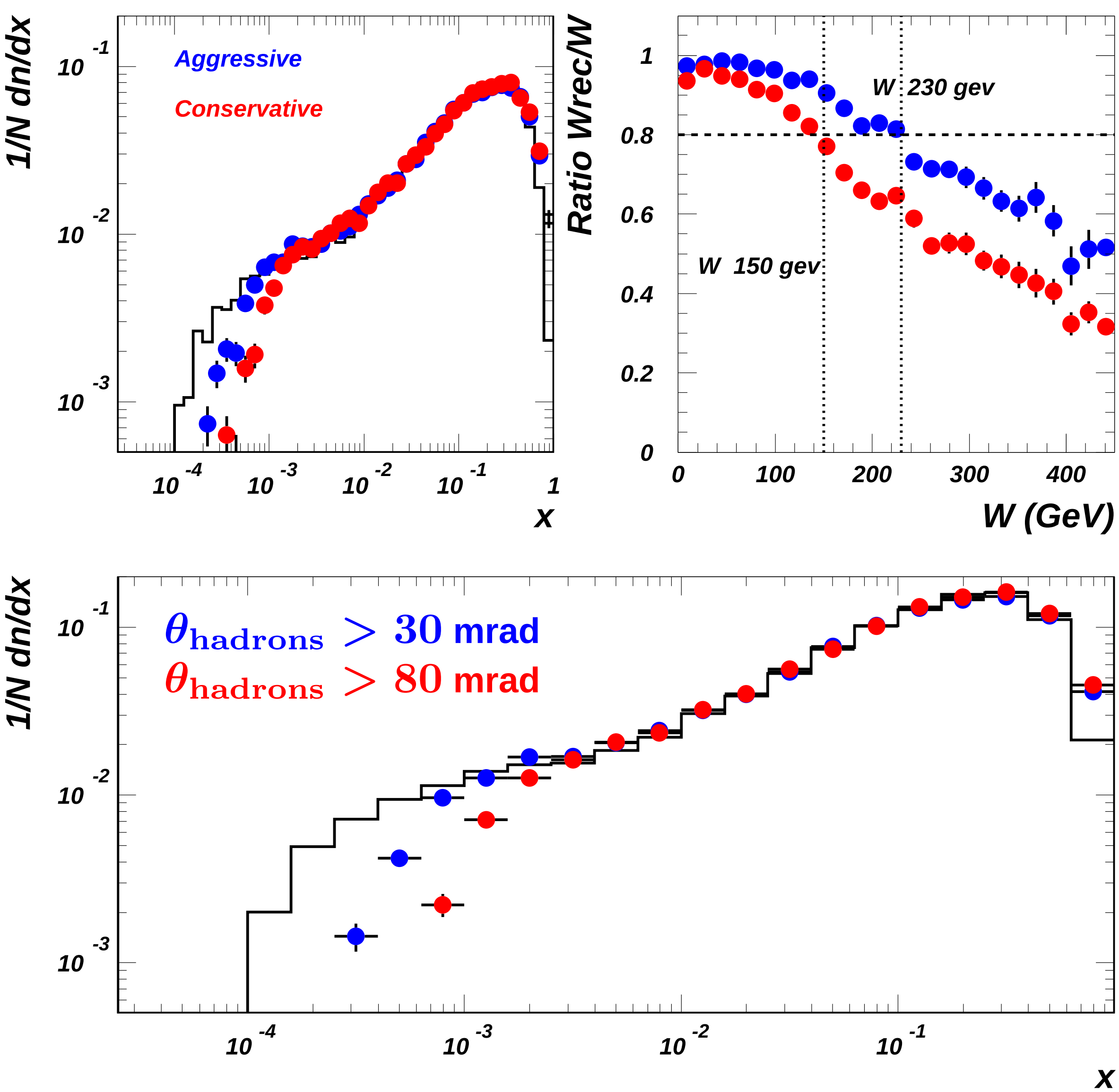

For $\frac{W_{\mathrm{vis}}}{W} > 0.8$ the reach in x is $4 \cdot 10^{-4}$ or 10^{-3} for $\theta_{\mathrm{hadrons}} > 30$ or 80 mrad.

The x and Q^2 reach for F_2^γ at a Photon Collider (I)

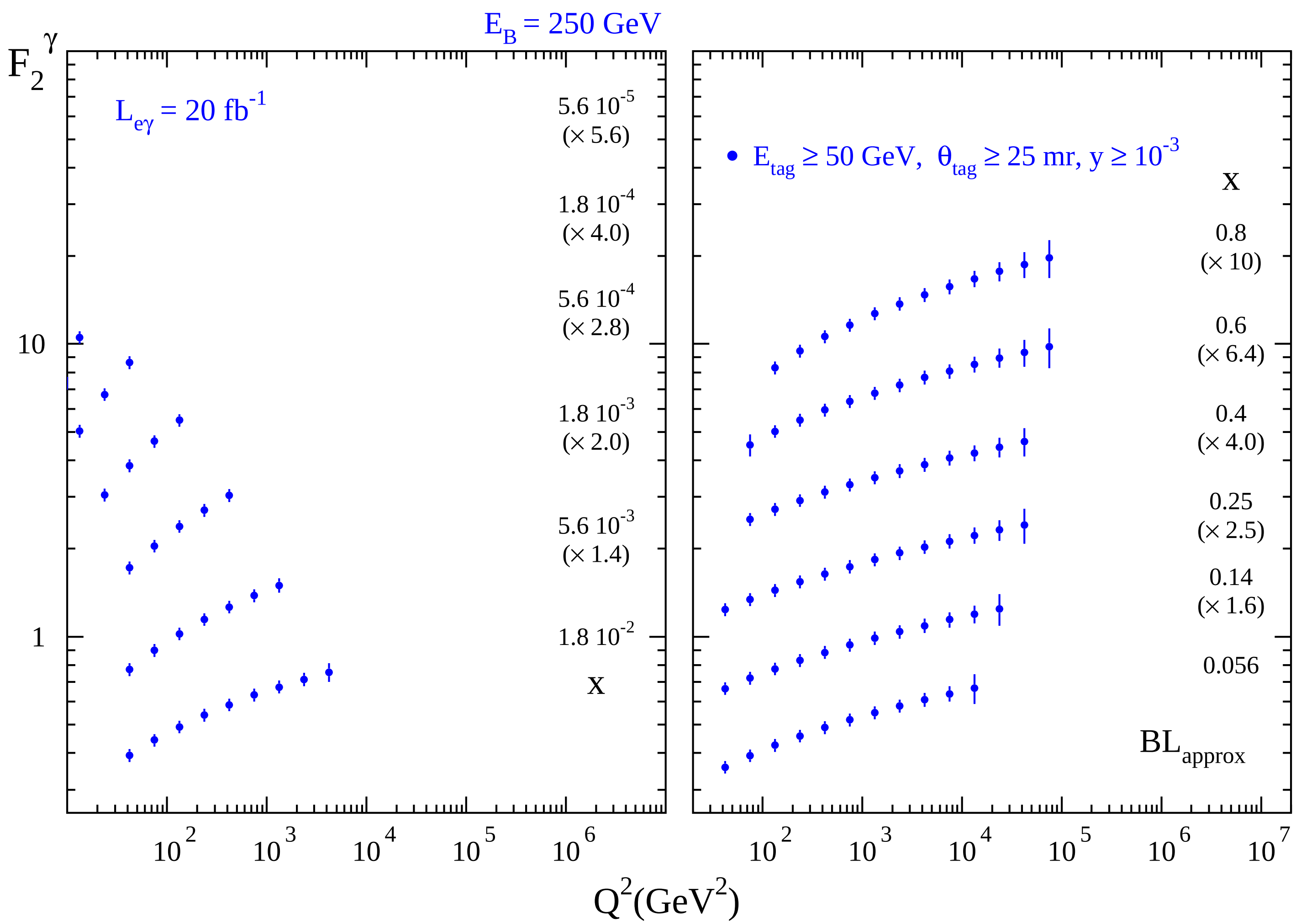

The phase space will be extended both to lower x and larger Q^2.

The x and Q^2 reach for F_2^γ at a Photon Collider (II)

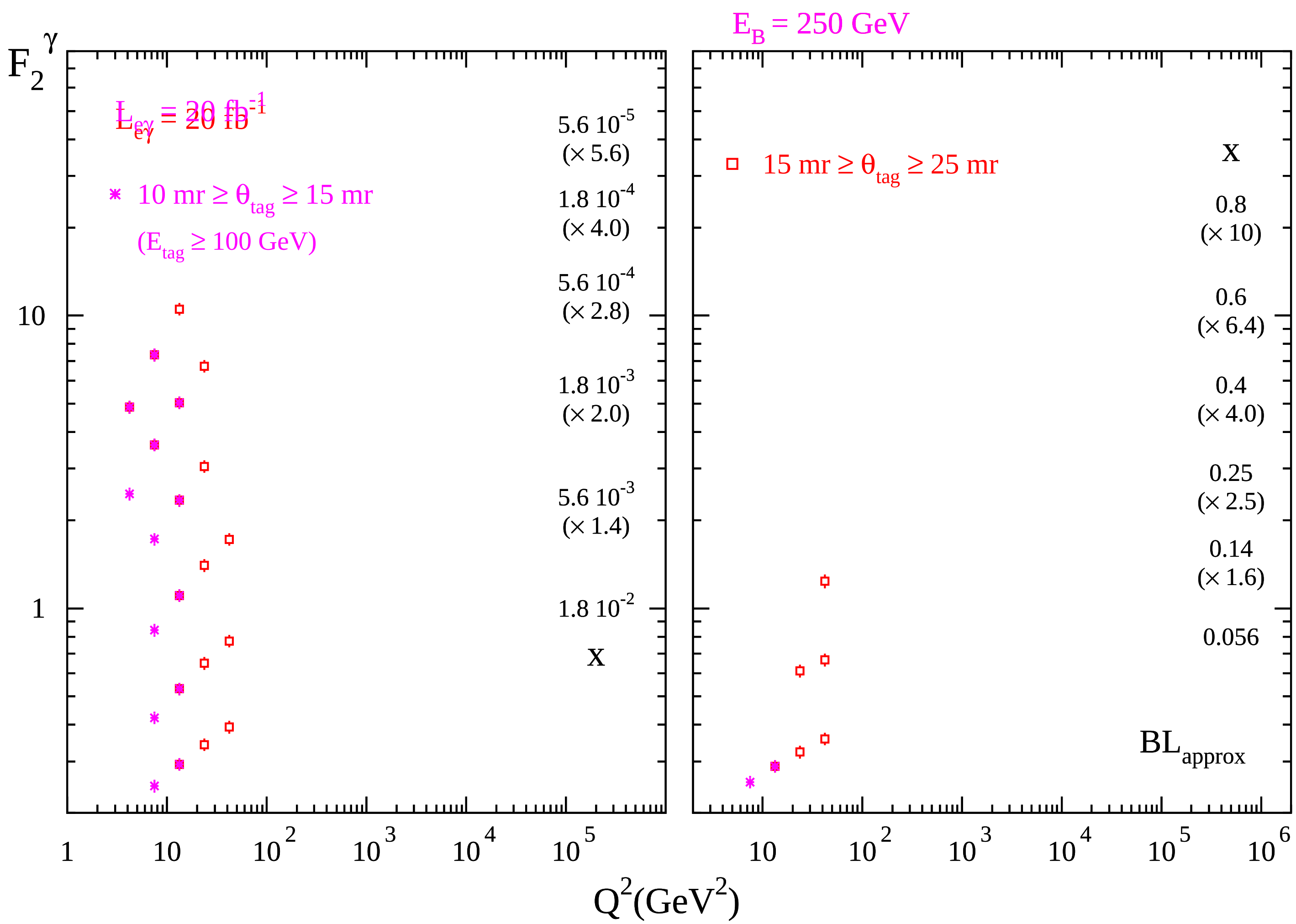

Never stop dreaming!

The sensitivity to α_s at large x

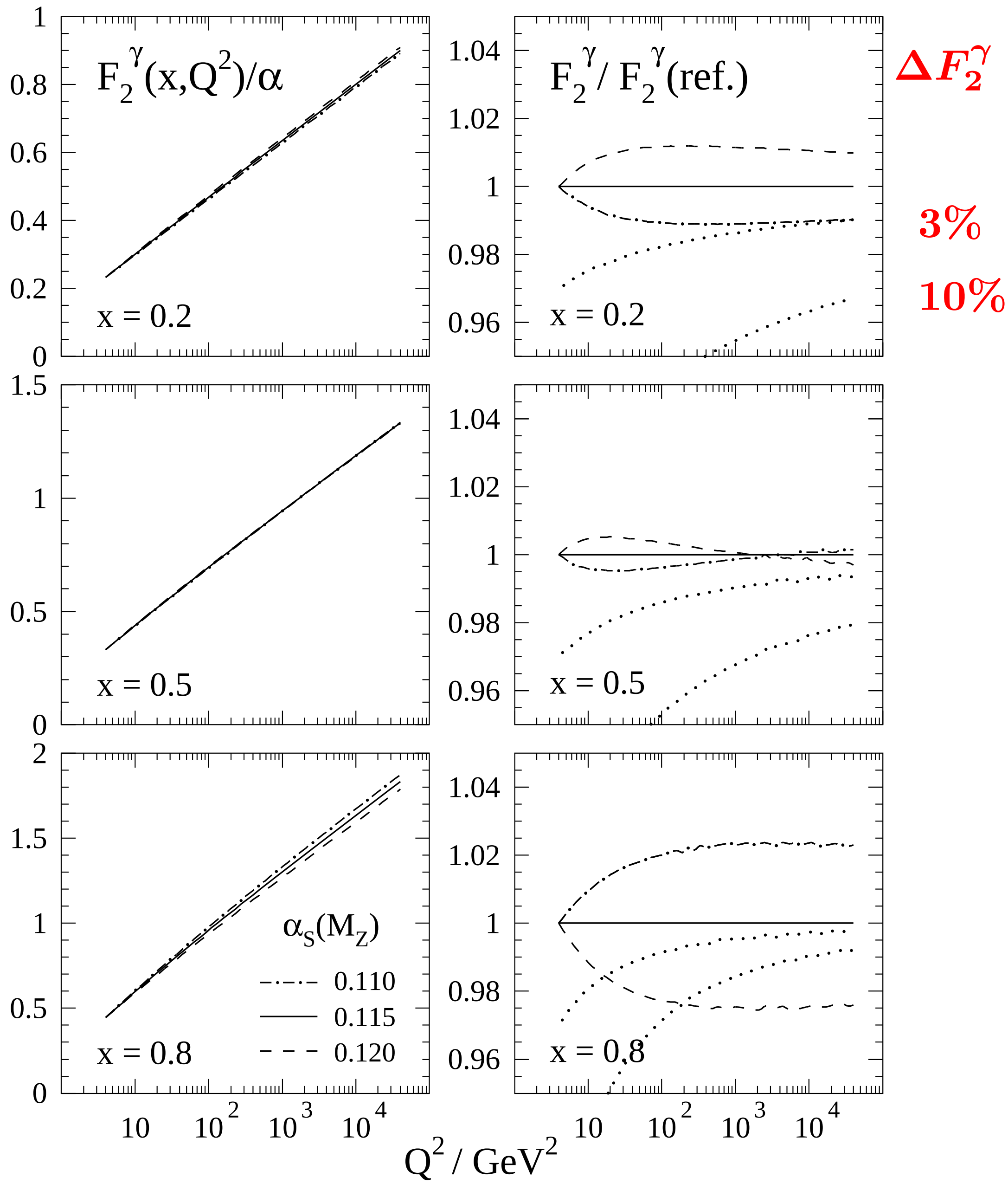

The normalisation of F_2^γ depends on α_s.

However, only very small effects are predicted:
e.g. at $x = 0.8$ a variation of $\Delta\alpha_s = 5\%$ means $\Delta F_2^\gamma = 3\%$. This will be hard to measure.

Flavour decomposition of F_2^γ

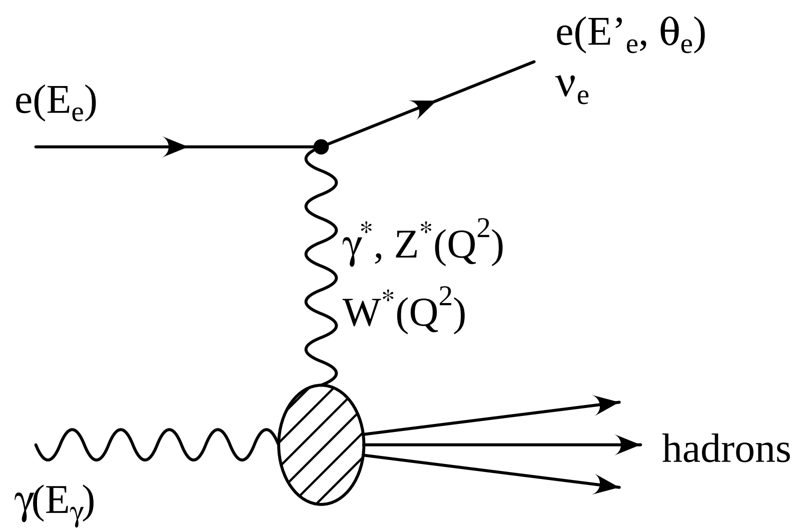

$$\frac{d\sigma}{dx\,dy}(e\gamma \to eX) \;\propto\; \sum_{q=u..}^{b} \hat{e}_q^2\, x\, q(x, Q^2)$$

$$\frac{d\sigma}{dx\,dy}(e\gamma \to \nu_e X) \;\propto\; x\,\left[(u+c) + (1-y)^2\,(d+s)\right]$$

Effective charge and cross-section

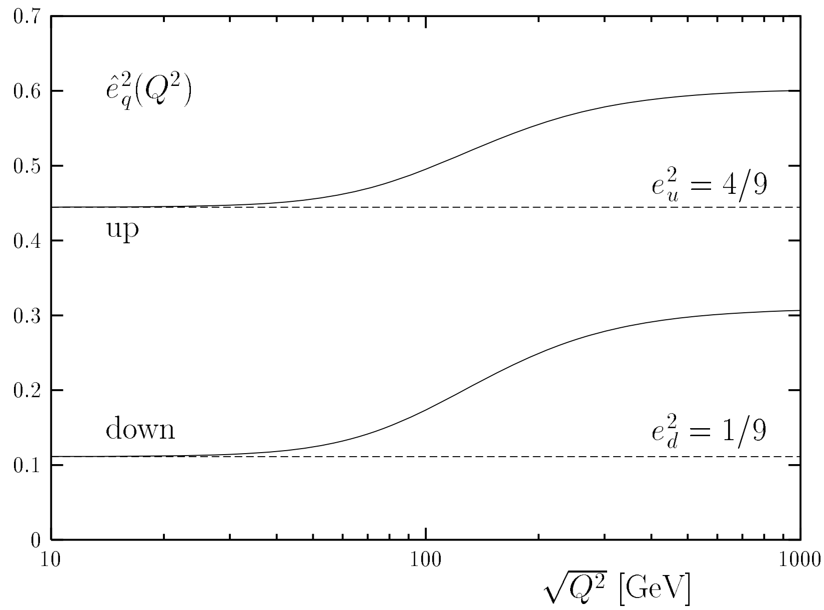

$0.44 \longrightarrow 0.60$

$0.11 \longrightarrow 0.31$

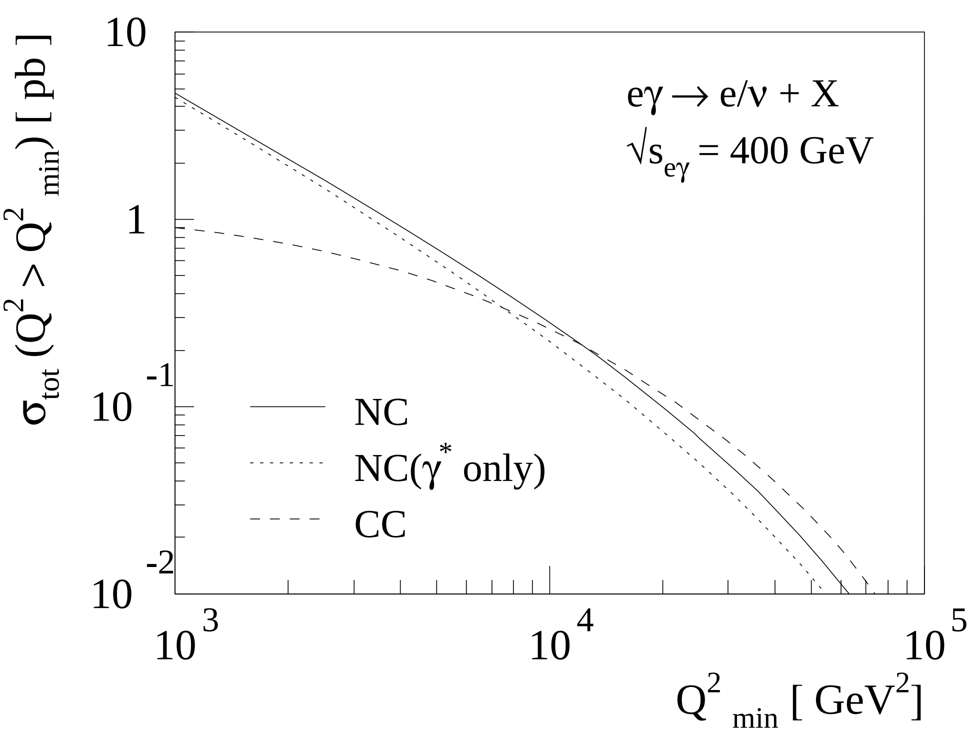

This gives 10^4 CC and $4 \cdot 10^4$ NC events per year.

Predictions of the u to d ratio

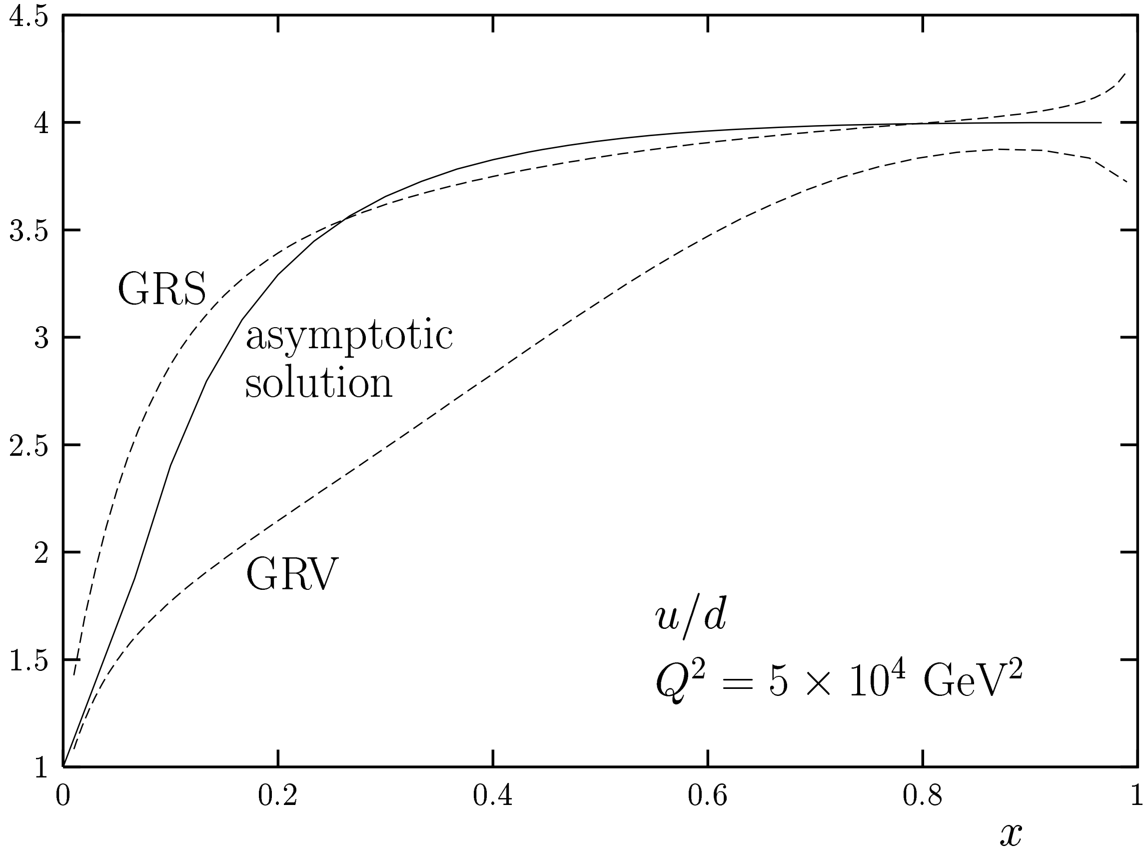

At present the predictions for the u to d ratio vary within a factor of 2 to 3.

Polarized parton distributions

Definition: $\Delta f^{\gamma} \equiv f_{+}^{\gamma +} - f_{-}^{\gamma +}$ for $f = q, \bar{q}, g$

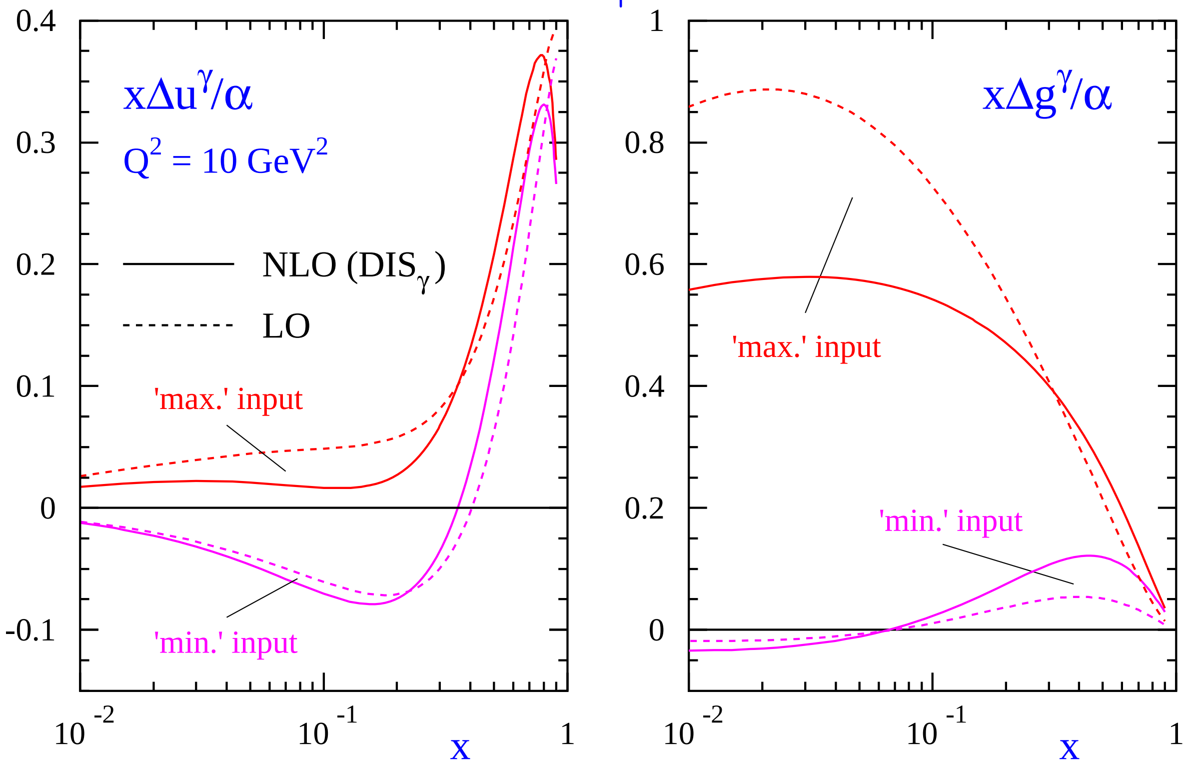

Asymmetries: $\frac{\Delta\sigma}{\sigma} \equiv \frac{\sigma(++)-\sigma(+-)}{\sigma(++)+\sigma(+-)}$

At present we have NO experimental information on Δf^{γ}.

Constraint: $\Delta\sigma \leq \sigma \Rightarrow |\Delta f^{\gamma}(x,Q^2)| \leq f^{\gamma}(x,Q^2)$

Fullfilled for $\Delta f^{\gamma}_{\mathrm{point-like}}$ but needs to be enforced for $\Delta f^{\gamma}_{\mathrm{hadron-like}}$.

Choices:

$$\Delta f^{\gamma}_{\mathrm{hadron-like}}(x,\mu^2) = \begin{cases} f^{\gamma}(x,\mu^2) & \text{('max input')} \\ 0 & \text{('min input")} \end{cases}$$

Experimental information is highly desirable.

The ratio g_1^γ / F_1^γ from DIS

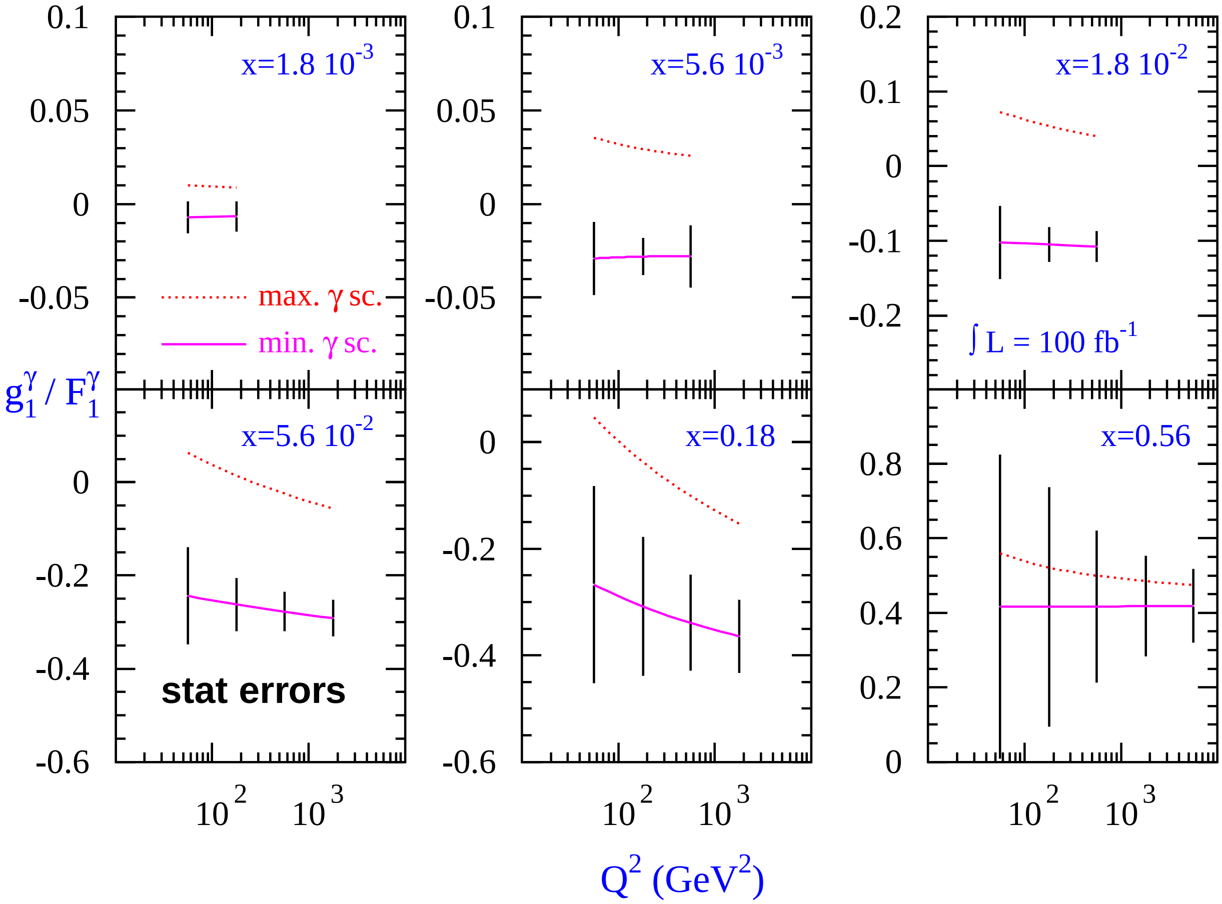

Asymmetry: $\frac{\Delta\sigma}{\sigma} \propto \frac{g_1^\gamma}{F_1^\gamma}$

with: $g_1^\gamma \propto \Delta q^\gamma + \alpha_s \Delta g^\gamma$

The structure function g_1^γ is mainly sensitive to quarks. Use F_1^γ from unpolarized DIS to determine the polarized distribution function Δq^γ.

The di-jet sensitivity to Δg^{γ}

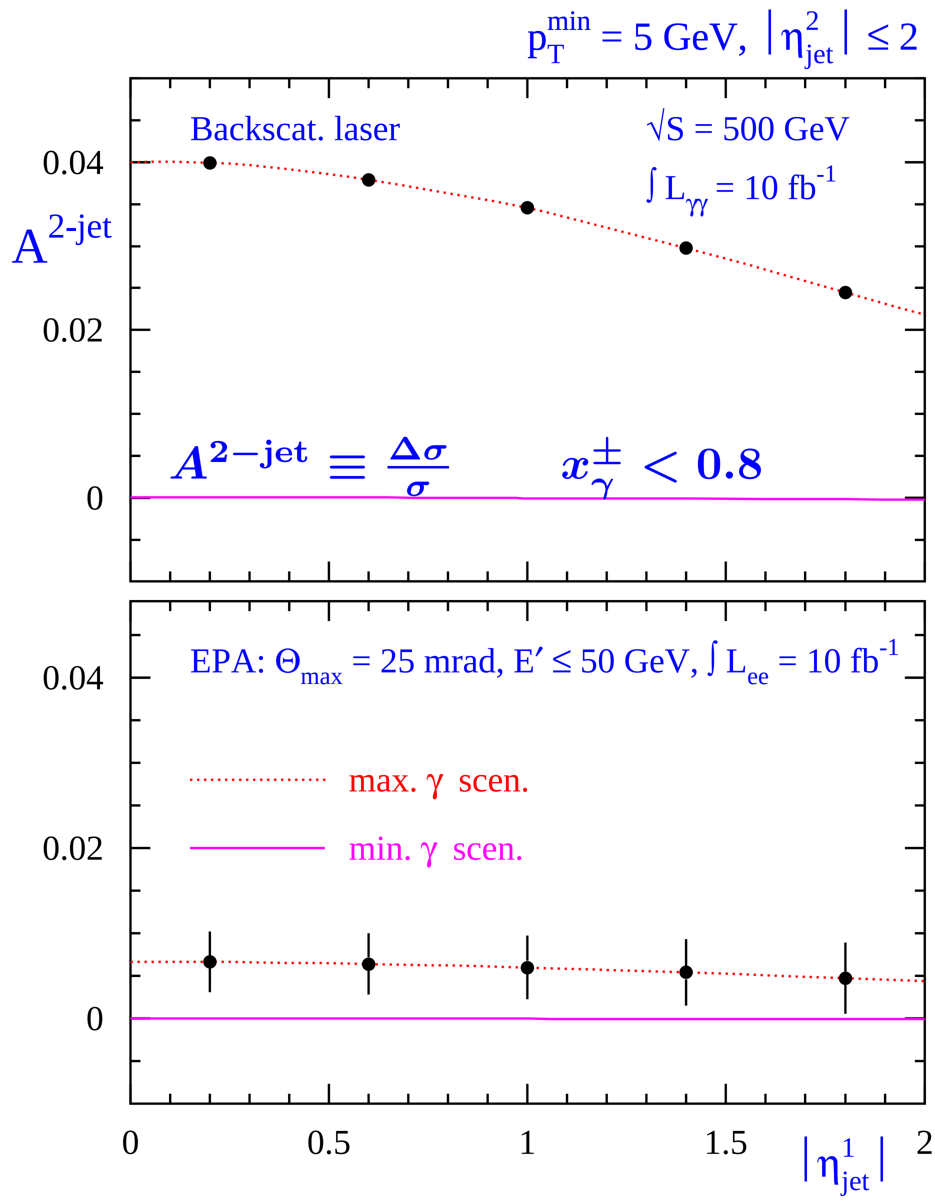

For double-resolved events $A^{2-\text{jet}}$ is mainly sensitive to $gg \longrightarrow q\bar{q}$, but also other processes contribute.

$\Rightarrow$ Use effective parton distribution function.

Extract Δg^{γ} from $A^{2-\text{jet}}$ together with Δq^{γ} obtained from DIS. A Photon Collider is probably needed.

F_2^γ for virtual photons

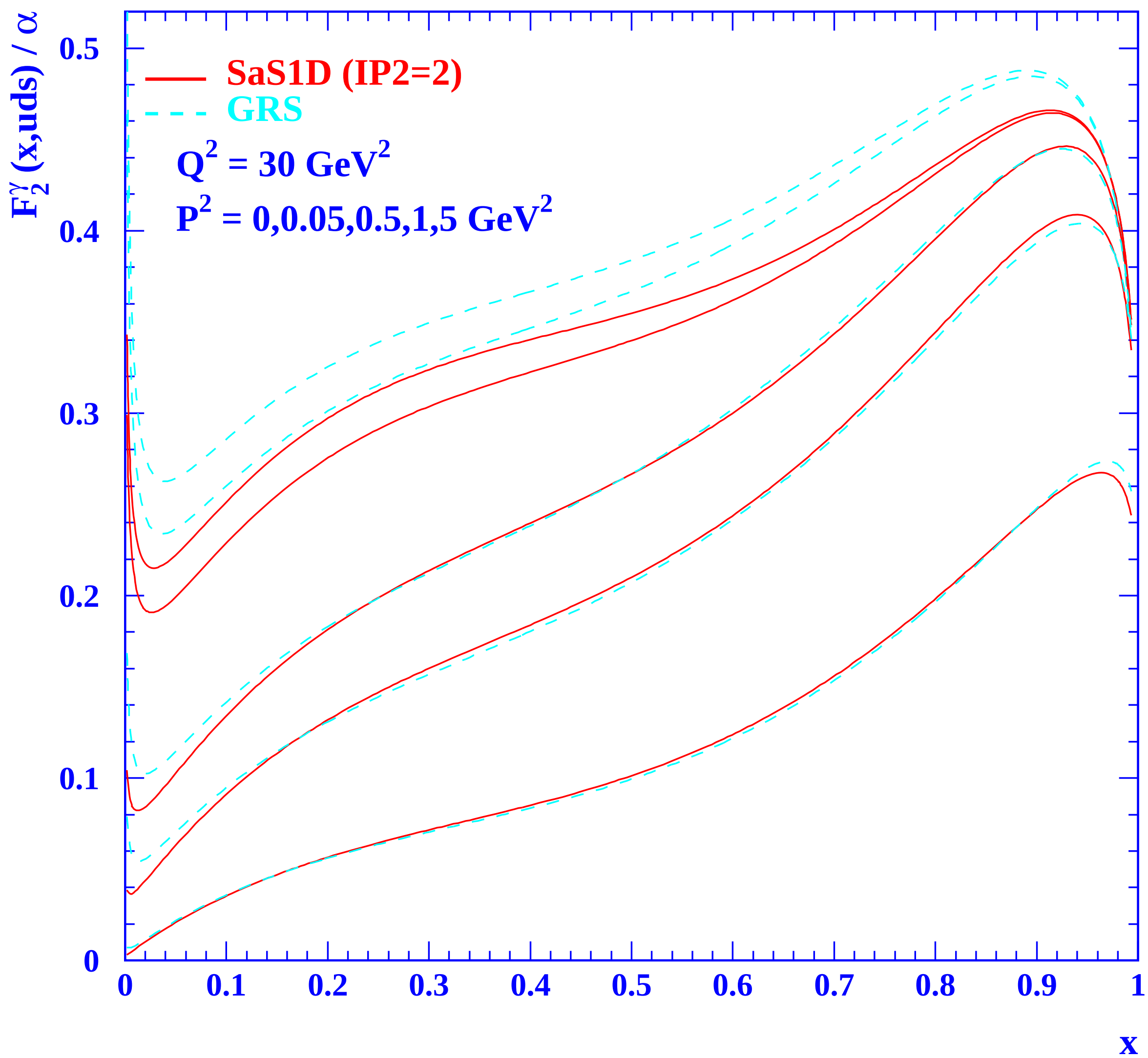

The absolute predictions agree for $P^2 > 0.5\ \mathrm{GeV}^2$, when using SaS1D ($IP2 = 2$)

The double tag limit: $Q^2, P^2 \gg m_e^2, \frac{\rho_i^{00}}{2\rho_i^{++}} \to 1$

$$\mathrm{d}^6\sigma = \frac{\mathrm{d}^3\mathrm{p}_1'\mathrm{d}^3\mathrm{p}_2'}{E_1'E_2'} \frac{\alpha^2}{16\pi^4 q^2 p^2} \left[\frac{(q\cdot p)^2 - q^2p^2}{(p_1\cdot p_2)^2 - m_e^2 m_e^2}\right]^{1/2} 4\rho_1^{++}\rho_2^{++} \cdot \left(\sigma_{TT} + \sigma_{TL} + \sigma_{LT} + \sigma_{LL} + \frac{1}{2}\tau_{TT}\cos 2\bar{\phi} - 4\tau_{TL}\cos\bar{\phi}\right)$$

$$\mathrm{d}^6\sigma = \frac{\mathrm{d}^3\mathrm{p}_1'\mathrm{d}^3\mathrm{p}_2'}{E_1'\,E_2'} \mathcal{L}_{TT}\,\sigma_{\gamma^\star\gamma^\star}\,,$$

$$\mathrm{d}^6\sigma = L_{TT}\,\sigma_{\gamma^\star\gamma^\star}$$ with: $$L_{TT} = \int \frac{\mathrm{d}^3\mathrm{p}_1'\mathrm{d}^3\mathrm{p}_2'}{E_1'\,E_2'}\mathcal{L}_{TT}$$

The Measurements of F_{eff}^{γ}

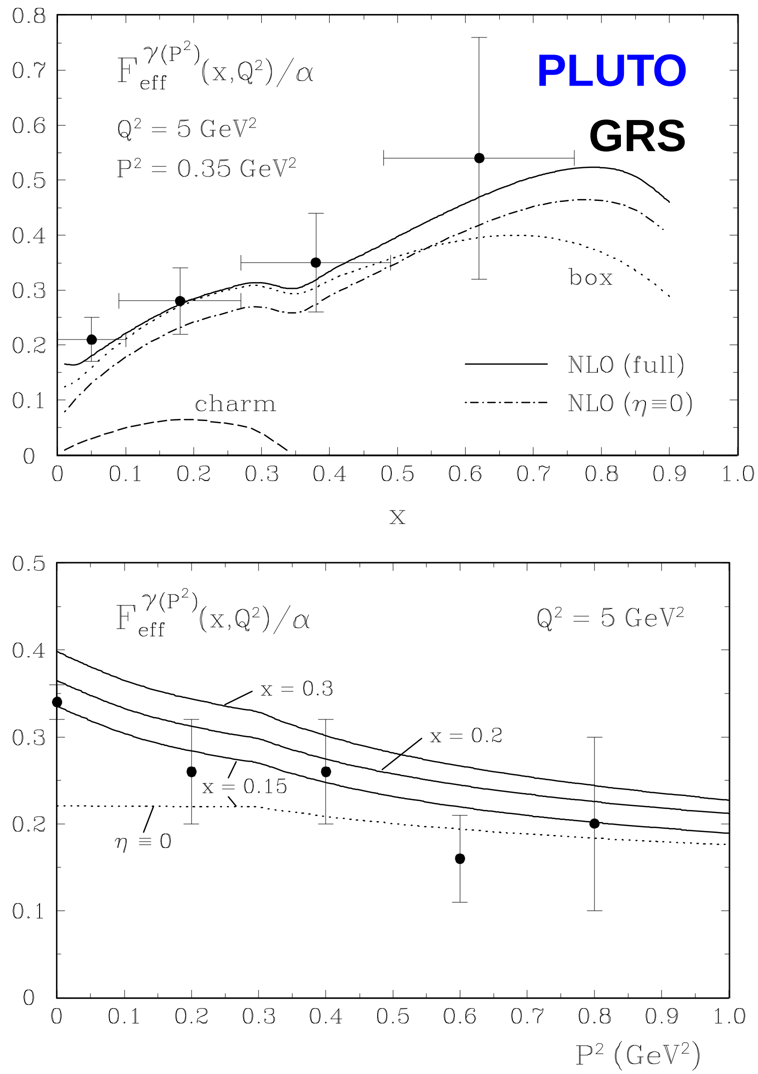

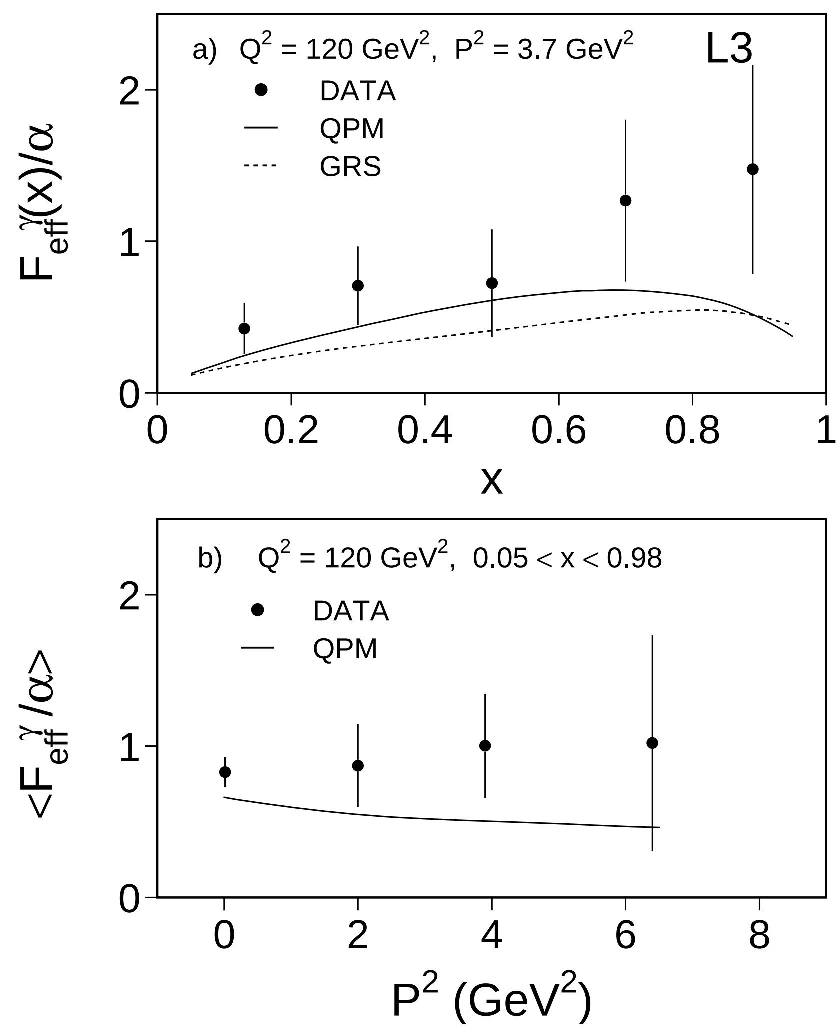

The cross-section for double tags for $e^+e^- \xrightarrow{\gamma^\star\gamma^\star} e^+e^-\mu^+\mu^-$

OPAL

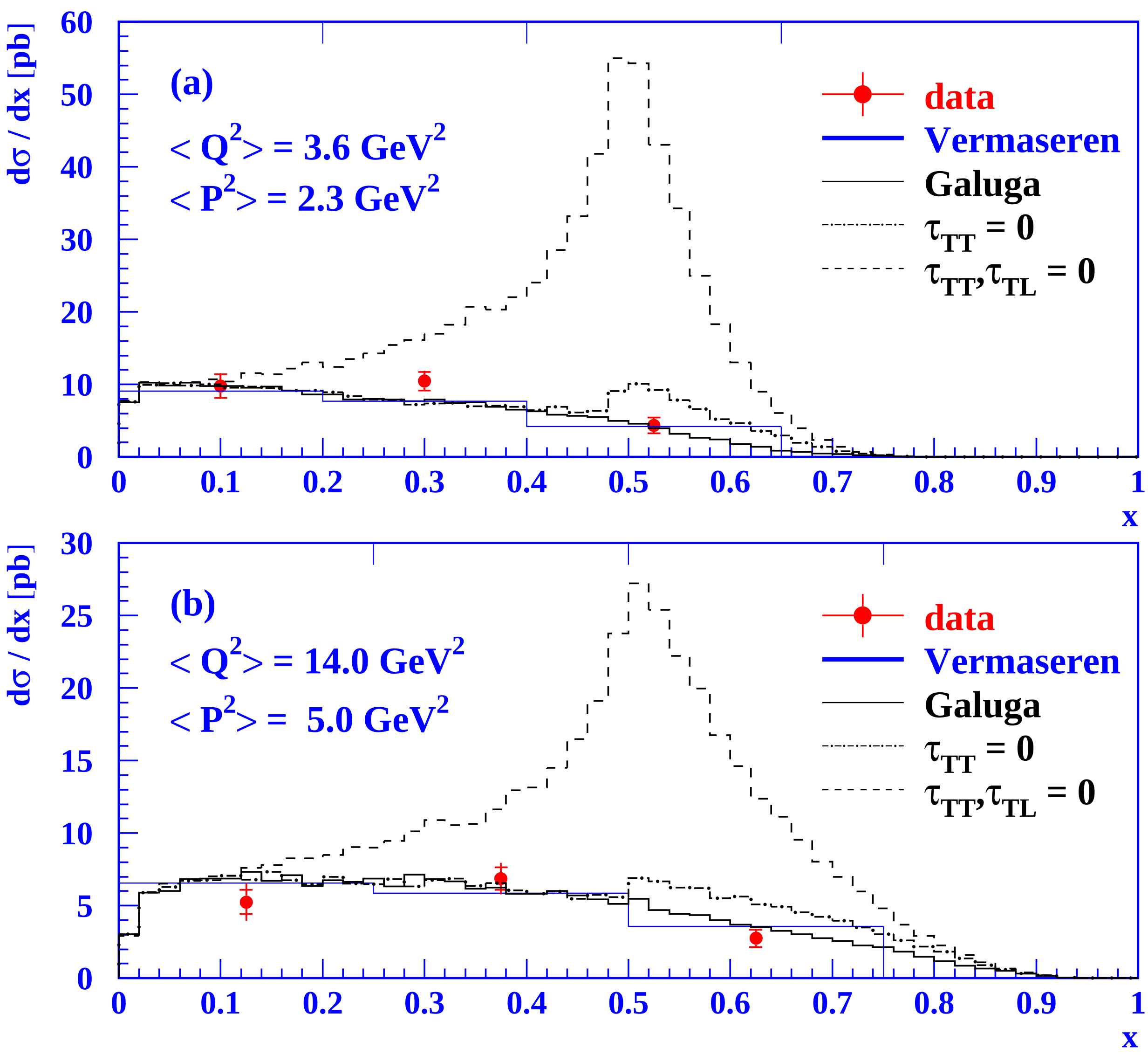

QED agrees well with the data and the presence of the interference terms is clearly seen for the first time.

$\sigma_{\gamma^\star\gamma^\star}$ as a signal of BFKL

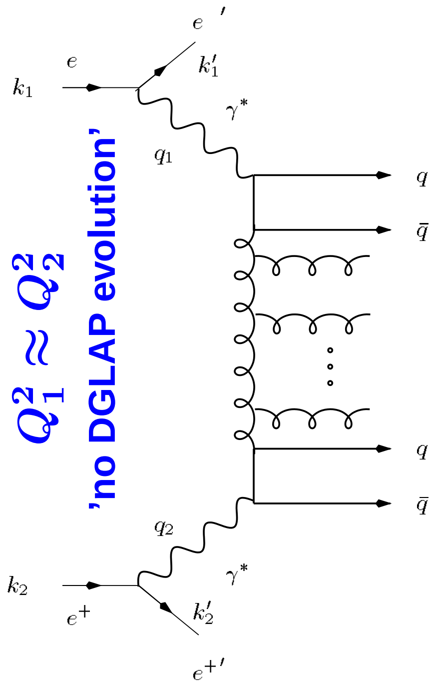

$$y_1 = \frac{q_1 k_2}{k_1 k_2}\,, \quad Q_1^2 = -q_1^2$$

$$s = (k_1 + k_2)^2, s_0 = \frac{\sqrt{Q_1^2 Q_2^2}}{y_1 y_2}$$

$$\hat{s} = W^2 \approx s\, y_1 y_2$$

1) Take $Q_i^2 \gg \Lambda^2_{\rm QCD}$ and $Q_1^2 \approx Q_2^2$ to allow for a perturbative prediction without DGLAP evolution.

2) Look at a region where the phase space for gluon emission is large $\Rightarrow$ $W^2 \gg Q_1^2, Q_2^2$.

3) Define:

$$Y = \ln\left(\frac{s y_1 y_2}{\sqrt{Q_1^2 Q_2^2}}\right) \simeq \ln\left(\frac{W^2}{\sqrt{Q_1^2 Q_2^2}}\right) = \overline{Y}\,,$$

and measure the cross-section as a function of $Y\,or\,\overline{Y}$.

The importance of QED radiative corrections

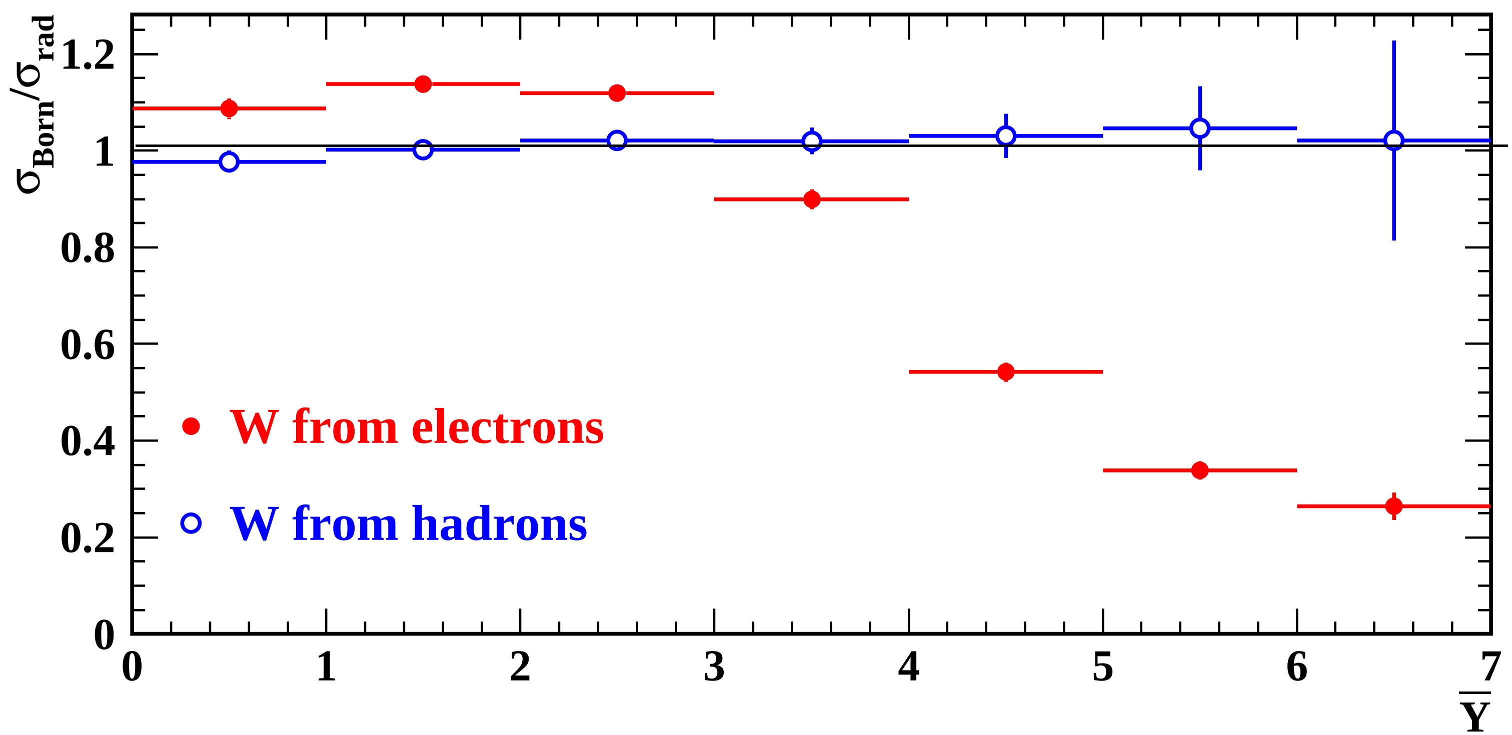

Radiative corrections are only important for the electron method, and they are large at large Y which means at low electron energies.

$\sigma_{\gamma^\star\gamma^\star}$ from OPAL

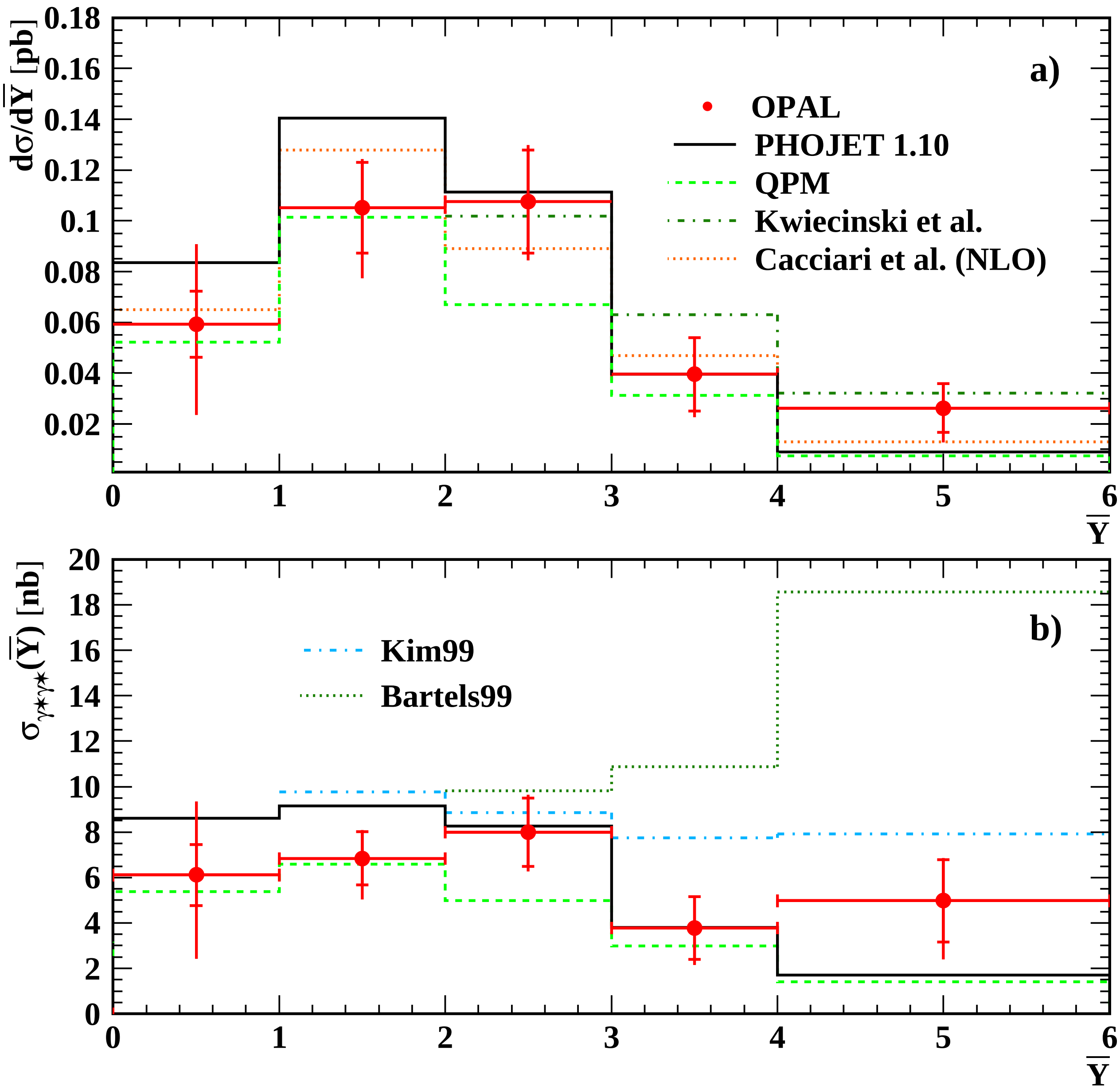

1) **Bartels99** ⇒ **LO BFKL is too high.**

2) **Cacciari et. al** ⇒ **NLO DGLAP QCD is sufficient.**

3) **Kwiecinski et. al** ⇒ **HO BFKL also fits the data.**

Double tag hadronic cross-section from L3

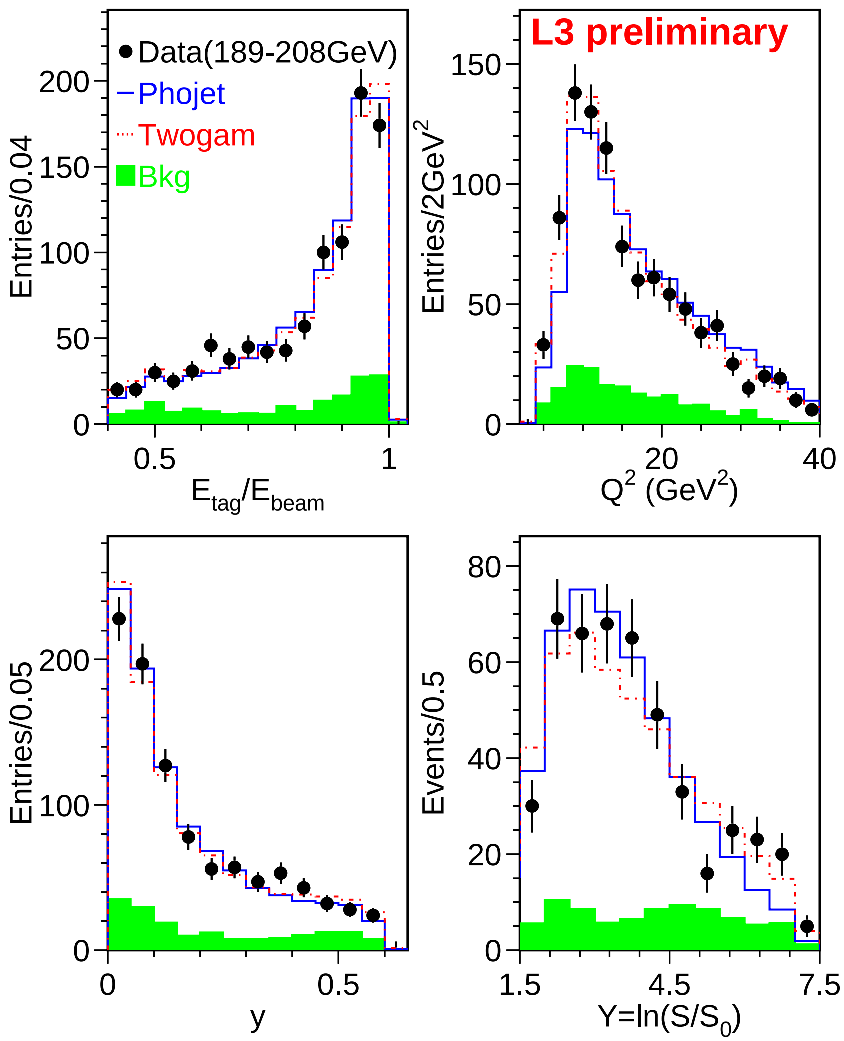

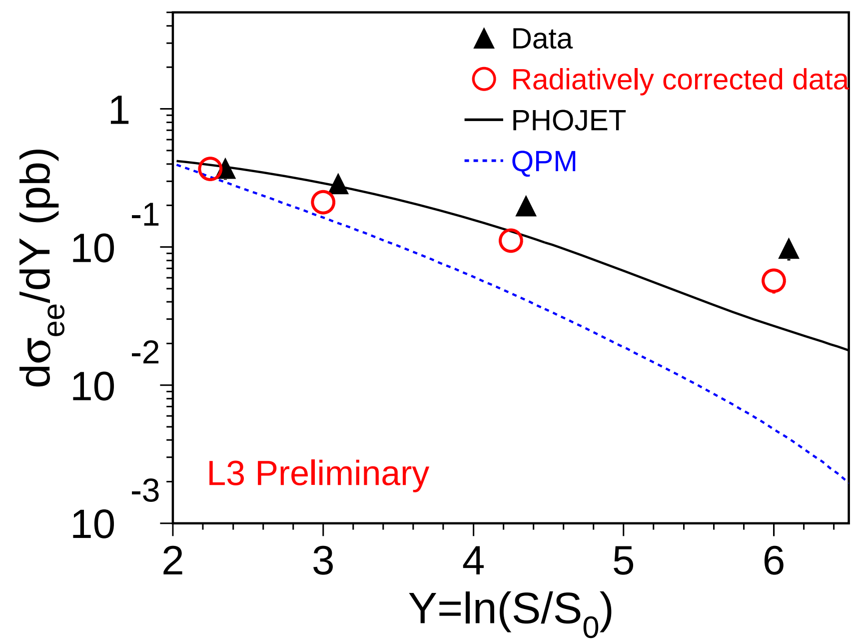

Some excess is seen at large Y

BFKL expectation for large W

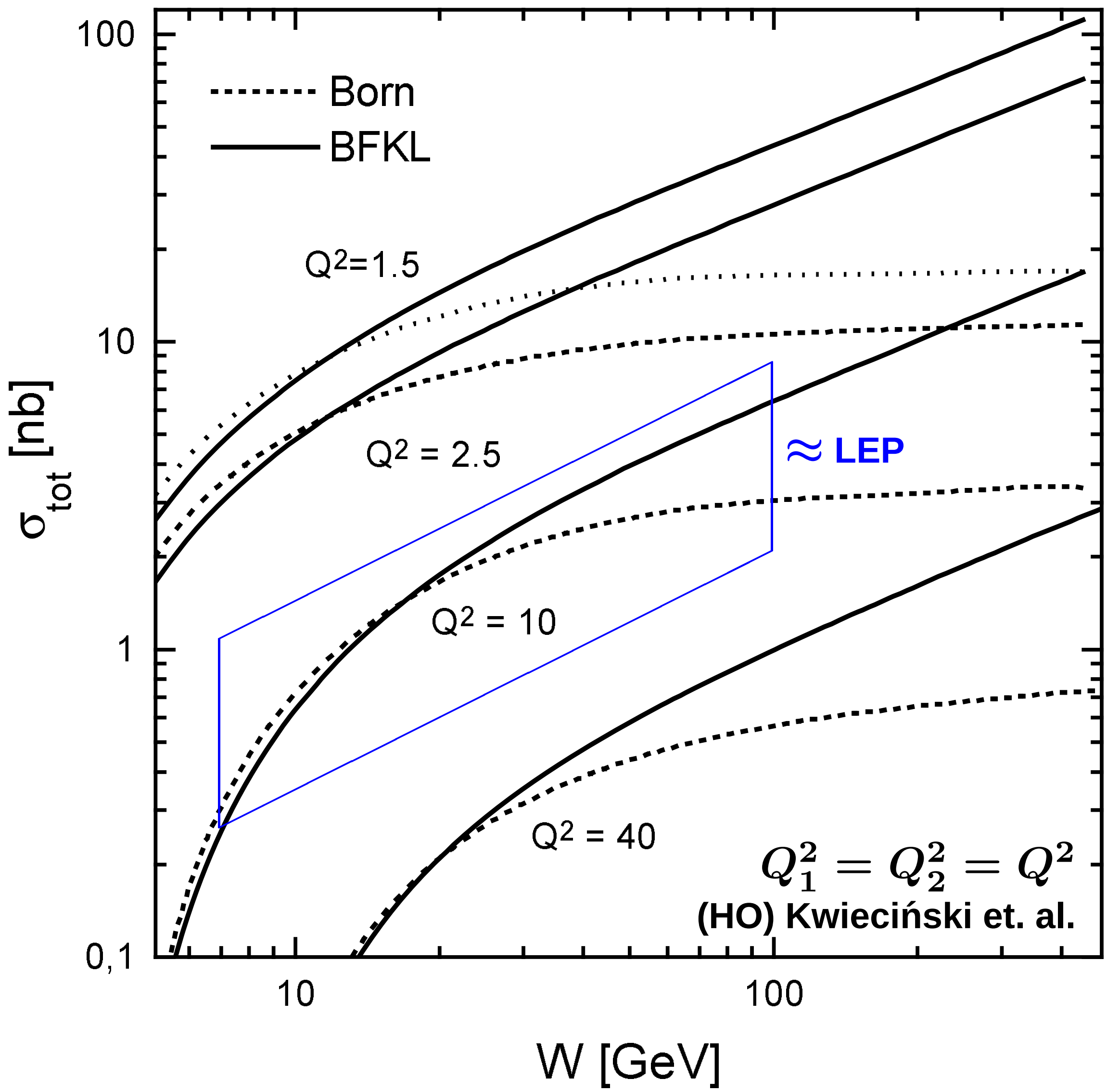

1) LEP probes the region for W up to about 100 GeV and $\langle Q^2 \rangle \approx 15\,\mathrm{GeV}^2$.
2) The Linear Collider will extend the region to larger W^2 for moderate Q^2, giving access to large Y.

QCD Pomeron and J/ψ production

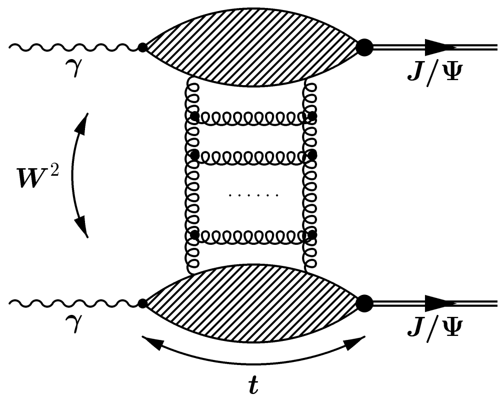

$\sigma(\gamma\gamma \to J/\psi\, J/\psi)$

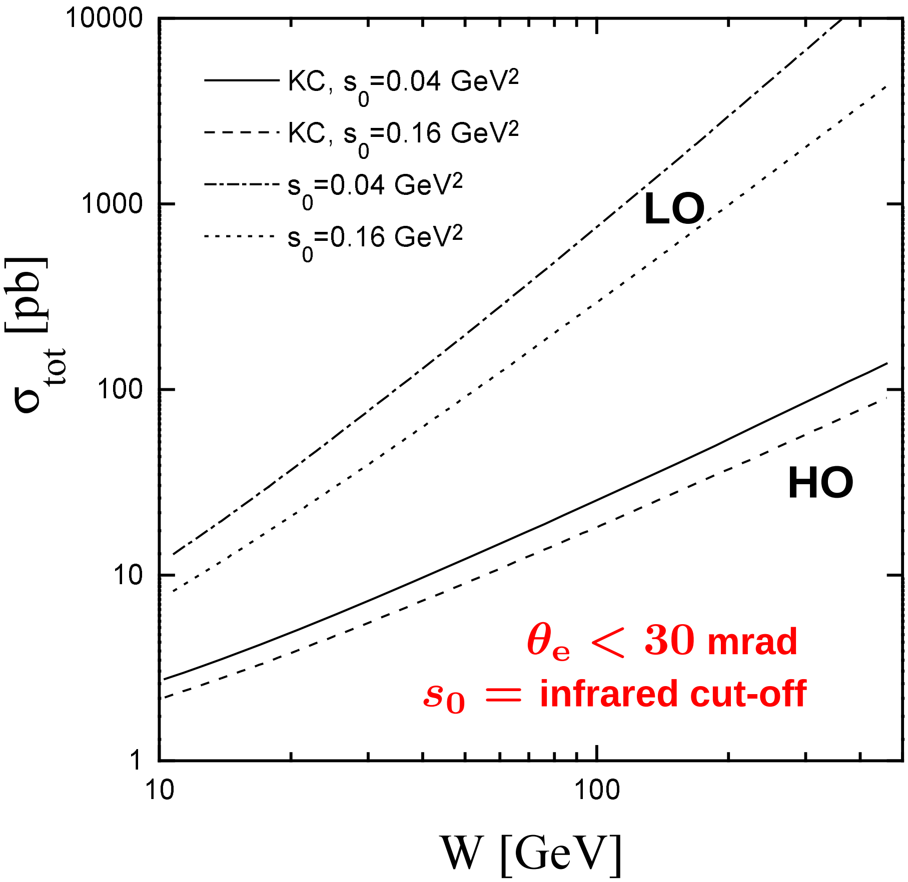

$\sigma(e^+e^- \longrightarrow e^+e^- J/\psi\, J/\psi) = 0.75$ pb.

This yields 75k events for $\mathcal{L}_{int} = 100\ fb^{-1}$, but the J/ψ are mainly produced at low angles $\Rightarrow$ acceptance?

Properties of $\mathrm{J}/\psi\,\mathrm{J}/\psi \to 4\mu$

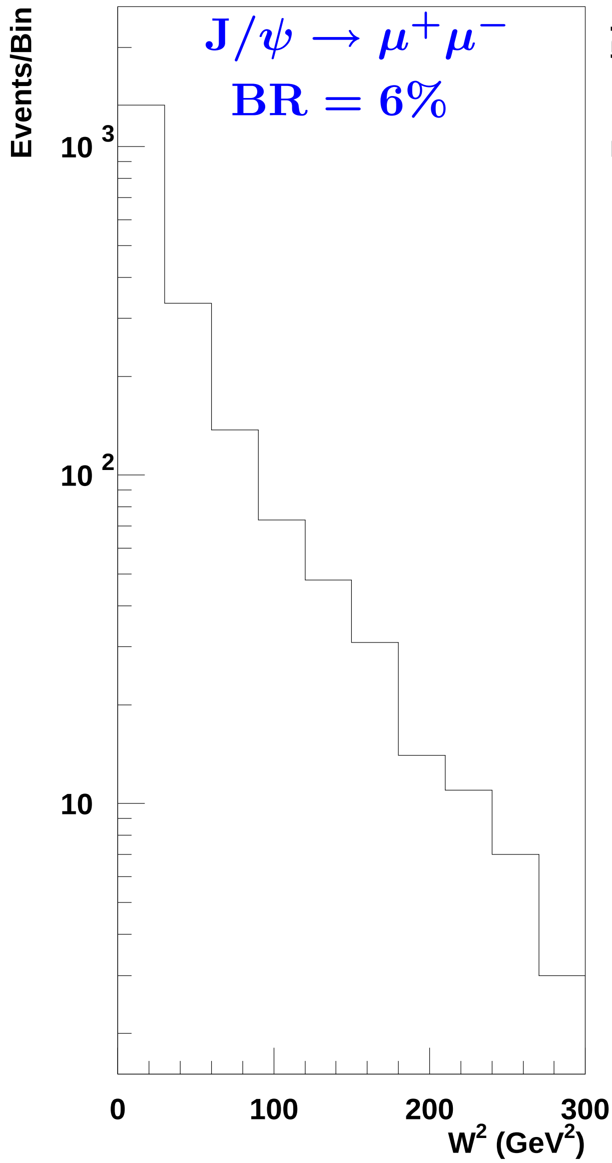

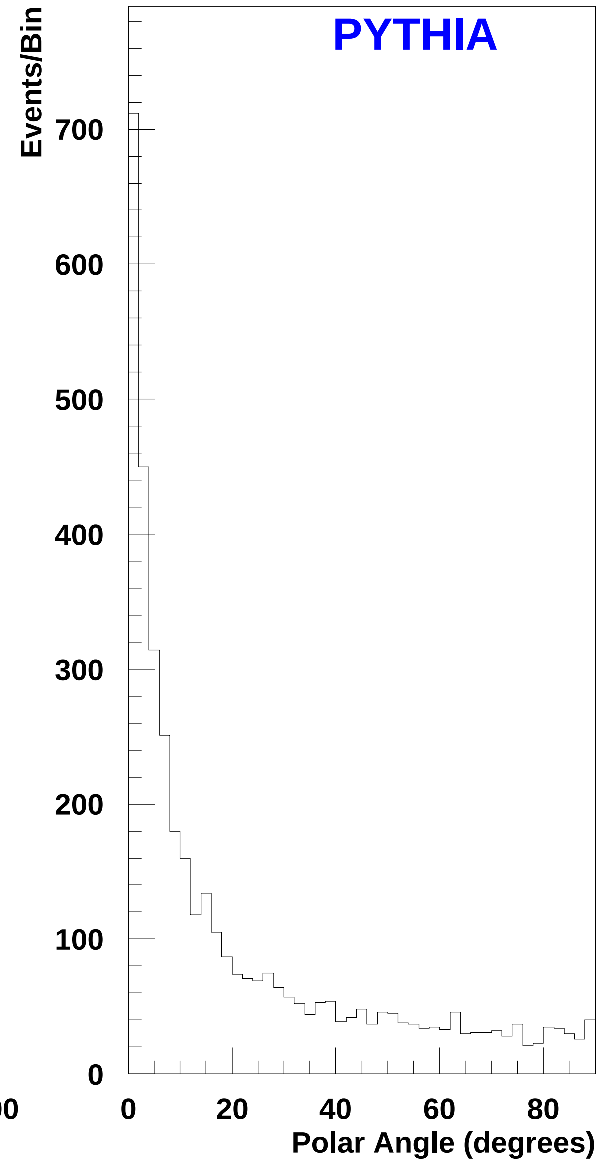

For $p_\mu \geq 2\,\mathrm{GeV}$ and $\theta_\mu > 20/100/150$ mrad the acceptance is only 40/17/10%, which yields about 10-100 events for $\mathcal{L}_{\mathrm{int}} = 100\ \mathrm{fb}^{-1}$.

With small acceptance and branching ratio a large luminosity is needed to observe the process.

Higgs search in $\gamma\gamma \longrightarrow h_0 \longrightarrow \mathrm{X\overline{X}}$

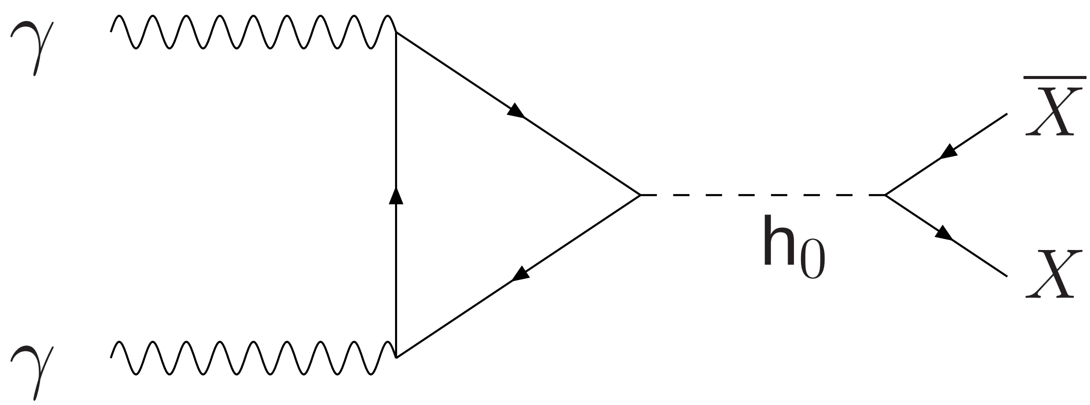

1. The Higgs is produced as an s-channel resonance. A measurement of $\Gamma(\gamma\gamma \longrightarrow h_0)$ is very fundamental as it is sensitive to all charged particles in the loop which couple to the Higgs.
2. The required accuracy for $\Gamma(\gamma\gamma \longrightarrow h_0)$ is at the few percent level to be sensitive to new particles in the decoupling limit.
3. Combined measurements of $\Gamma(\gamma\gamma \longrightarrow h_0)$ and $\mathrm{BR}(h_0 \longrightarrow \gamma\gamma)$ at the e^+e^- and $\gamma\gamma$ collider provide a model independent measurement of the total width of the Higgs.

Higgs production $\gamma\gamma \rightarrow h_0$

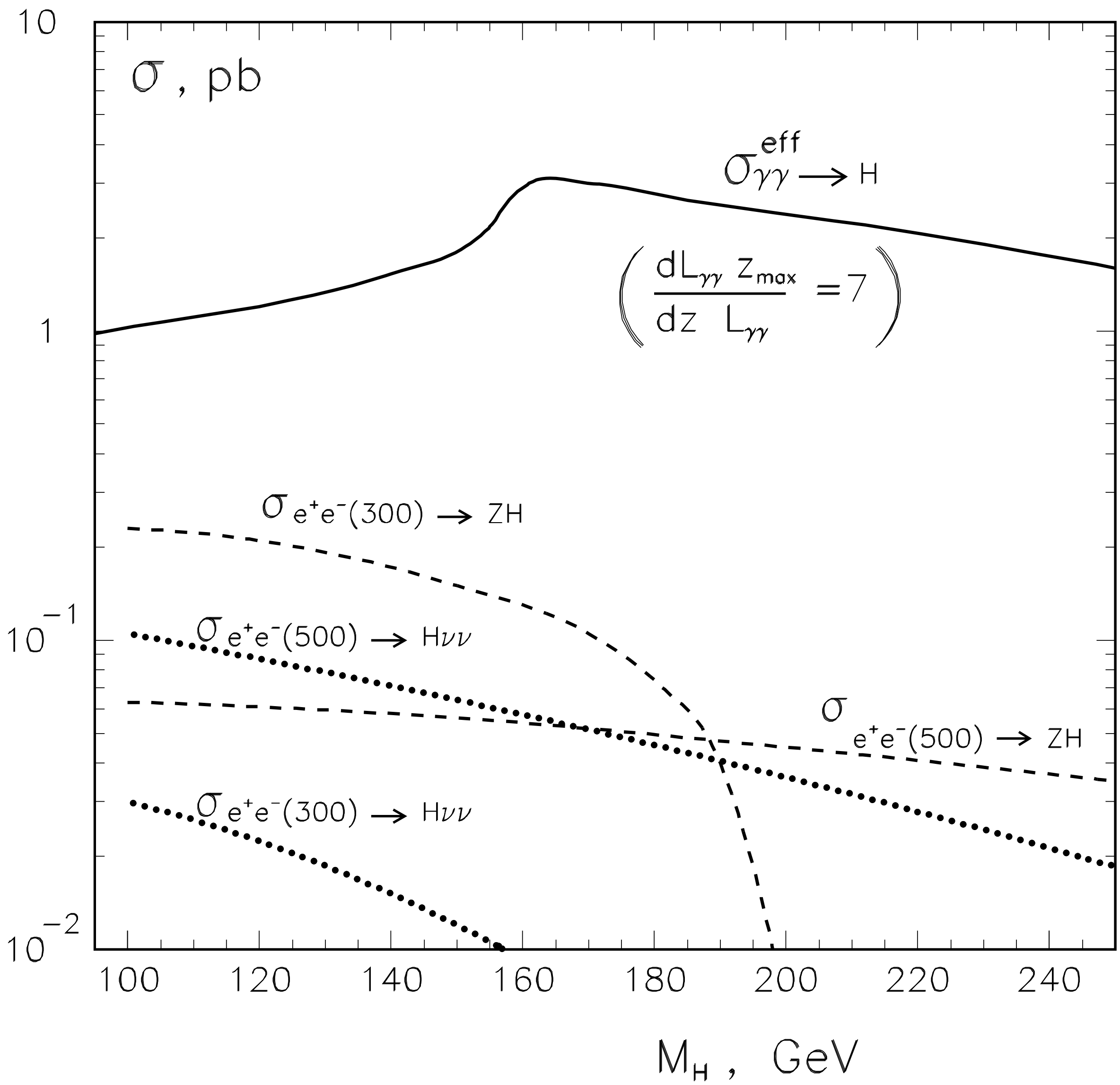

$$\sigma_{\gamma\gamma}^{\text{eff}} = \frac{\mathrm{d}L_{\gamma\gamma}}{\mathrm{d}W_{\gamma\gamma}} \frac{M_{h_0}}{L_{\gamma\gamma}} \frac{4\pi^2\Gamma(\gamma\gamma \rightarrow h_0)(1-\lambda_1\lambda_2)}{M_{h_0}^3}$$

Good prospects for $\gamma\gamma$ production of Higgs bosons, because of the larger cross-section and the reach to higher masses than for e^+e^-.

$\gamma\gamma \longrightarrow$ hadrons as underlying event

$$\mathrm{d}\Omega = \mathrm{d}\phi\mathrm{d}\eta\,\sin^2\theta$$

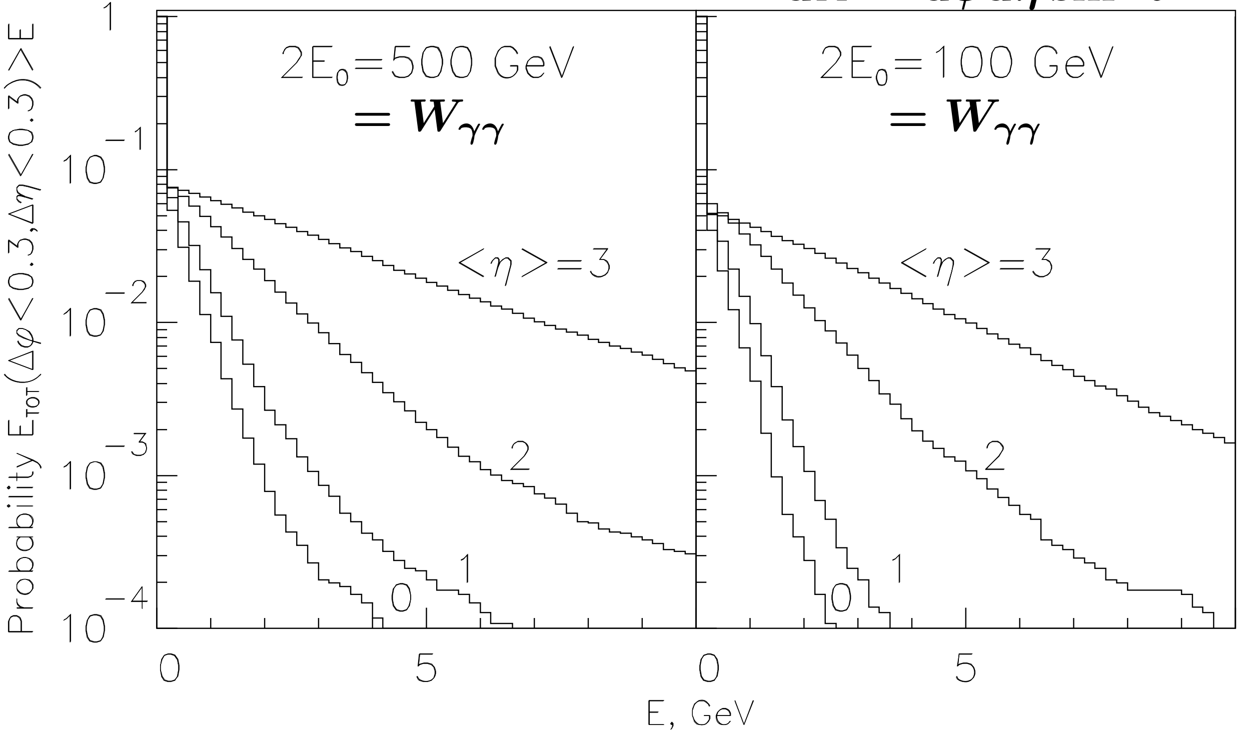

1) The energy resolution for a jet of $100\ \mathrm{GeV}$ energy is about $3\ \mathrm{GeV}$.

2) Assuming two $\gamma\gamma \longrightarrow$ hadrons reactions per event, the probability to have an additional energy of $2\ \mathrm{GeV}$ in a jet at $\eta = 0(2)$ is $1.5(60)\%$.

3) The background potentially degrades the mass resolution, especially at large rapidities, and most likely has to be measured directly from the data.

The test case $\gamma\gamma \rightarrow h_0 \rightarrow \mathrm{b\bar{b}}$

1. To reduce the continuum production of $\mathrm{b\bar{b}}$ and $\mathrm{c\bar{c}}$ one needs to select $J_z = 0$, because then $\sigma(\gamma\gamma \rightarrow \mathrm{q\bar{q}}) \propto m_\mathrm{q}/W_{\gamma\gamma}$.
2. In addition, good b tagging and c suppression is mandatory.
3. Assume 100$\%$ laser and 85$\%$ electron polarization and run the collider at $\sqrt{s_\mathrm{ee}} = M_{h_0}/0.8$ such that the Higgs mass corresponds to the peak of the $\gamma\gamma$ luminosity spectrum.
4. Use additional cuts to further suppress the background.

For $L_{\gamma\gamma} = 43\ \mathrm{fb}^{-1}$ in the peak, which means about $400\ \mathrm{fb}^{-1}$ $\mathrm{e}^+\mathrm{e}^-$ luminosity, $\Gamma(\gamma\gamma \rightarrow h_0)$ can be determined with a precision of about 2-10$\%$ in the mass range $120 < M_{h_0} < 160\ \mathrm{GeV}$.

Higgs reconstruction for $\gamma\gamma \rightarrow h_0 \rightarrow b\bar{b}$

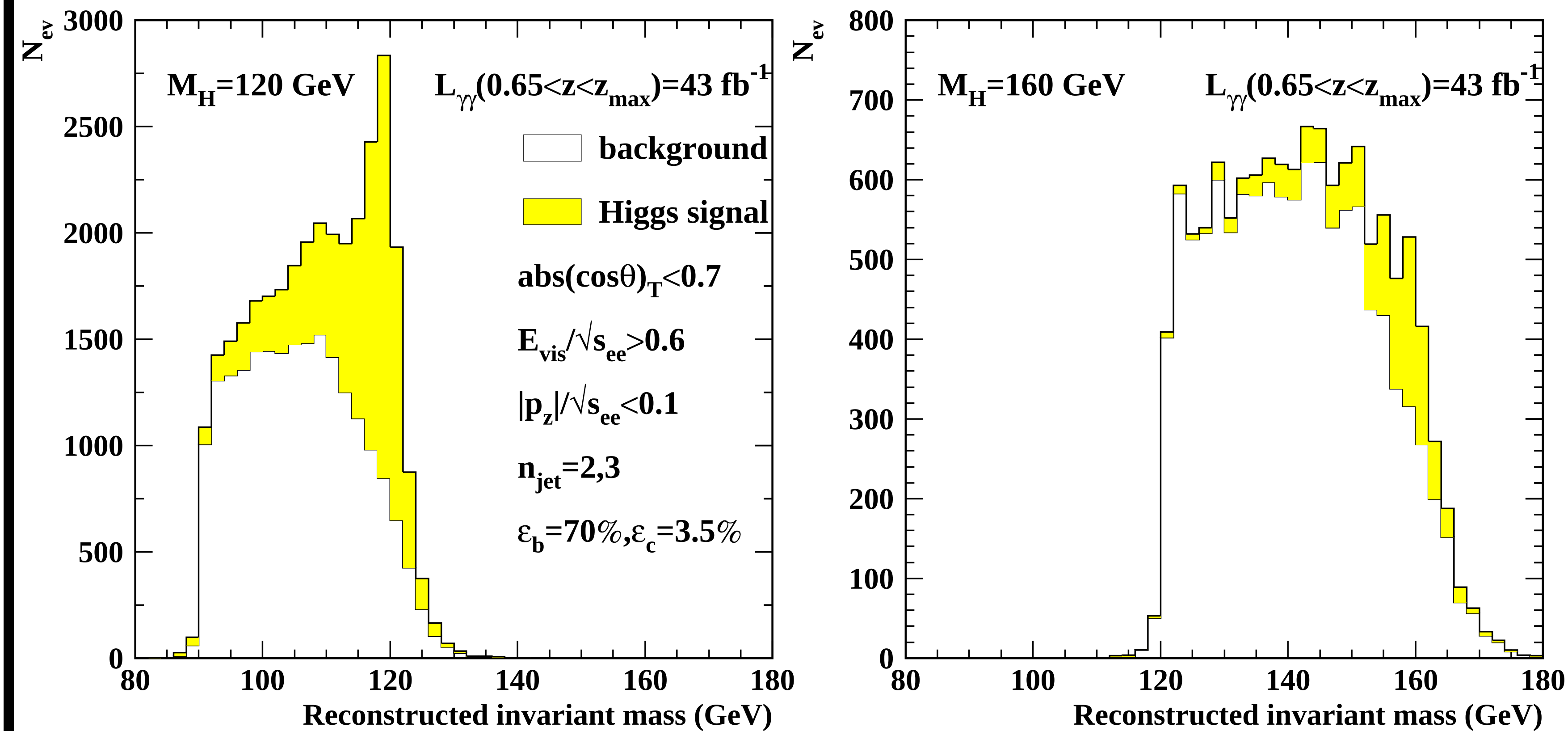

Clear signals are observed, especially for low Higgs masses.

Search for MSSM Higgs bosons

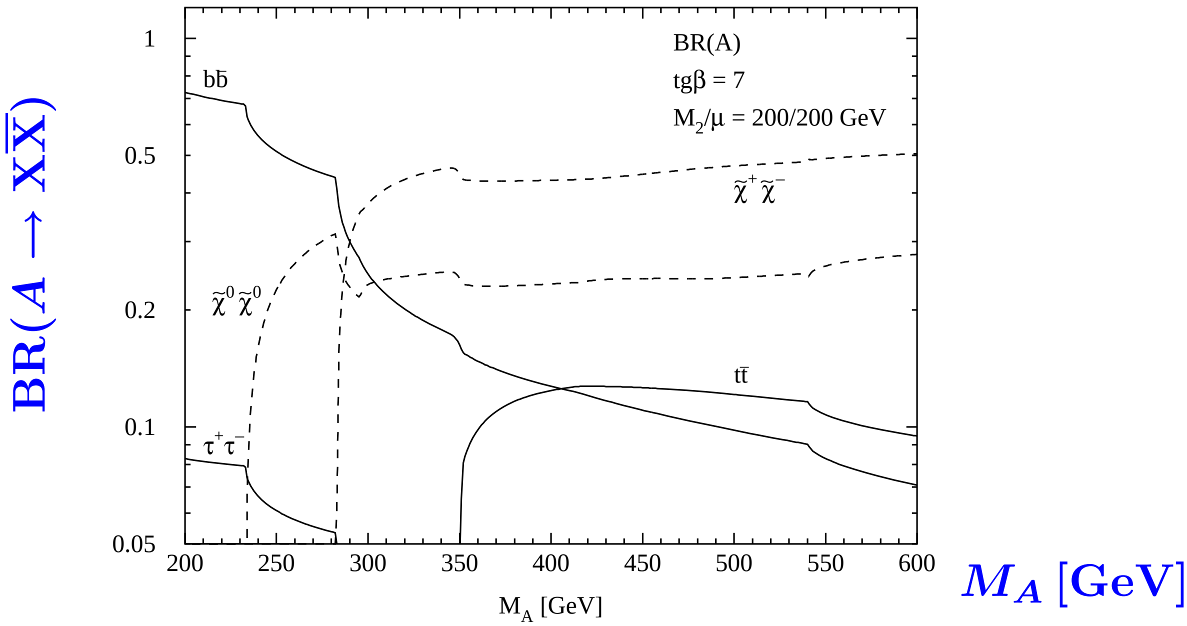

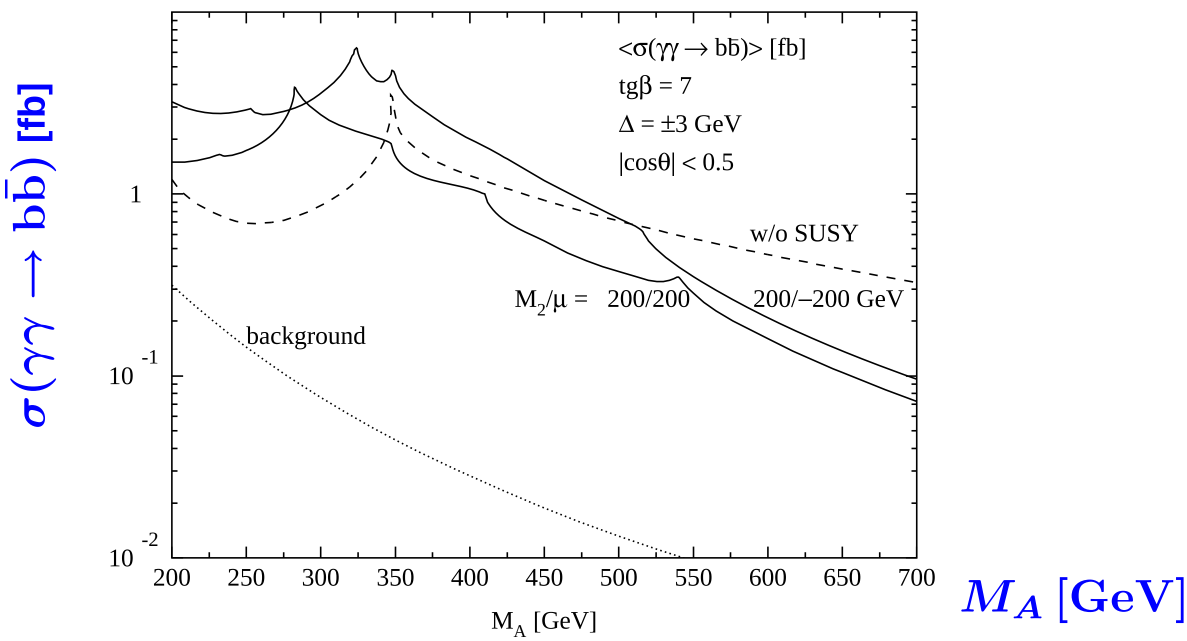

Good prospects for $\gamma\gamma$ production of MSSM neutral Higgs bosons up to $M_A = 400$ GeV in a region of parameter space where the LHC is blind $[\tan(\beta) = 7, M_2/\mu = 200/200$ GeV$]$.

Some $\gamma\gamma$ and eγ cross sections

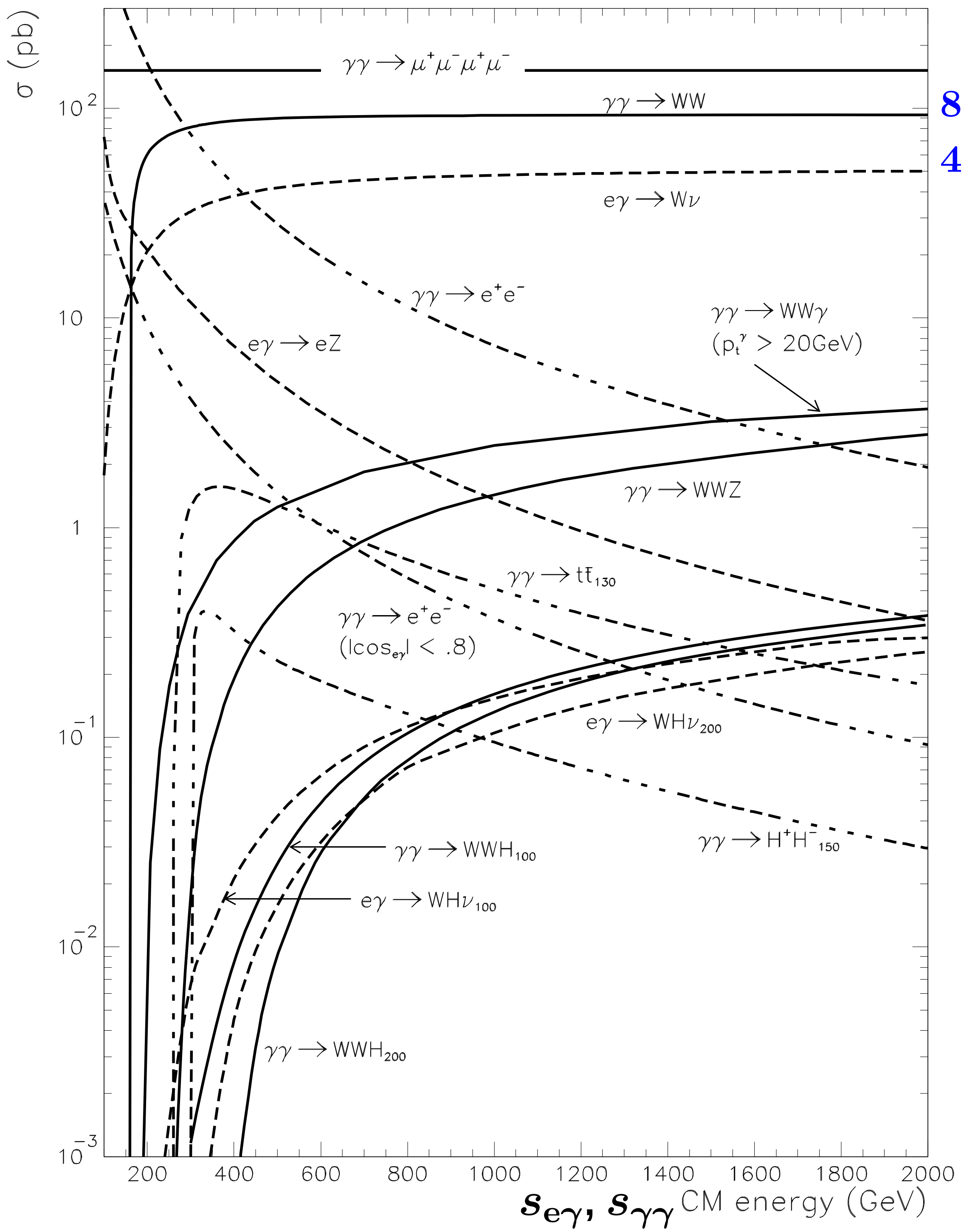

81*pb*

43*pb*

The WW(γ) final state

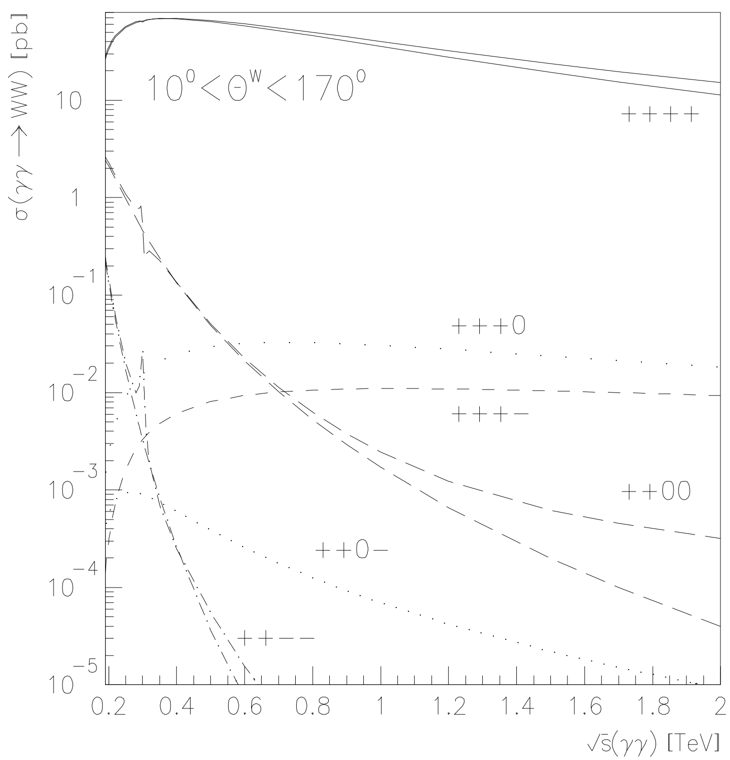

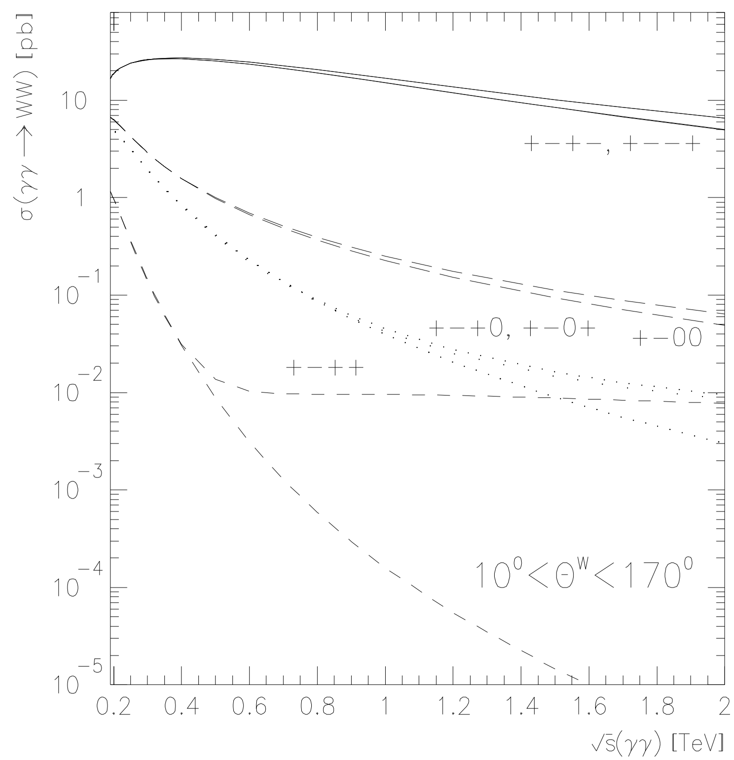

1. The $\mathcal{O}(\alpha)$ cross-sections yield $\sigma_{\gamma\gamma}\ (\sigma_{\rm ee}) = 61\ (6.6)$ pb within cuts.
2. The radiative corrections are moderate but strongly depend on θ^W.
3. About 10^6 $\mathrm{W}^+\mathrm{W}^-$ pairs per year are produced. A sample well suited for studies of anomalous couplings of the W.

The production of Z^0 pairs at a Photon Collider

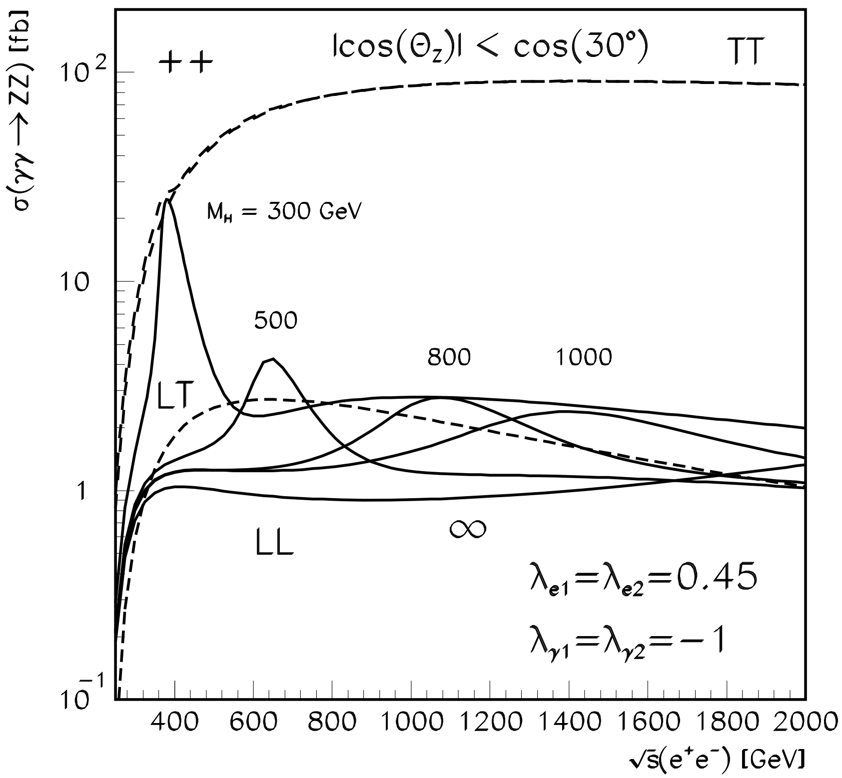

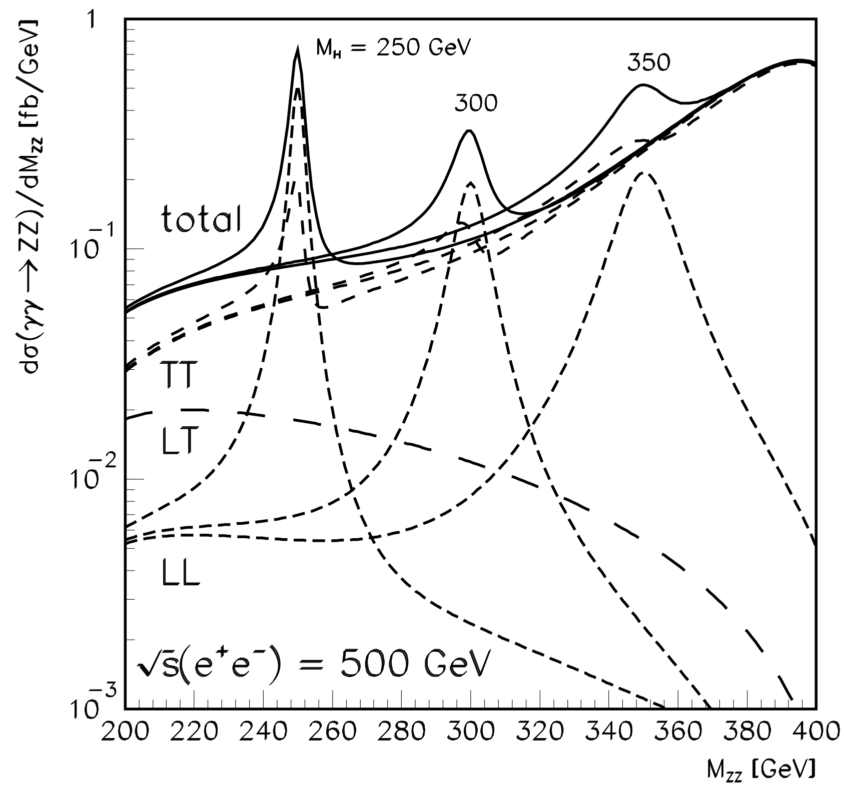

1. The cross-section strongly depend on the helicities of the Z bosons.
2. Higgs signals up to $M_H = 350$ GeV can be observed, for higher masses the background from the continuum $Z_T Z_T$ production is too high.

The various options for single top production

reaction	no. of diagrams	polarization	$t\bar{t}$	$\sigma_{\rm top}$ [fb] 0.5 TeV	$\sigma_{\rm top}$ [fb] 1 TeV
$e^+e^- \longrightarrow e^-\bar{\nu}_e t\,\bar{b}$	20	LR	yes	10.0	16.9
$\gamma\gamma \longrightarrow e^-\bar{\nu}_e t\,\bar{b}$	21	++	yes	11.1	19.2
$e^-e^- \longrightarrow e^-\nu_e \bar{t}\,b$	20	LL	no	2.6	19.1
$e^-\gamma \longrightarrow \nu_e \bar{t}\,b$	4	L+	no	94.3	174.7

$e^-\gamma \longrightarrow \nu_e \bar{t}\,b$ is the best option since it has the largest cross-section, no $t\bar{t}$–pair background and a high degree of polarization is possible. It has excellent sensitivity to V_{tb} and to anomalous couplings at the Wtb vertex.

Diagrams for single top production

e^+e^-: N = 20

$\gamma\gamma$: N = 20

e^-e^-: N = 4

$e^-\gamma$: N = 21

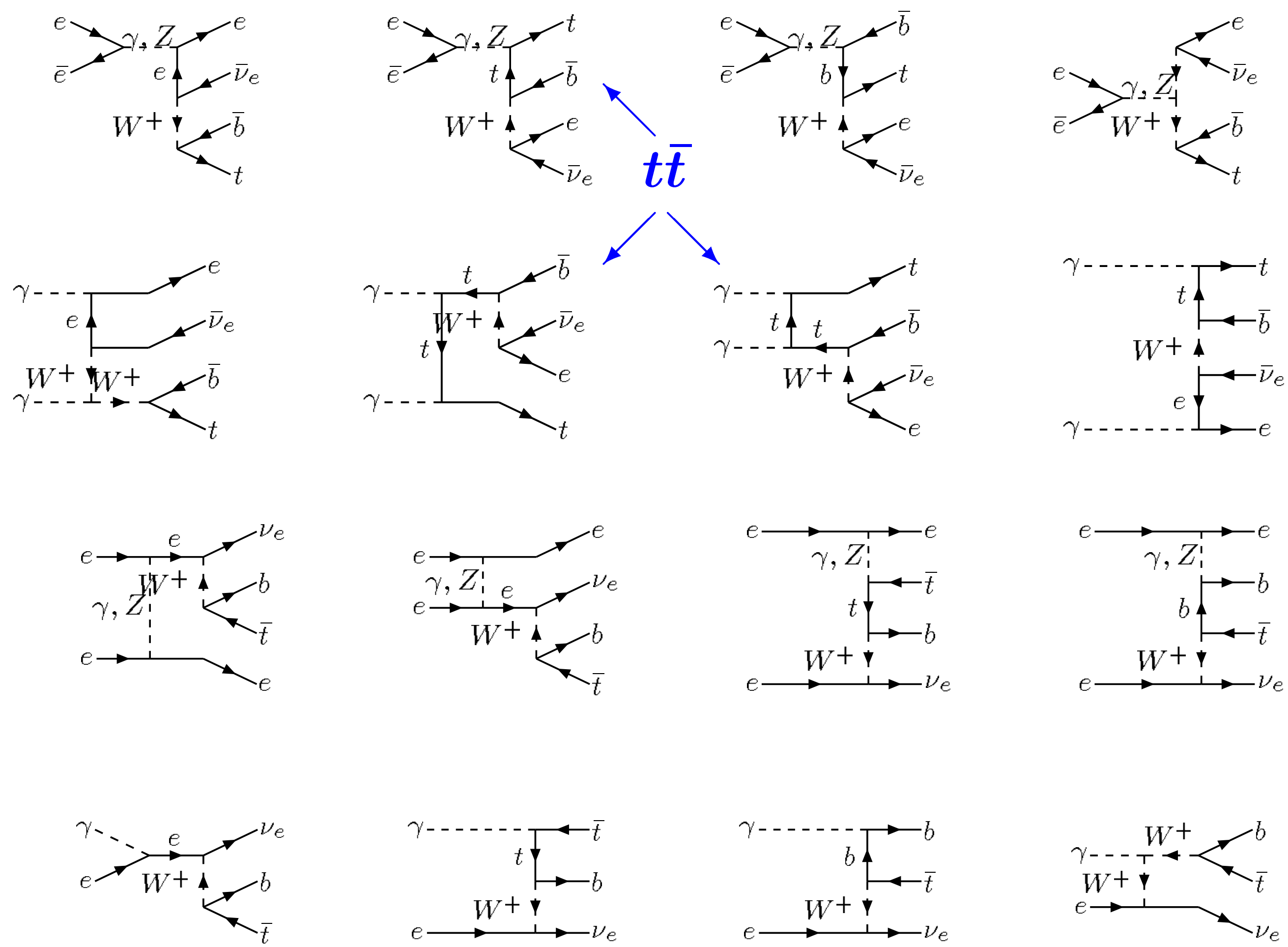

Single top production

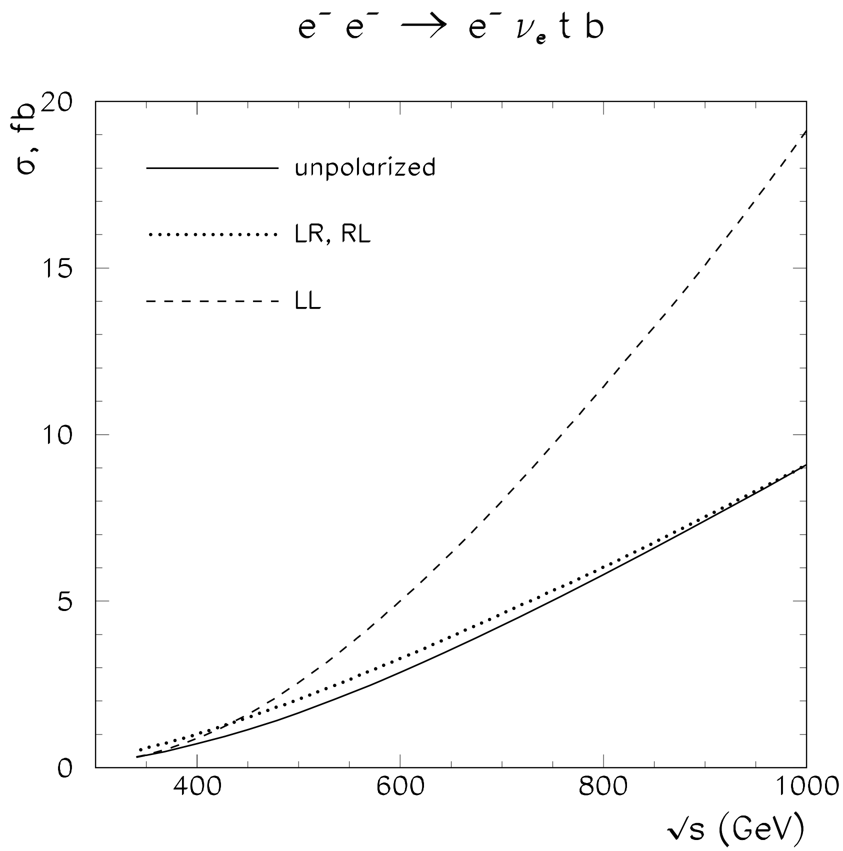

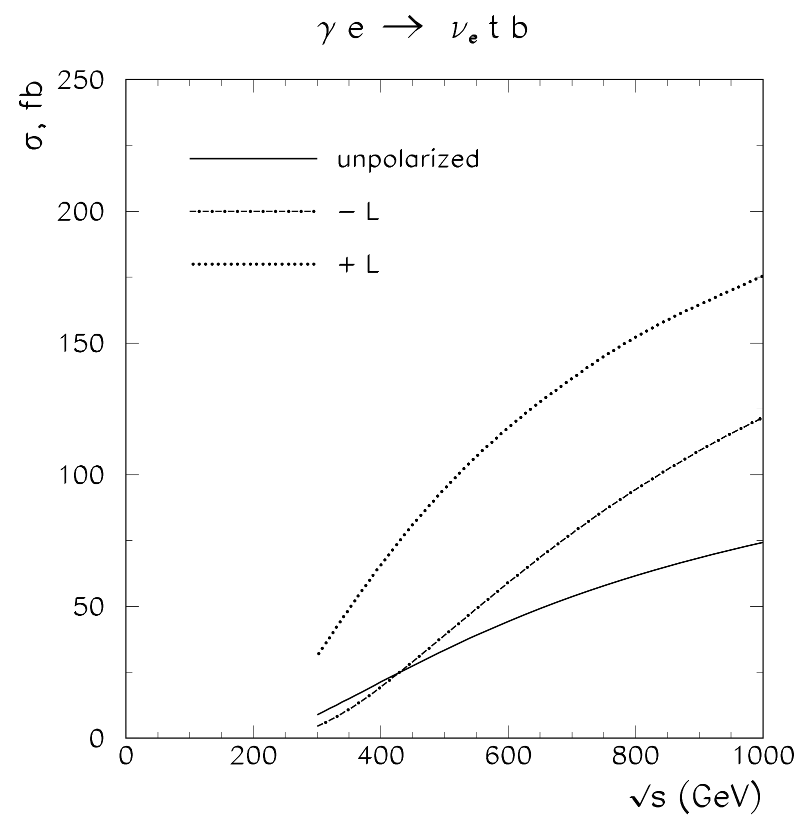

For $\mathcal{L}_{\rm int} = 100\ \rm fb^{-1}$ at $\sqrt{s_{\rm ee}} = 500\ \rm GeV$, the matrix element V_{tb} can be measured with 3.5% and 0.5% statistical precision for $e^-e^- \to e^-\nu_e \bar{t}\, b$ and $e^-\gamma \to \nu_e \bar{t}\, b$.

Conclusion

1. The Linear Collider is an ideal tool to investigate photon–photon physics at the highest energies.

2. The tagging of electrons down to the lowest possible angles is a challenging task, but it is mandatory to achieve overlap with the results from LEP II in several areas, i.e. structure function measurements.

3. Due to the high centre-of-mass energy, especially in the Photon Collider mode, new channels (Higgs, W, Z^0, LQ, ...) are open to be copiously produced.

4. For some of the reactions the Photon Collider extends the reach of a e^+e^- Collider significantly, and in some cases it is unique.

Much work is ahead of us to bring a Linear Collider to life, but it should be fun and the physics potential is certainly worth the effort.

Slides: http://home.cern.ch/nisius